

DOKUZ EYLÜL UNIVERSITY
GRADUATE SCHOOL OF NATURAL AND APPLIED SCIENCES

**FEATURE EXTRACTION AND
CLASSIFICATION OF
ELECTROENCEPHALOGRAPHIC (EEG)
SIGNALS TOWARDS THE USE OF BRAIN-
COMPUTER INTERFACE IN COGNITIVE
APPLICATIONS**

by
Sezin TUNABOYLU

July, 2017
İZMİR

**FEATURE EXTRACTION AND
CLASSIFICATION OF
ELECTROENCEPHALOGRAPHIC (EEG)
SIGNALS TOWARDS THE USE OF BRAIN-
COMPUTER INTERFACE IN COGNITIVE
APPLICATIONS**

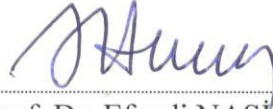
**A Thesis Submitted to the
Graduate School of Natural and Applied Sciences of Dokuz Eylül University
In Partial Fulfillment of the Requirements for the Degree of Doctor of
Philosophy in Department of Statistics, Statistics Program**

**by
Sezin TUNABOYLU**

**July, 2017
İZMİR**

Ph.D. THESIS EXAMINATION RESULT FORM

We have read the thesis entitled “**FEATURE EXTRACTION AND CLASSIFICATION OF ELECTROENCEPHALOGRAPHIC (EEG) SIGNALS TOWARDS THE USE OF BRAIN-COMPUTER INTERFACE IN COGNITIVE APPLICATIONS**” completed by **SEZİN TUNABOYLU**, under supervision of **PROF. DR. EFENDİ NASİBOĞLU** and we certify that in our opinion it is fully adequate, in scope and in quality, as a thesis for the degree of Doctor of Philosophy.



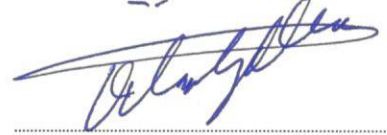
Prof. Dr. Efendi NASİBOĞLU

Supervisor



Prof. Dr. Mehmet KUNTALP

Thesis Committee Member



Prof. Dr. Özlem EGE ORUÇ

Thesis Committee Member



Prof. Dr. Urfat NURİYEV

Examining Committee Member



Doç Dr. Serdar DEMİR

Examining Committee Member



Prof. Dr. Emine İlknur CÖCEN

Director

Graduate School of Natural and Applied Sciences

ACKNOWLEDGEMENT

Firstly, I would like to express my sincere gratitude to my thesis Advisor Prof. Dr. Efendi NASİBOĞLU for the continuous supports, his patience, and motivation during my doctorate thesis studies. I have gained different perspectives thanks to my advisor. His scientific guidance helped me in research and writing of this thesis. Besides my advisor, I would like to thank the rest of my thesis committee: Prof. Mehmet KUNTALP, Prof. Dr. Özlem EGE ORUÇ, for their valuable comments and encouragement, also their confidence to me.

My sincere thanks also goes to Dr. Alper VAHAPLAR for all supports, his valuable inspiration, spending his time to me and sharing all their experience. Also, I would like to thank Erhan KEŞFEDEN for all supports and motivations.

Last but not the least, I would like to thank my parents and my brother for supporting me in all my life and this doctorate thesis. Without their precious support it would not be possible to conduct this research. I would like to express my special thanks of gratitude to my husband for his support and understanding. I dedicate this thesis to my mother Leyla TANSI, my father Hasan TANSI, my brother Serkan TANSI, my dear husband Çağdaş TUNABOYLU and my honey son Çınar TUNABOYLU.

I am grateful to the Scientific and Technological Research Council of Turkey, TÜBİTAK, for whom supporting me throughout my graduate studies.

Sezin TUNABOYLU

FEATURE EXTRACTION AND CLASSIFICATION OF ELECTROENCEPHALOGRAPHIC (EEG) SIGNALS TOWARDS THE USE OF BRAIN-COMPUTER INTERFACE IN COGNITIVE APPLICATIONS

ABSTRACT

In this thesis, the brain computer interface system is developed for the cursor movement through the cognitive signals. The EEG data is handled from the Emotiv Neuroheadset device via our developed program written in c# language.

We have worked on classification of five cognitive tasks; up, down, left, right and no movement. Before the movement of the cursor, the participants need to be trained to control the brain signals. In the training phase, the training screen is designed to consist of the visual stimuli. The participants have trained the program three times in different days and each session includes 24 trainings. EEG signals are very complex and the extracting information is difficult. Also, EEG signals has many artifacts occurred by the eye movement, muscle movement and the noise in environment. Therefore, median filtering and the normalization method are used in the preprocessing phase. Then the specific features for all cognitive tasks are extracted by the multifractal detrended fluctuation analysis and the fast Fourier transform. The P_h values and beta signals calculated from the MFDFA and FFT methods respectively, are used as features.

Finally these features are classified by the nearest neighbor algorithms. Nearest neighbor (NN) algorithms are simple but effective methods for performing pattern classification. The CxK nearest neighbor algorithm is firstly used for cognitive EEG signal classification in this thesis and this method has given acceptable results when compared with the other studies in literature.

Keywords: EEG, BCI, feature extraction, classification, k-nearest neighbor algorithm, CxK-nearest neighbor algorithm.

BİLİŞSEL UYGULAMALARDA BEYİN-BİLGİSAYAR ARAYÜZÜNÜN KULLANIMINA YÖNELİK ÖZELLİK ÇIKARIMI VE ELEKTROENSEFALOGRAFİK (EEG) SİNYALLERİN SINIFLANDIRILMASI

ÖZ

Bu tez çalışmasında, bilgisayar imlecinin düşünce gücüyle hareket ettirilmesi için beyin-bilgisayar arayüzü geliştirilmiştir. EEG sinyalleri, Emotive Neuroheadset cihazının c# diliyle geliştirdiğimiz programa entegre edilerek elde edilmiştir. Düşünce gücüyle imlece yukarı, aşağı, saga, sola ve hareket etmeme komutlarını yaptırma üzerinde çalışılmıştır. Öncelikle katılımcıların beyin sinyallerini kontrol edebilmesi için eğitilmeleri gerekmektedir. Eğitim için komutların görsel resimlerini içeren bir ekran geliştirilmiştir. Katılımcılar 3 farklı günde eğitim programına tabi tutulmuştur. Her bir eğitimde görsel uyaranları içeren uygulama 24 kere gösterilerek elde edilen veriler sonraki çalışmalar için kaydedilmiştir.

EEG verileri kompleks ve ham halinden bilgi çıkarılması zordur. Ayrıca, göz hareketleri, kas hareketleri ve ortam sesleri EEG sinyallerinde gürültüye neden olmaktadır. Bu nedenle ön işleme aşamasında medyan filtreleme ve normalizasyon yöntemleri kullanılmıştır. Ön işleme işleminden sonra spesifik özellikler her bir komut için çıkarılmıştır. Özellik çıkarmak için MFDFA ve FFT yöntemleri kullanılmıştır. MFDFA yöntemi ile elde edilen dağılım değerleri ve FFT yöntemi ile elde edilen beta sinyalleri özellik olarak kullanılmıştır. Böylece büyük veri setinden daha küçük veri seti oluşturularak boyut indirgeme yapılmıştır. Son olarak, çıkarılan özellikler en yakın komşu algoritmalarıyla sınıflandırılmıştır. Sınıflandırma yöntemi olarak basit fakat örüntü sınıflandırma iyi performans değerlerine sahip olan k-en yakın komşu yöntemi ile EEG sinyal örüntülerinin sınıflandırılmasında daha önce kullanılmamış olan CxK en yakın komşu yöntemi kullanılmıştır ve literatürdeki çalışmalarla karşılaştırıldığında kabul edilebilir sonuçlar elde edilmiştir.

Anahtar kelimeler: EEG, BCI, özellik çıkarma, sınıflandırma, K-en yakın komşu algoritması, CxK- en yakın komşu algoritması.

CONTENTS

	Page
PH.D. THESIS EXAMINATION RESULT FORM	II
ACKNOWLEDGEMENT	III
ABSTRACT.....	IV
ÖZ	V
CONTENTS.....	VI
LIST OF FIGURES	IX
LIST OF TABLES	XI
 CHAPTER ONE - INTRODUCTION	 1
1.1 The Organization of the Thesis	3
1.2 Significance of this Study	5
 CHAPTER TWO - STRUCTURE OF THE BRAIN	 7
2.1 Lobes and the Functional Areas of the Brain	7
2.2 Cortical Homunculus.....	10
2.3 Brain Cell	11
 CHAPTER THREE - BIOMEDICAL SIGNALS.....	 13
3.1 Electroencephalogram (EEG).....	13
3.2 Measuring Brain Activity	15
3.3 Brain Waves	17
 CHAPTER FOUR - BRAIN COMPUTER INTERFACE.....	 21
4.1 The Structure of the BCI	21

CHAPTER FIVE - DATA	24
5.1 Data Acquisition.....	24
5.2 Training Experiments	26
5.3 Data Preprocessing	26
5.3.1 Median Filtering	27
5.3.2 Normalization	27
 CHAPTER SIX - SOFTWARES	 28
6.1 Emotiv Epoc Neuroheadset Software.....	28
6.1.1 Training Program.....	29
6.1.2 TestBench	30
6.2 Sycamore BCI Software.....	35
 CHAPTER SEVEN - FEATURE EXTRACTION METHODS.....	 42
7.1 Multifractal Detrended Fluctuation analysis	42
7.2 Brain Bandpowers Extraction	44
7.2.1 Fast Fourier Transform	46
7.2.2 Hanning Window.....	47
 CHAPTER EIGHT - CLASSIFICATION AND VALIDATION METHODS ..	 49
8.1 Statistical Signal Similarity	49
8.2 K-Nearest Neighbor Algorithm.....	53
8.3 $C \times K$ -Nearest Neighbor Algorithm	55
8.4 k-fold Cross Validation Method.....	56

CHAPTER NINE - EXPERIMENTAL RESULTS.....	58
9.1 Data Validation.....	58
9.2 Offline and Online Results	67
CHAPTER TEN - CONCLUSION	84
REFERENCES.....	86



LIST OF FIGURES

	Page
Figure 2.1 Anatomy of the brain and functions.	7
Figure 2.2 The lobes of the cerebrum.	8
Figure 2.3 The parts of the brainstem.	10
Figure 2.4 The motor homunculus visualizes the mapping of body muscles to the motor cortex. The mapping is not isomorph as important areas like tongue, hands and lips are overly represented.....	11
Figure 2.5 The cell of the human motor cortex.....	12
Figure 3.1 First recording of EEG signals made by Hans Berger.....	14
Figure 3.2 EEG sensing device.	16
Figure 3.3 Delta wave	17
Figure 3.4 Theta wave.....	18
Figure 3.5 Alpha wave	19
Figure 3.6 Beta wave.....	19
Figure 3.7 Gamma wave	20
Figure 4.1 The flow of the BCI system.....	22
Figure 5.1 Emotiv Epoch device.	24
Figure 5.2 Emotiv electrode locations.	25
Figure 5.3 Timing diagram of a motor imagery trial performed by the subject. The direction of the arrows provides instruction to the subject.....	26
Figure 5.4 Median filtering example.....	27
Figure 6.1 Emotiv Epoc control panel	28
Figure 6.2 Emotive Cognitive Suite for training	30
Figure 6.3 Emotiv Test Bench display showing EEG suit.....	31
Figure 6.4 Emotiv FFT suit.....	32
Figure 6.5 Emotiv gyro suit	33
Figure 6.6 Emotiv data packet counter and packet loss display	33
Figure 6.7 Sycamore training screen.....	35
Figure 6.8 Sycamore starting image of training screen.....	36
Figure 6.9 Sycamore up image of training screen.....	37
Figure 6.10 Sycamore down image of training screen.....	37

Figure 6.11 Sycamore right image of training screen.	38
Figure 6.12 Sycamore left image of training screen.	38
Figure 6.13 Sycamore no movement image of training screen.	39
Figure 6.14 Sycamore statistical similarity calculation screen.	39
Figure 6.15 Sycamore MFDFA calculation screen.	40
Figure 6.16 Sycamore BCI online test screen.	41
Figure 7.1 A discrete Fourier analysis of a sum of cosine waves at 10, 20, 30, 40, and 50 Hz.	46
Figure 7.2 Hanning window.	48
Figure 8.1 K-nearest neighbor.	54
Figure 8.2 10-fold cross validation.	57
Figure 9.1 The signals of mental tasks for the electrode locations of Subject1.	62
Figure 9.2 The power of the Beta and Alpha signals of Subject1.	63
Figure 9.3 The power of the Beta and Alpha signals of Subject2.	64
Figure 9.4 The power of the Beta and Alpha signals of Subject3.	65
Figure 9.5 The power of the Beta and Alpha signals of Subject4.	66
Figure 9.6 The power of the Beta and Alpha signals of Subject5.	67

LIST OF TABLES

	Page
Table 3.1 Brain wave frequencies	17
Table 9.1 The statistical similarity between mental tasks for session 1.....	59
Table 9.2 The statistical similarity between mental tasks for session 2.....	59
Table 9.3 The statistical similarity between mental tasks for session 3.....	60
Table 9.4 The statistical similarity of same mental tasks between sessions.	60
Table 9.5 The statistical similarity of different mental tasks for session's average. .	61
Table 9.6 The accuracy rates of K – nearest neighbor algorithm for subject 1.	70
Table 9.7 The accuracy rates of K – nearest neighbor algorithm for subject 2.	70
Table 9.8 The accuracy rates of K – nearest neighbor algorithm for subject 3.	71
Table 9.9 The accuracy rates of K – nearest neighbor algorithm for subject 4.	72
Table 9.10 The accuracy rates of K – nearest neighbor algorithm for subject 5.	72
Table 9.11 The accuracy rates of CxK – nearest neighbor algorithm for subject 1...	73
Table 9.12 The accuracy rates of CxK – nearest neighbor algorithm for subject 2...	74
Table 9.13 The accuracy rates of CxK – nearest neighbor algorithm for subject 3...	75
Table 9.14 The accuracy rates of CxK – nearest neighbor algorithm for subject 4...	75
Table 9.15 The accuracy rates of CxK – nearest neighbor algorithm for subject 5...	76
Table 9.16 The overall accuracy rates of CxK and K – nearest neighbor algorithm for all cognitive tasks.	77
Table 9.17 The accuracy rates of K – nearest neighbor algorithm for all subjects....	78
Table 9.18 The accuracy rates of CxK–nearest neighbor algorithm for all subjects.	78
Table 9.19 The accuracy rates of the online analysis for K-NN classifier.	80
Table 9.20 The accuracy rates of the online analysis for CxK-NN classifier.....	81
Table 9.21 The accuracy rates of the different classifiers in the literature.	82
Table 9.22 The offline analysis accuracy rates of the different classifiers of the Bhattacharyya et al. (2015) method.	83
Table 9.23 The online analysis accuracy rates of the different classifiers of the Bhattacharyya et al. (2015) method.	83

CHAPTER ONE

INTRODUCTION

The human body is controlled by the brain. The brain is very complex and the all functions have not found yet. But we know that it is responsible for perception, cognition, attention, emotion, memory and physical actions (Carlson, 2002; Purves et al., 2004). It works by the electrical activities between the neurons. When the person is thinking, reading, speaking or doing motor activities, the electrical signals are generated with chemical synapses in the different part of the brain. These electrical activities are measured and the occurred signals are monitored through the many techniques such as the electroencephalography (EEG), electrocorticography (ECoG), magnetic resonance imaging (MRI), functional magnetic resonance imaging (fMRI), positron emission tomography (PET) and single photo emission computed tomography (SPECT). These non-invasive techniques are used easily and they give an opportunity to analyze human brain functions.

We have use EEG technique in this thesis because the EEG has been generally used method to capture brain signals, noninvasiveness, usability and low set-up costs (Blankertz, et al., 2008; Grosse-Wentrup et al. 2009). EEG has been generally used as non-invasive technique for the brain signal analysis. It is very useful in diagnosis and treatment of mental and neurological brain diseases. The extracted features have been used in the classification of the mental tasks of the EEG signals. These features are very important for both diagnosis of the brain diseases and better understanding of the cognitive process. For this reason, it is vital to develop automated classification methods for EEG to ensure proper evaluation and treatment of neurological diseases (Agarwal et al., 1998). The unsupervised and supervised classification methods can be used to separate EEG signal features. In the unsupervised methods, the classes are not known but in the supervised classification, classes are known. We have used the supervised classification methods.

Recently, EEG signal are used in brain computer interface studies. Brain computer interface is the very useful tool for the communication between brain and

computer by controlling components of EEG signals. Many studies have demonstrated the relationship between EEG signals and mental tasks (Keirn & Aunon, 1990; Lang et al., 1996; Pfurtscheller et al., 1997; Anderson et al., 1998; Altenmuller & Gerloff, 1999; McFarland et al., 2000).

Generally, BCI Technology composed of four basic processes: recording the raw EEG signals as *signal acquisition*, removing noises as *signal preprocessing*, extraction of the intended action or desired features from the mental activity as *feature extraction*, and finally classification of the desired features.

There have been many BCI applications in the literature. Brain computer interface works are started with the study of Farwell & Donchin (1998). The basic BCI applications are computer games, biofeedback therapy such as reduction of epileptic seizures, treatment of attention deficit hyperactivity disorder (ADHD), navigation in virtual reality and cursor control applications (Blankertz et al. 2007; Pfurtscheller et al 2006; Sellers & Donchin, 2006). The increasing technology allow the control more complex devices such as prostheses, robot arms and mobile robots (Graumann et al., 2009; Velliste et al., 2008). Also, BCI has been used for the disabled subjects. Therefore, BCI communication could improve the quality of life for disabled peoples such as lack of muscle control (McFarland et al., 1993; Wolpaw & McFarland, 1994).

In the signal acquisition process, the raw EEG signals are recorded by the Emotiv Epoc Neuro Headset brain computer interface technology. Signals were filtered with the band-pass filtering method for the removing artifacts. Also, the median filtering and normalization methods are used as preprocessing. The features are extracted by the Fast Fourier Transform (FFT) and multifractal detrended fluctuation analysis method. The probability distribution and midrange beta signals are used as features extracted by MFDFA and FFT analysis respectively.

The multifractal detrended analysis has been commonly used method in the literature. Stan et al. (2013) have used the multifractal detrended cross correlation

analysis for investigating characteristics of series of length of coding and non-coding DNA sequences. Zheng et al. (2005) have used multiplicative multifractals for characterizing neuronal firing recordings. The MFDFA is used in linguistic analysis for the characterization of the text (Ausloos, 2012; Suckling et al., 2008). Also, it is used for EEG pattern recognition (Wang et al., 2003; Dutta et al., 2014; Kumar et al., 2013) and eye movement analysis (Shelhamer, 2005; Ihlen & Vereijken, 2010; Schmeisser et al., 2001; Kelty-Stephen & Nixon, 2013; Astefanoaei et al., 2013).

In this thesis, the cursor movement will be achieved using the imaginary EEG signals. We aim to classify the brain signals for the left, right, up, down and no movement mental tasks. K-Nearest Neighbor and C-KNN algorithms (Ulutagay & Nasibov, 2016) are used for the classification of the mental tasks.

1.1 The Organization of the Thesis

Thesis consists of ten chapters and in each chapter gives valuable information for this thesis. The organization of this thesis is briefly explained as follows:

Chapter 2 provides an overview of the brain structure and functional areas. The brain is the complex organ of the human body. It is composed of the millions of neurons. Beyond controlling the vital functions of the body, it controls the motor functions, sensations, thinking and visual activities. In this chapter, these issues are explained in a detail.

Chapter 3 gives the overview of the biomedical signals. The biomedical signals are the observations of physiological activities of organisms, ranging from gene and protein sequences, to neural and cardiac rhythms, to tissue and organ images (Chang & Moura, 2010). The aim of the biomedical signal processing is to extract specific and important information from the biomedical signals. The Electroencephalogram is the one and the mostly used biomedical signal. The EEG and its band power frequency waves are mentioned in this chapter.

Chapter 4 explains the brain computer interface system. The BCI is the communication between human and machine. It allows the user to control computer or machines through his/her thoughts. For this reason, many processing are carried out in four phases.

Chapter 5 provides the collection of the data, training phase and preprocessing methods. The data set is captured by the Emotiv Epoc Neuroheadset. The training phase is applied to the participants for the improvement of the classification results. The EEG signals are affected from the environment, muscle and eye movements and these effects cause to the artifacts. The preprocessing methods are applied to the raw EEG signal for removing artifacts.

Chapter 6 presents the Emotiv Epoc Neuroheadset and our developed software Sycamore BCI. The Emotiv is easy to use device. It is non-invasive and, has 14 electrode location and two reference electrode. It capture the electrical signal of the brain with this 14 electrodes. Firstly, we use the Emotiv cognitive application for the test. Also, we take the EEG data from the Emotiv application program Test Bench and make our analysis from this data with the Weka and Matlab. Then we develop the Sycamore BCI program for the preprocessing, feature extraction and classification processes. Also, the online test interface is developed to work with extracted features and selected classification method. In this chapter these programs and the interfaces are displayed and explained.

Chapter 7 illustrates the feature extraction methods in a detail. The feature extraction is very important process because of the reduce curse of dimentionality. The probability distribution of the Hurst exponent, extracted by the multifractal detrended fluctuation analysis. Also the specific brain signals are extracted from the time domain EEG data with the fast Fourier transform method. The midrange and the beta signals are used as feature too.

In Chapter 8, the classification methods are mentioned. Statistical similarity method is the statistical hypothesis test method. It used for the validation of the data

by measuring similarity of the each cognitive task. The commonly used method K-nearest neighbor classifier is used to classify P_h , midrange beta and beta feature signals. Also, newly proposed CxK-nearest neighbor classifier is applied to the classification of the features. These methods are explained by the algorithm steps. Finally, 10-fold cross-validation method used for the performance evaluation is explained.

Chapter 9 shows the experimental results for offline and online analysis. In offline analysis, extracted features are classified for five subjects with the K-nearest neighbor algorithm and CxK-nearest neighbor algorithm. This cursor movement BCI application is subject based application. Therefore, the feature extraction process is done for all subjects and the subjects features are classified separately.

Chapter 10 is the final chapter. In this chapter the conclusion is explained. The advantages of the used processes are discussed.

1.2 Significance of this Study

Contributory disciplines of BCI are known as Cognitive Psychology, Social and Organizational Psychology, Ergonomics and Human Factors, Engineering, Design, Anthropology, Sociology, Philosophy, Linguistics, Artificial Intelligence and Computer Science.

Scope of a user interface includes design of input and output devices, workstation environment, context of use, information layout and meaning.

User characteristics such as cognitive ability, expertise/experience, level of education, age, attitude, physical ability and culture will be affected by the improvements and outcomes of BCI studies.

In a business context, user interface and related studies such as BCI may improve efficiency, effectiveness, productivity, safety and user satisfaction yielding;

- Completeness and accuracy with which users achieve specified goals (effective)
- The speed with accuracy in which users can complete the tasks for which they use the product (efficient)
- Pleasant and satisfying to use (engaging)
- Prevent errors caused by the user's interaction & help the user recover from any errors that do occur (error tolerant)
- Allows users to build on their knowledge without deliberate effort (easy to learn)

In this thesis;

- The statistical similarity method is used as first time for the data validation.
- The newly developed classifier the CxK-nearest neighbor algorithm is applied to the EEG signal classification as a first time. This method is basic and gives acceptable results in both online and offline analysis.
- In the literature, it is known that thinking signals occurs in the midrange beta signal frequency but the Ph values give the better results than the midrange beta signal. This shows that the Ph values represent the specific features of the cognitive tasks.
- The BCI studies are done as a project with the team, in this study we have carried out this works with a small team. Nevertheless, we take acceptable results.

Any contribution to the BCI system is valuable. This proposed classification method can be used for the wheel chair management for disable people, games, and linguistic comments etc.

CHAPTER TWO

STRUCTURE OF THE BRAIN

The human brain is the mysterious organ which controls all essential functions of the body. The brain receives the information from the outside world through five senses organ: eye (vision), nose (smell), skin (touch), tongue (taste), and ear (hearing). Then it interprets the received information to meaningful information for us and stores in memory. Also, thoughts, speech, movement of the limb, function of many organs within body, breathing are a few of the things controlled by the brain.

2.1 Lobes and the Functional Areas of the Brain

Brain is the most complex organ of the human body. All physical and mental tasks are managed through the brain. The brain anatomically consists of three important parts; cerebrum, cerebellum and brainstem (Gray, 2002) as displayed in Figure 2.1.

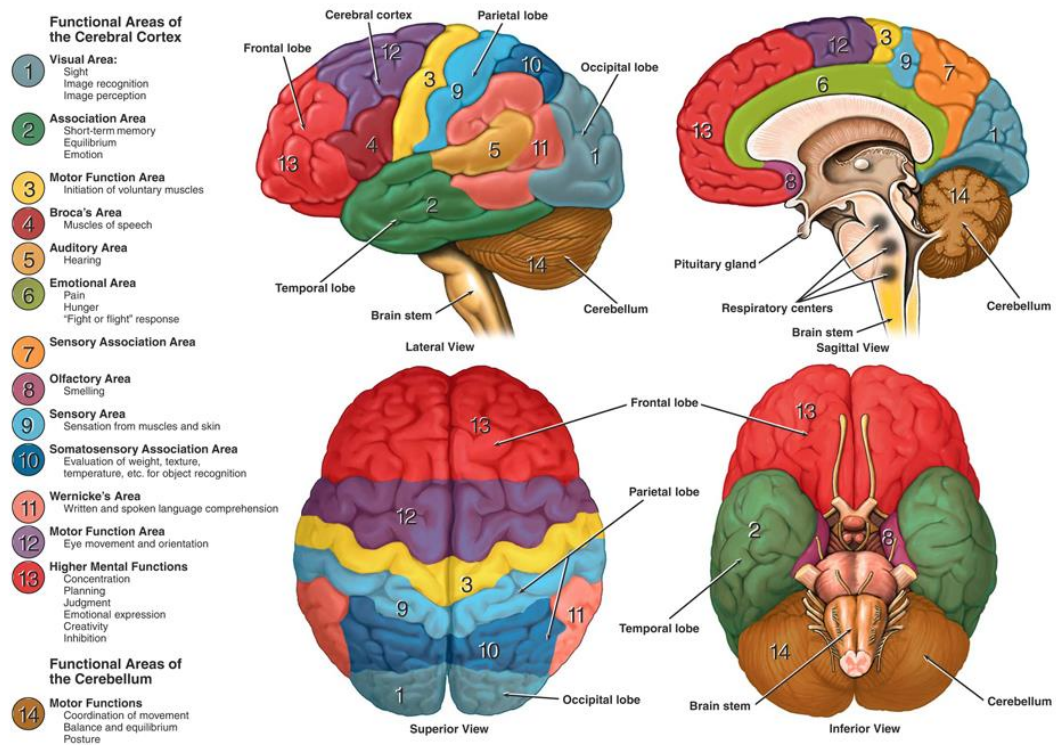


Figure 2.1 Anatomy of the brain and functions (Gray, 2002).

The afformentioned parts are explained as follows:

Cerebrum:

The cerebrum is the largest and principle part of the brain. It is located in the in the front area of the skull and consisting of left and righ hemispheres. Each hemisphere composed of the four parts called as lobes: frontal, parietal, occipital, and temporal (Purves et al., 2004) as shown in Figure 2.2. The outer layer of the cerebrum is made up of neural tissues known as the cerebral cortex. The cerebrum part of the brain is generally responsible from thoughts, movements, emotions and motor brain functions. These lobes are responsible for variety functions.

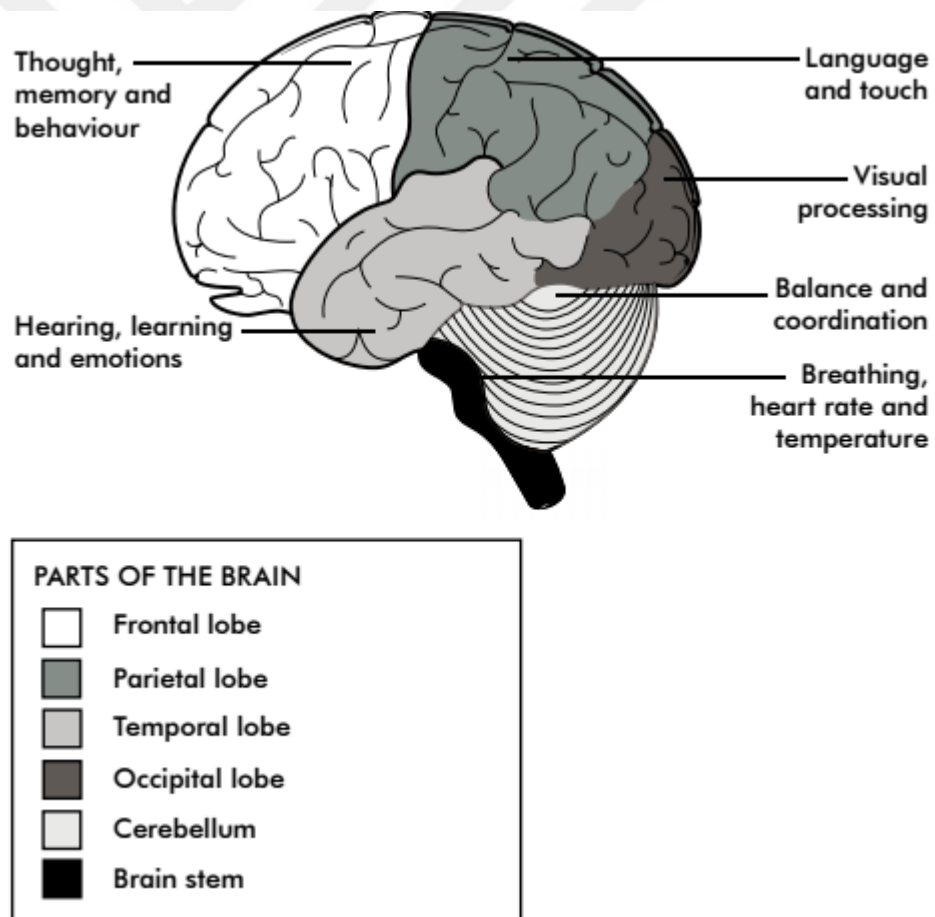


Figure 2.2 The lobes of the cerebrum (Purves et al., 2004).

- Frontal Lobe is located at the front of the brain and positioned in front of the parietal lobe and above and in front of the temporal lobe. The frontal lobe controls voluntary movement, emotions, problem solving, motor development, reasoning, planning, parts of speech and movement.
- *Parietal Lobe* is positioned above the occipital lobe and behind the frontal lobe. The parietal lobe is responsible for sensation such as pain, touch etc., sensory comprehension, and recognition, perception of stimuli, orientation and movement.
- *Occipital Lobe* is responsible for visual processing, such as color differentiation, and motion perception.
- *Temporal Lobe* is positioned under the lateral fissure on both cerebral hemispheres. The temporal lobe is involved in processing sensory inputs of visual memories, language comprehension, and emotion association.

Cerebellum:

The cerebellum is the part of the brain at the lower back of the skull in vertebrates. Also, cerebellum composed of the two hemispheres: left and right. It is the second largest part of the brain and contains more than half of the brain neurons. This part is generally responsible for the sensory perception, coordinates and regulates muscular activities. The cerebellum is also associated with voluntary muscle movements, fine motor skills, posture and balance regulation.

Brainstem:

The brainstem is the posterior part of the brain and connects the cerebrum and spinal cord. In the human brain, the brainstem contains the midbrain, pons and medulla. The midbrain is associated with vision, hearing, motor control, sleep/awake, alertness, and temperature regulation. The pons contains system that carry signals

from the cerebrum to the medulla and vice versa. Also it carries sensory signals to the thalamus.

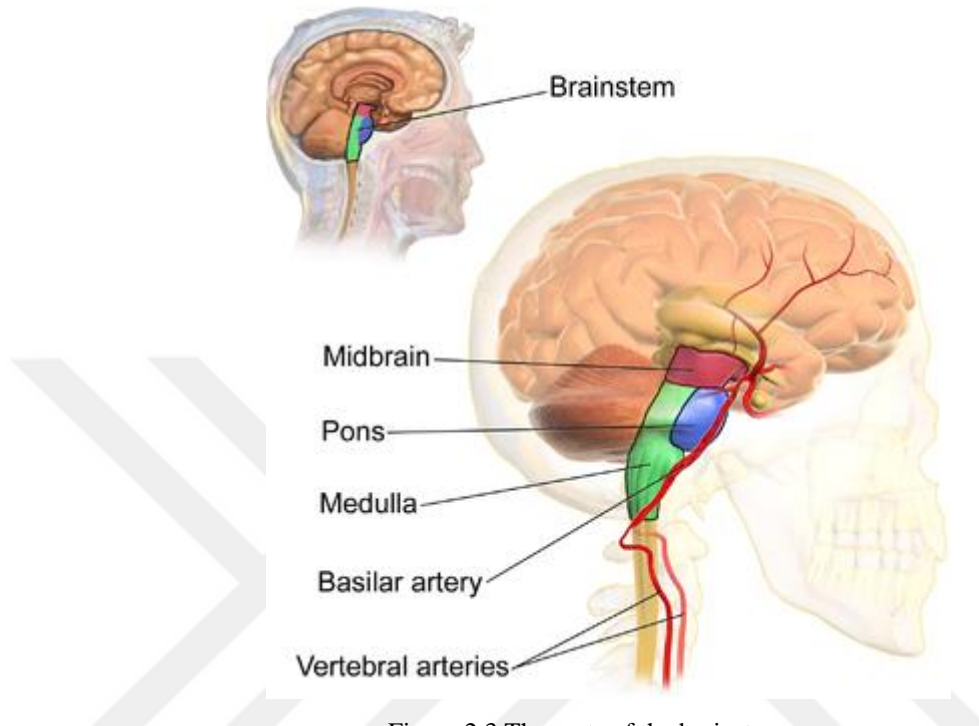


Figure 2.3 The parts of the brainstem.

The brain stem is the main control panel of the body. It is responsible for vital functions of the body, including breathing, consciousness, movements of the eyes and mouth, and the relaying of sensory messages (pain, heat, noise etc), heartbeat, blood pressure and hunger.

2.2 Cortical Homunculus

The homunculus shows in which the body parts are rendered according to how much of the somatosensory cortex is devoted to them (Schacter et al., 2009). The homunculus scheme was useful to determine a good choice of discrimination tasks for each patient, leading to motor imagery of left hand vs. right hand or little left finger vs. tongue.

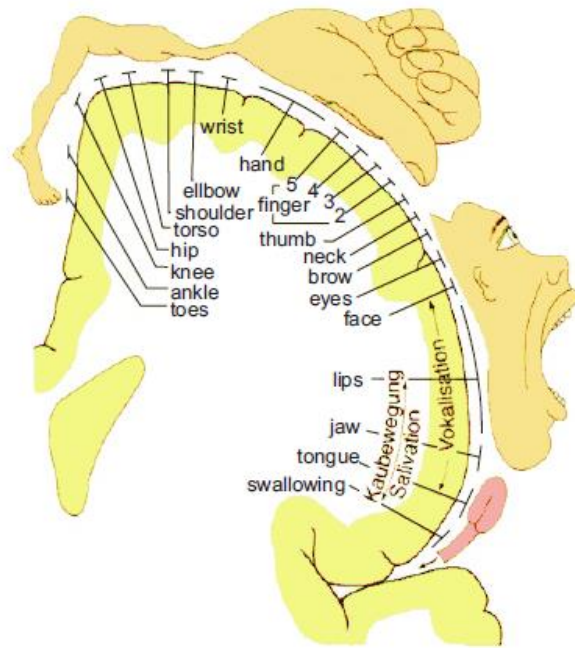


Figure 2.4 The motor homunculus visualizes the mapping of body muscles to the motor cortex. The mapping is not isomorph as important areas like tongue, hands and lips are overly represented (according to (Gohlenhofen, 1997)).

2.3 Brain Cell

The human nervous system consists of approximately 10^{10} to 10^{11} neurons, cells specialized in information processing, and of about the same number of neuroglia cells that support the neurons' activities in various ways (Eckert et al., 1993). Most of the neurons are situated in the central nervous system consisting of the brain and the spinal cord. The single pyramidal neuron cell is in Figure 2.5:

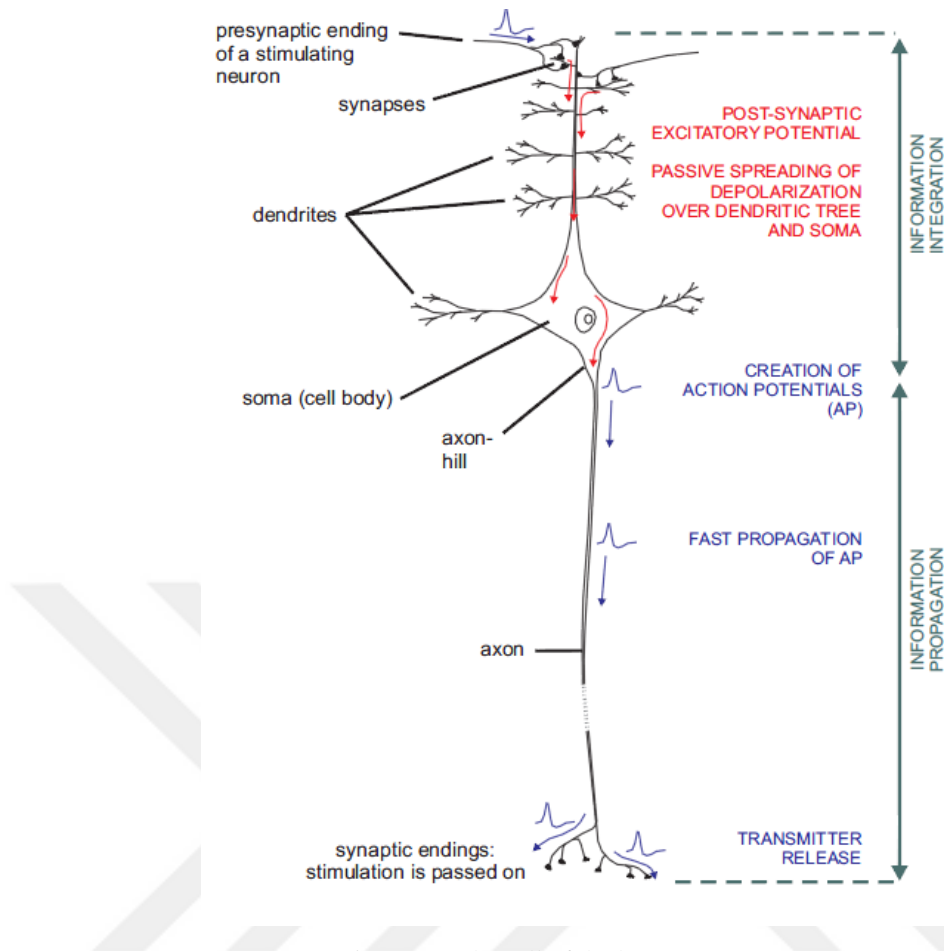


Figure 2.5 The cell of the human motor cortex.

The neuron is the basic unit and messenger of the peripheral nervous system. It is composed of four basic parts:

- soma (or cell body),
- dendrites,
- axon, and
- axon terminals.

The *soma* surrounds the nucleus. *Dendrites* sense information from neighboring cells. The *axon* can be part of the spinal cord, connect with muscle or sensory nerves, or branch into small fibers. The *axon terminals* branch off from the axon and send the action potential to nearby neurons.

CHAPTER THREE

BIOMEDICAL SIGNALS

The human body consists of the many systems. These are the nervous system, the cardiovascular system, and the musculoskeletal system. Each system is composed of subsystems that perform many physiological processes. For example, the cardiac system performs the rhythmic pumping of blood throughout the body to facilitate the delivery of nutrients, as well as pumping blood through the pulmonary system for oxygenation of the blood itself.

Physiological processes are including:

- Nervous or hormonal stimulation and control;
- Inputs and outputs that could be in the form of physical material,
- Neurotransmitters,
- Mechanical, electrical, or biochemical actions.

The physiological processes are described by the signals. These signals have many types; biochemical, electrical and physical. The signal reflects the form of hormones and neurotransmitters is called biochemical signals. The electrical signals reflect the form of potential or current. Also, the physical signals reflect the form of pressure or temperature.

3.1 Electroencephalogram (EEG)

EEG represents the electrical activity of the brain (Cox et al., 1972; Cooper et al., 1980; Kooi et al., 1978, Rangayyan 2002). The electrical activity in the brain was discovered in 1875 by an English physician Richard Caton. Caton observed the EEG signals of rabbits and monkeys.

In 1924 Hans Berger, a German neurologist, used his ordinary radio equipment to amplify the brain's electrical activity measured on the human scalp. He announced that weak electric currents generated in the brain can be recorded without opening the skull, and depicted graphically on a strip of paper.

The activity that he observed changed according to the functional status of the brain, such as in sleep, anesthesia, lack of oxygen and in certain neural diseases, such as in epilepsy.

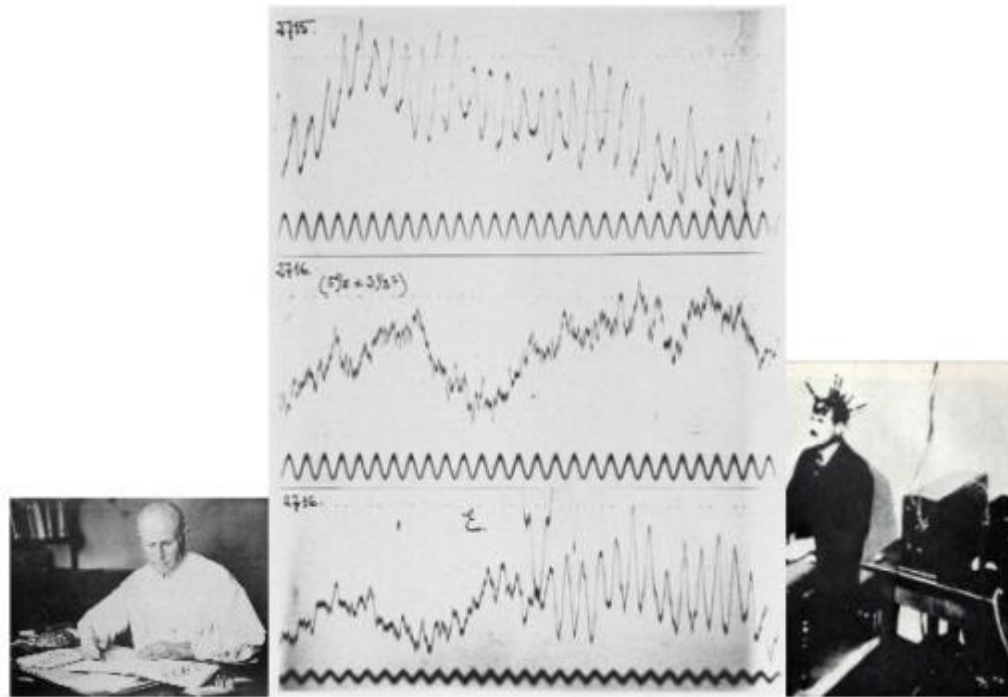


Figure 3.1 First recording of EEG signals made by Hans Berger (Berger, 1929).

Berger laid the foundations for many of the present applications of electroencephalography. He also used the word electroencephalogram as the first for describing brain electric potentials in humans. He was right with his suggestion that brain activity changes in a consistent and recognizable way when the general status of the subject changes, as from relaxation to alertness (Bronzino, 1995).

Later in 1934 Adrian & Matthews published the paper verifying concept of “human brain waves” and identified regular oscillations around 10 to 12 Hz which they termed “alpha rhythm” (Bronzino, 1995).

3.2 Measuring Brain Activity

The brain analysis is composed of structural and functional analysis. Structural analysis is used to analyze the anatomy of the brain, in order to find structural features. These could be tumors, hemorrhages, blood clots and lesions, or even deficits present at birth.

The magnetic resonance imaging (MRI) is the structural analysis method. Functional analysis is used to measure and locate brain activity. It is used for exploring the functions of special structures, and to diagnose epileptic seizures or diseases affecting brain activity.

The electroencephalography (EEG) and functional magnetic resonance imaging (fMRI) are used as functional analysis methods. Functional imaging is also used to aid surgical treatment of brain lesions when it becomes necessary to determine the locality of essential functional cortex to help guide the best surgical approach. Many times a structural and functional method will be used in conjunction to better assess how the activity and region are related.

The EEG and fMRI are two commonly used methods for investigating human brain states in cognitive neuroscience experiments. Both are noninvasive, but in other respects they are complimentary. EEG measures voltage changes in electrodes placed on the scalp (Figure 3.2), whose number ranges commonly from 32 to 256.

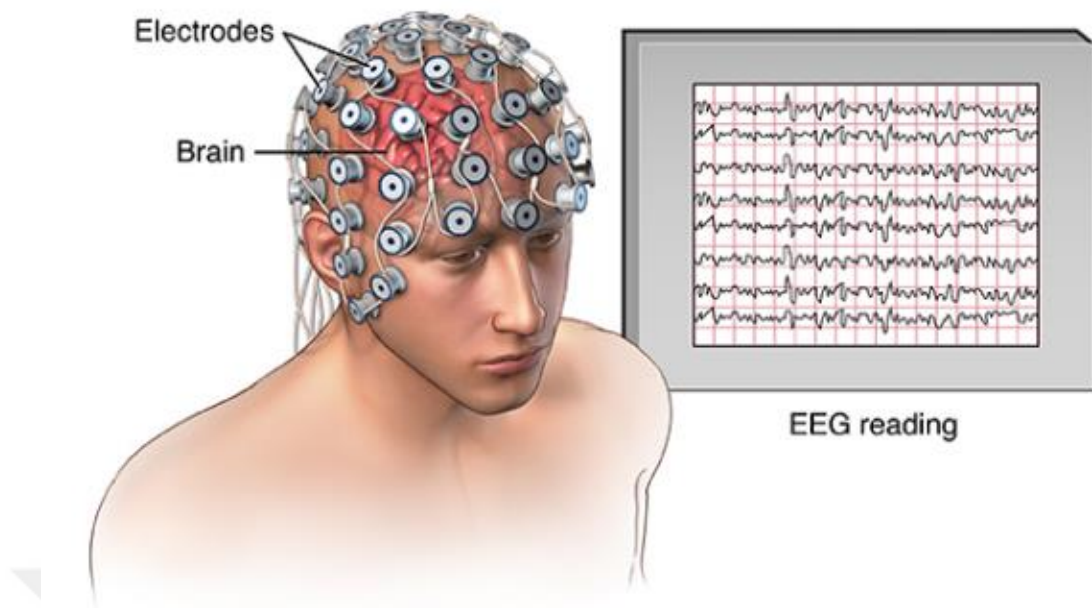


Figure 3.2 EEG sensing device.

EEG has millisecond time sensitivity, but spatial information must be inferred through an inversion process, and has at most as many independent spatial measurements as there are electrodes (Grave de Peralta Menendez et al., 2001).

The fMRI measures changes in blood oxygen level also called the BOLD signal, throughout the brain (Ogawa et al., 1990; Frahm et al., 1992). It produces a 3D image with a spatial resolution of roughly a few millimeters, but temporal resolution is on the order of a few seconds.

Furthermore the BOLD signal is a complicated convolution of brain activity because the blood oxygen level takes several seconds to rise and even longer to fall in response to an impulse of activity. Thus EEG provides an excellent measure of temporal dynamics but a poor measure of spatial locations, and fMRI provides an excellent measure of spatial locations but a poor measure of temporal dynamics.

3.3 Brain Waves

Brain patterns are commonly formed sinusoidal wave shapes. Usually, these signals are measured from peak to peak and normally range from 0.5 to 100 μV in amplitude. The power spectrum is derived from the raw EEG signal by the Fourier transform. The contribution of sine waves with different frequencies can be seen in power spectrum.

The brain waves have been categorized into basic groups as Delta, Theta, Alpha, Beta and Gamma (Table 3.1) (Teplan, 2002). For the detailed analysis in this work Beta signals are separated to Low, Midrange and High frequency bands.

Table 3.1 Brain wave frequencies (Teplan, 2002)

Brainwave Type	Frequency Range	Mental States and Conditions
Delta	0.1 Hz. to 3 Hz.	Deep, dreamless sleep, NON-Rem sleep, unconscious
Theta	4 Hz. to 7 Hz.	Intuitive, creative, recall, fantasy, imaginary, dream
Alpha	8 Hz. to 12 Hz.	Relaxed, but not drowsy, tranquil, conscious
Low Beta	12 Hz. to 15 Hz.	Formerly SMR, relaxed yet focused, integrated
Midrange Beta	16 Hz. to 20 Hz.	Thinking, aware of self & surroundings
High Beta	21 Hz. to 30 Hz.	Alertness, agitation
Gamma	30 Hz. to 100 Hz.	Motor functions, higher mental activity

Delta (0.1 – 3 Hz): Delta waves are between 0.1 Hz and 3 Hz frequency range (Figure 3.3). Delta waves are usually associated with the deep sleep. Sleep is generally divided into two types: non-rapid eye movement sleeps (NREM) and REM sleep. NREM and REM occur in alternating cycles. NREM is further divided into stage I, stage II, stage III, and stage IV. The last two stages correspond to deeper sleep, where slow delta waves show higher proportions.

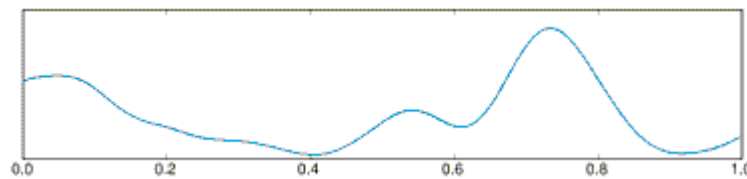


Figure 3.3 Delta wave

Theta (4 - 7 Hz): Theta waves are between 4 Hz and 7 Hz frequency range (Figure 3.4). Theta activity is seen in drowsiness, arousal and often during meditation. Dominant Theta activity is associated with relaxed, meditative, and creative states, memory recall and flow states.

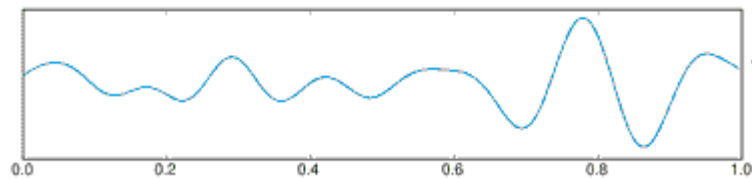


Figure 3.4 Theta wave

Alpha (8 - 12 Hz): Alpha waves are between 8 Hz and 12 Hz frequency range (Figure 3.5). Alpha activity is induced when closing the eyes and relaxation, and abolished by eye opening or alerting by any mechanism (e.g. thinking, mathematical calculations) (Teplan, 2002). Most of people, when close their eyes their wave pattern significantly changes from beta into alpha waves.

High Alpha levels appear in the frontal lobes during relaxation and are suppressed when other activities take place. It is quite common in EEG signal analysis to compare the Alpha suppression between different regions in order to determine the functional areas which are currently in use. For example, linguistic processing tends to depress Alpha activity in the left frontal lobe, while abstract spatial thinking can suppress Alpha in the right frontal lobe. Trained meditators often produce much higher levels of Alpha activity during normal activities, especially in the frontal lobes.

Similar rhythms in the motor cortex called as Mu-rhythms which around the same frequency range indicate muscle relaxation. Suppression of Mu-rhythms in the motor cortex in specific regions corresponds with activation of particular muscle groups. For example, clenching your right fist is directly associated with a dip in Mu-rhythm near the F3 sensor on the left side of the head.

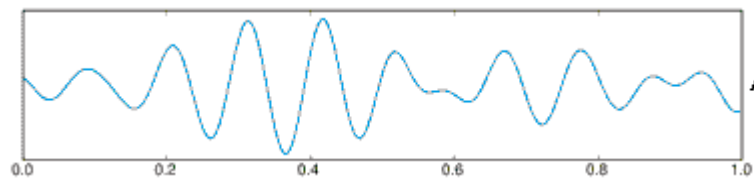


Figure 3.5 Alpha wave

Beta (12 - 30Hz): Beta waves are between 12 Hz and 30 Hz frequency range (Figure 3.6). Beta wave is the terms used to designate the frequency range of human brain activity between 12 and 30Hz.

Beta activity of multiple and varying frequencies is often associated with active, task-oriented, busy or anxious thinking and active concentration. Beta waves can be separated to three parts: Low Beta, Midrange Beta and High Beta. The low beta waves are between 12 Hz and 15 Hz frequency range.

It is active, when people relaxed yet focused, formerly SMR and integrated situations. The midrange beta waves are between 16 Hz and 20 Hz frequency range. It is active in thinking, aware of self and surroundings situations. The high beta waves are between 21 Hz and 30 Hz frequency range. It is active in alertness and agitation situations.

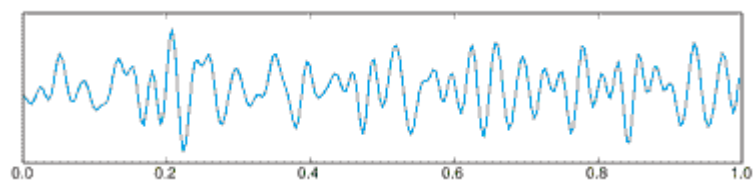


Figure 3.6 Beta wave

Gamma (> 30Hz): Gamma waves are higher than 30 Hz frequency range (Figure 3.7). Gamma rhythms occur when different populations of neurons network together to carry out demanding cognitive or motor functions.

Generally Gamma waves are observed in the frontal regions when fast, coupled processing is required, such as in fight/flight mode and when task switching during multi-tasking. In task switching, Gamma bursts are clearly evident when the current

task is archived to short term memory and a new task is retrieved for 'concurrent' processing.

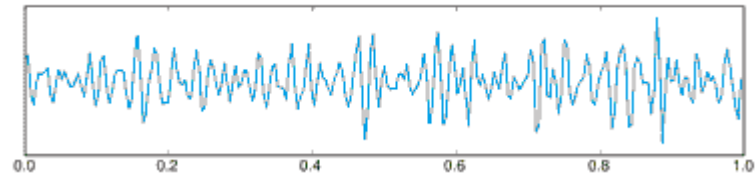


Figure 3.7 Gamma wave

CHAPTER FOUR

BRAIN COMPUTER INTERFACE

BCI is a communication system that recognizes user's command only from his or her brainwaves and feedback according to commands. For this purpose subject is trained. Simple task can consist of desired motion of an arrow displayed on the screen only through subject's imaginary of the motion of his/her left or right hand. As the consequence of imaging process, certain characteristics of the brainwaves are raised and can be used for user's command recognition.

4.1 The Structure of the BCI

BCI Technology composed of four basic processes: recording the raw EEG signals as *signal acquisition*, removing noises as *signal preprocessing*, extraction of the intended action or desired features from the mental activity as *feature extraction*, and finally *classification* of the desired features.

1. EEG Data Acquisition: The effectively acquisition of the brain signal is the most important phases of the brain computer interface system communication. Human thoughts produce the electrical activities. These activities could be measured many types of EEG devices. The measured electrical activities are analog signals and analog signals are converted to the digital signals. In this thesis, EEG signals are captured by the Emotiv Epoc Neuroheadset.

2. Signal Preprocessing: The EEG signals are affected from the environment sounds, eye movement and muscle movements. Because of the outside effects, the noises called as artifacts, are occurred in the captured EEG signal. Therefore, the preprocessing is required for the removing these artifacts. In the preprocessing phase, the recorded data is cleaned and purified from the noisy data (Bashashati et al. 2007). After the preprocessing, the quality of the data is improved.

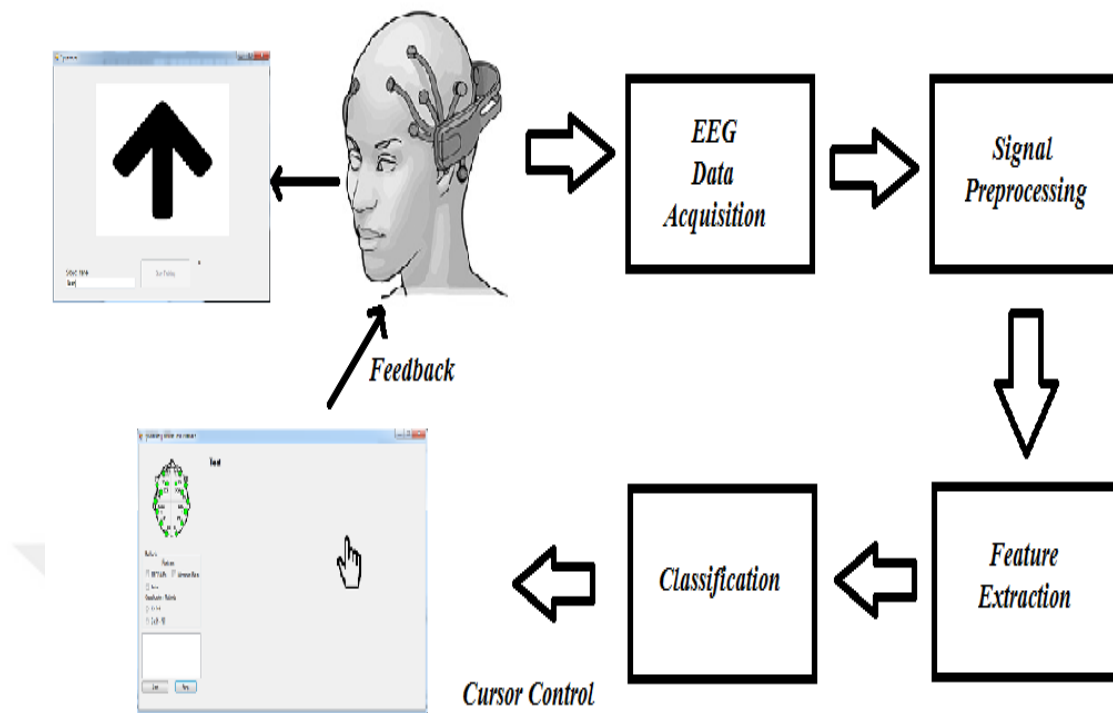


Figure 4.1 The flow of the BCI system.

3. Feature Extraction: EEG signals are very complex and the patterns are not recognized easily. In this phase, feature extraction methods extract the signal features that encode the user's messages or commands. Thus, the raw EEG signals have been characterized by the features. The feature extraction phase is very important because of the effective classification results. Also, dimension of the features are lower than the dimension of the raw EEG signal. So, we avoid from the curse of the dimensionality.

4. Classification: In the classification phase, the extracted specific features are assigned to the accurate classes. The classes are defined as the type of cognitive states. There are the supervised and unsupervised methods. When the classes are known, the supervised classifiers are used; otherwise the unsupervised classifiers are used for the classification of the EEG signal.

5. Feedback: Finally, in this phase the feedback according to the identified cognitive task is provided to the participant. The goal of the feedback is that helping the control brain activity of the participant.



CHAPTER FIVE

DATA

The EEG signals can be captured through invasive and non-invasive methods. The invasive methods require surgery, therefore this method do not preferred. There are many non-invasive devices for measuring EEG signals. In this thesis, the Emotiv Epoc Neuroheadset is used for capturing EEG signals.

5.1 Data Acquisition

The raw EEG signals are recorded using an Emotiv Epoc amplifier device (Figure 5.1). Signals were measured from 14 EEG channels plus 2 references (CMS/DRL references, P3/P4 locations) offering optimal positioning for accurate spatial resolution.



Figure 5.1 Emotiv Epoch device.

Channel names based on the international 10-20 electrode location system are: AF3, F7, F3, FC5, T7, P7, O1, O2, P8, T8, FC6, F4, F8, AF4, with CMS/DRL references in the P3/P4 locations (Figure 5.2).

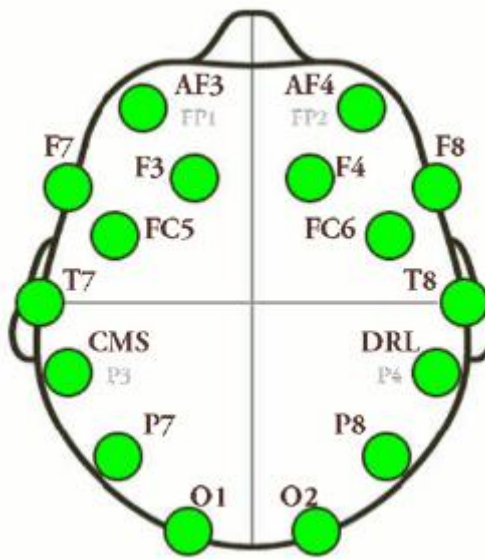


Figure 5.2 Emotiv electrode locations.

The 10–20 system or International 10–20 system is an internationally recognized method to describe and apply the location of scalp electrodes in the context of an EEG test or experiment. This method was developed to ensure standardized reproducibility so that a subject's studies could be compared over time and subjects could be compared to each other. This system is based on the relationship between the location of an electrode and the underlying area of cerebral cortex. The "10" and "20" refer to the fact that the actual distances between adjacent electrodes are either 10% or 20% of the total front–back or right–left distance of the skull.

Each part has a letter to identify the lobe and a number to identify the hemisphere location. The letters F, T, C, P and O mean as frontal, temporal, central, parietal, and occipital lobes, respectively.

Emotiv EPOC uses sequential sampling method, single ADC, at a rate of 128 SPS. It operates at a resolution of 14 bits per channel with frequency response between 0.16 - 43 Hz. The Emotiv Epoc System comprises of a built-in digital 5th order sinc filter with a bandwidth of 0.2-45 Hz and a digital notch filter at 50 and 60 Hz.

5.2 Training Experiments

The first step toward to classification of the cognitive states, is training of the subjects. The dataset accumulated during the subject trains itself to generate cognitive states. The visual stimuli is used in this study to provide instructions to the subject on the mental task he has to perform during the training phase. The visual cue contains instructions for five mental commands: Up, Down, Left, Right and No Movement in form of direction of an arrow and blank screen, as shown in Fig.5.3 (Bhattacharyya et al., 2015).

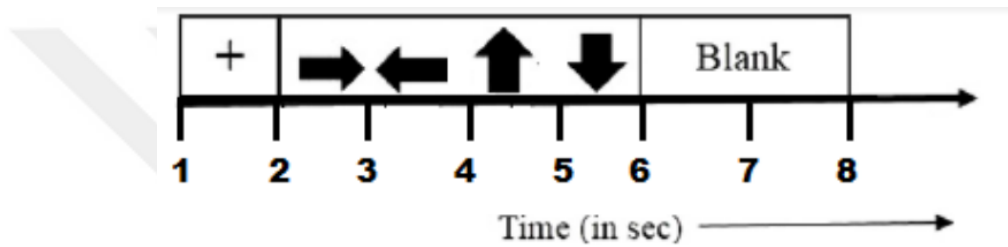


Figure 5.3 Timing diagram of a motor imagery trial performed by the subject. The direction of the arrows provides instruction to the subject (Bhattacharyya et al., 2015).

The subject is relaxing before the training. In the visual stimuli, when plus image appeared the subject knowing that the training will start. When the arrows appear, the subject both follows the arrows and thinks the control right hand according to the arrow rotation. In the blank screen, the subject thinks nothing. There is the breaks two second between each training. In a section, each training is repeated 24 times. Also, trainings of subject is undertaken over 3 different sessions and one session is performed on a single day.

5.3 Data Preprocessing

The EEG signals have many noises because of the various out affects, such as eye movement, head movement and the noises comes from the test environment. In the signal processing, many kinds of noise reduction methods are commonly used. In this thesis dissertation, median filtering and normalization is used for the preprocessing.

5.3.1 Median Filtering

The median filtering as a nonlinear digital filtering technique is used for the removing noises for improving the results of later processing. The median filtering is commonly used in signal processing because certain conditions, it maintains edges while removing noise.

The median is the middle value of the data. In the calculation of the median filtering, all values in all rows are sorted in ascending order and then the middle value is found. If the sorted count is even, This values calculated from the all rows are subtracted from each value.

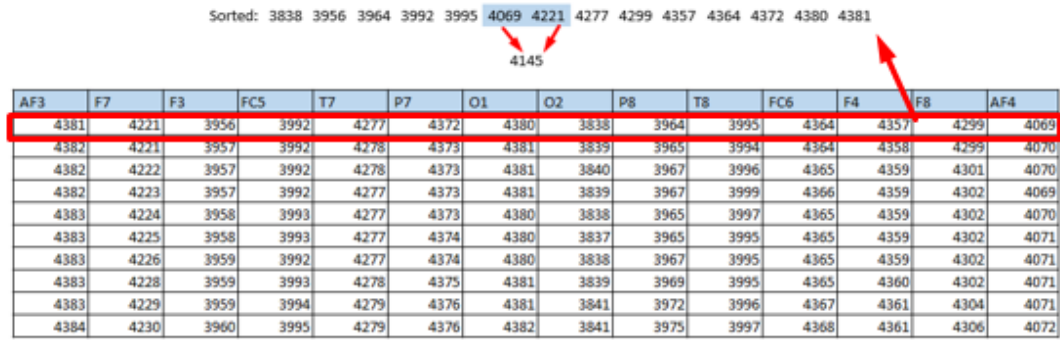


Figure 5.4 Median filtering example.

5.3.2 Normalization

The normalization is commonly used as a preprocessing method in biomedical signals. The normalization process transforms the measured data to a new interval from new minimum value to new maximum value for feature F. The basic formula is give by equation 5.1 .

$$v' = \frac{v - \min_F}{\max_F - \min_F} (\text{new_max}_F - \text{new_min}_F) + \text{new_min}_F \quad (5.1)$$

where v is the current value of feature F.

CHAPTER SIX

SOFTWARES

In this thesis, Emotiv Epoc Neuroheadset and our developed software Sycamore are used for acquisition of the raw EEG signal. The training studies are done both in Emotive control panel and our software program which is written in c# language. The analysis and online tests are carried on through our Sycamore software.

6.1 Emotiv Epoc Neuroheadset Software

The Emotive Headset Setup is opened by default when starting EPOC Control Panel (Figure 6.1). This screen is used to display contact quality of EPOC Neuroheadset's sensors and provide guidance to user in fitting the EPOC Neuroheadset correctly.

Achieving best results is possible with the contact quality. It is important that controlling the contact quality before starting to cognitive process. Poor contact quality will give poor detection results.

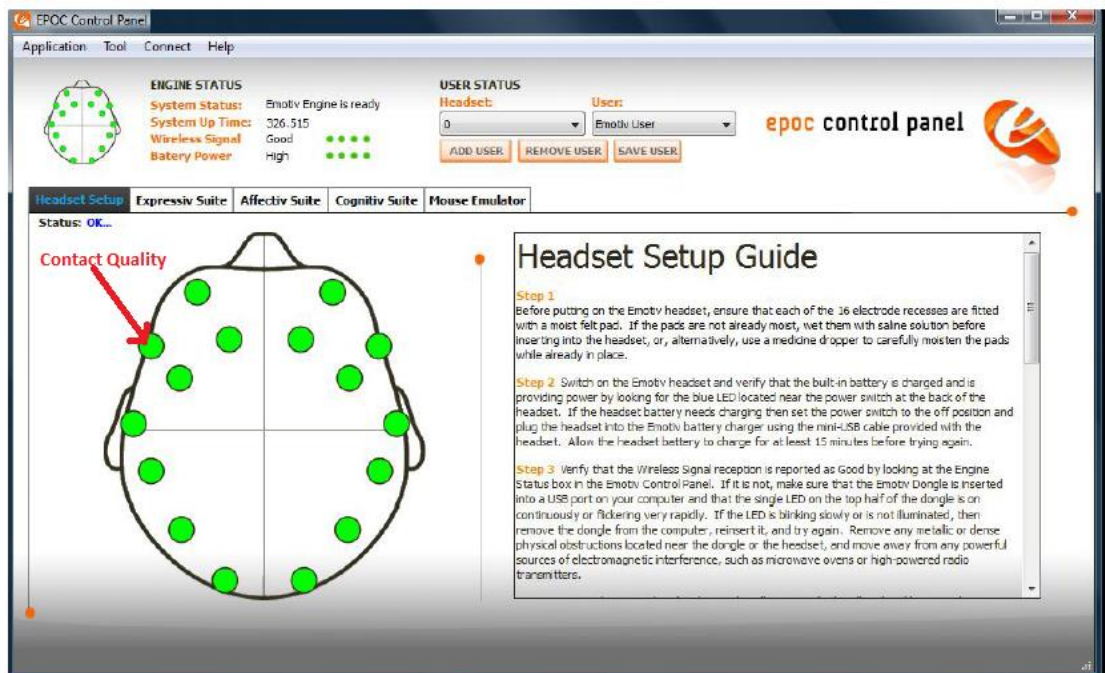


Figure 6.1 Emotiv Epoc control panel

The left side image is display the representation of the sensor and contact quality. Each circle represent one sensor and approximate location. The sensor colors give the contact quality. To achieve the the best signal, all sensors should be green.

Sensor colors indicate following results:

- Black : No Signal (Not Acceptable)
- Red : Very Poor Signal (Not Acceptable)
- Orange : Poor Signal
- Yellow : Fair Signal
- Green : Good Signal (Ideal Signal)

Green and some yellows can be acceptable but green and black/orange/red can not acceptable.

6.1.1 Training Program

The Cognitive Suite panel is used for the training phase (Figure 6.2). This panel uses a virtual 3D cube to display an animated representation of the detected commands. The real time brainwave activity of the user is evaluated for physical actions of real or virtual object according to user cognitive intent.

The detection is performed for 13 different cognitive actions: 6 directional movements (pull, push, left, right, up adn down) and 6 rotations (clockwise, counter-clockwise, left, right, forward, backward) and one additional action as disappear. The cognitive suit allows 4 action option to the user.

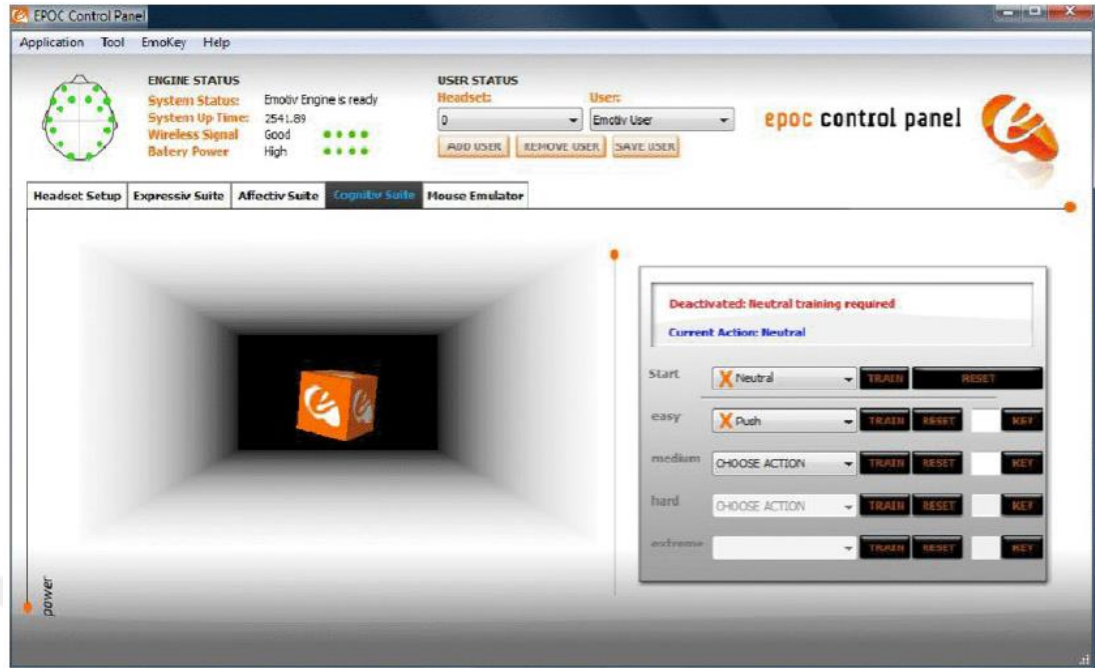


Figure 6.2 Emotive Cognitive Suite for training.

6.1.2 TestBench

Data set is recording by the Emotiv Epoc Test Bench. Emotiv neuro headset captures users' brainwave signals. Test Bench application independently collects data packets from the USB device and processes them to display, analyse, record and play-back time independent EEG signals (Figure 6.3).

The left side of TestBench Panel is the TestBench Status Pane. This pane shows neuroheadset sensor contact quality. It also exposes other functions which are described below.

The EEG Suite reports real time changes in the subjective emotional experiences by the users. EEG shows brainwave signals of 14 channels (AF3, F7, F3, FC5, T7, P7, O1, O2, P8, T8, FC6, F4, F8, AF4).

In this section, the users can choose to display one or more channels, and if users choose to display one channel, you can use AutoScale button. The main function of AutoScale button is automatic alignment of the upper and lower limits consistent

with the current channel values. You can set the vertical scale when more than one channel is displayed by changing the Channel Spacing value, which changes the vertical scale so that the difference between successive channel displays is equal to the number displayed in the box (to double the vertical resolution, change the number to 100 μ V).

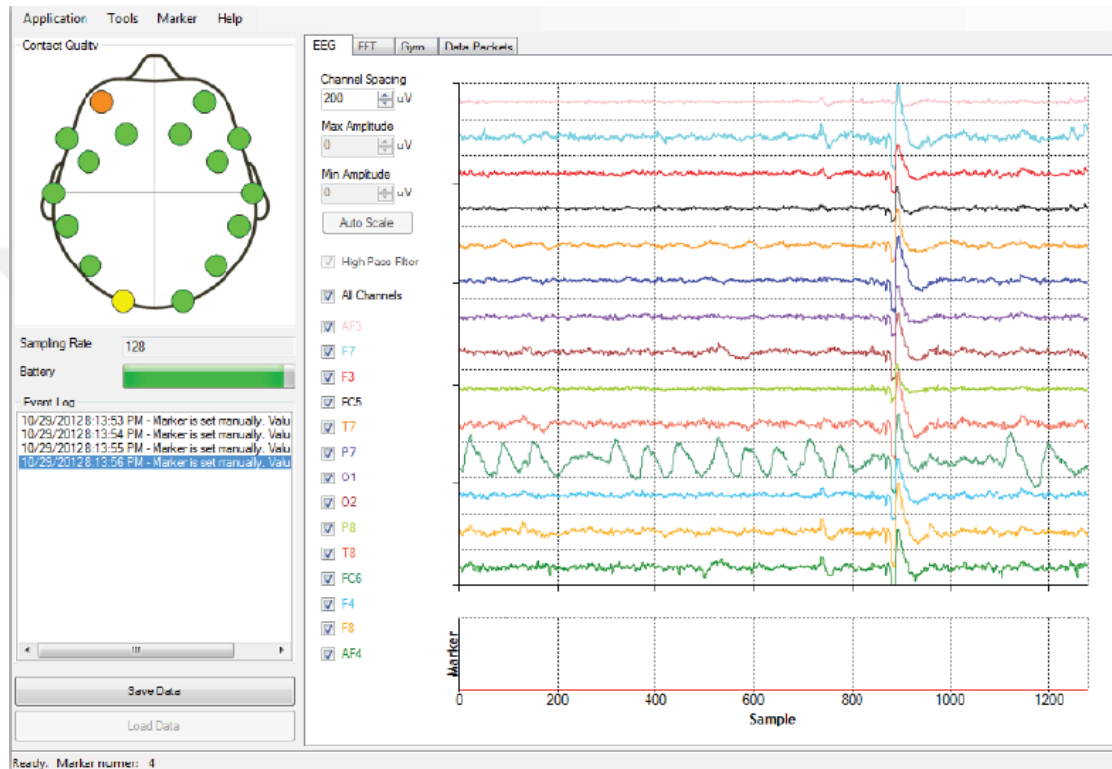


Figure 6.3 Emotiv Test Bench display showing EEG suite.

The FFT Suite shows EEG graph in the frequency domain and the power of signal in the frequency band. The FFT panel consists of a series of graphs. The first graph shows the FFT signal of a selected channel.

The second graph displays the power of a signal in specific frequency bands: Delta (0.1-3Hz); Theta (4-7Hz); Alpha (8-12Hz); Beta (12-30Hz); and one user-defined Custom band.

The function buttons changing the parameters of the graphs are in the left side of the FFT panel (Figure 6.4).

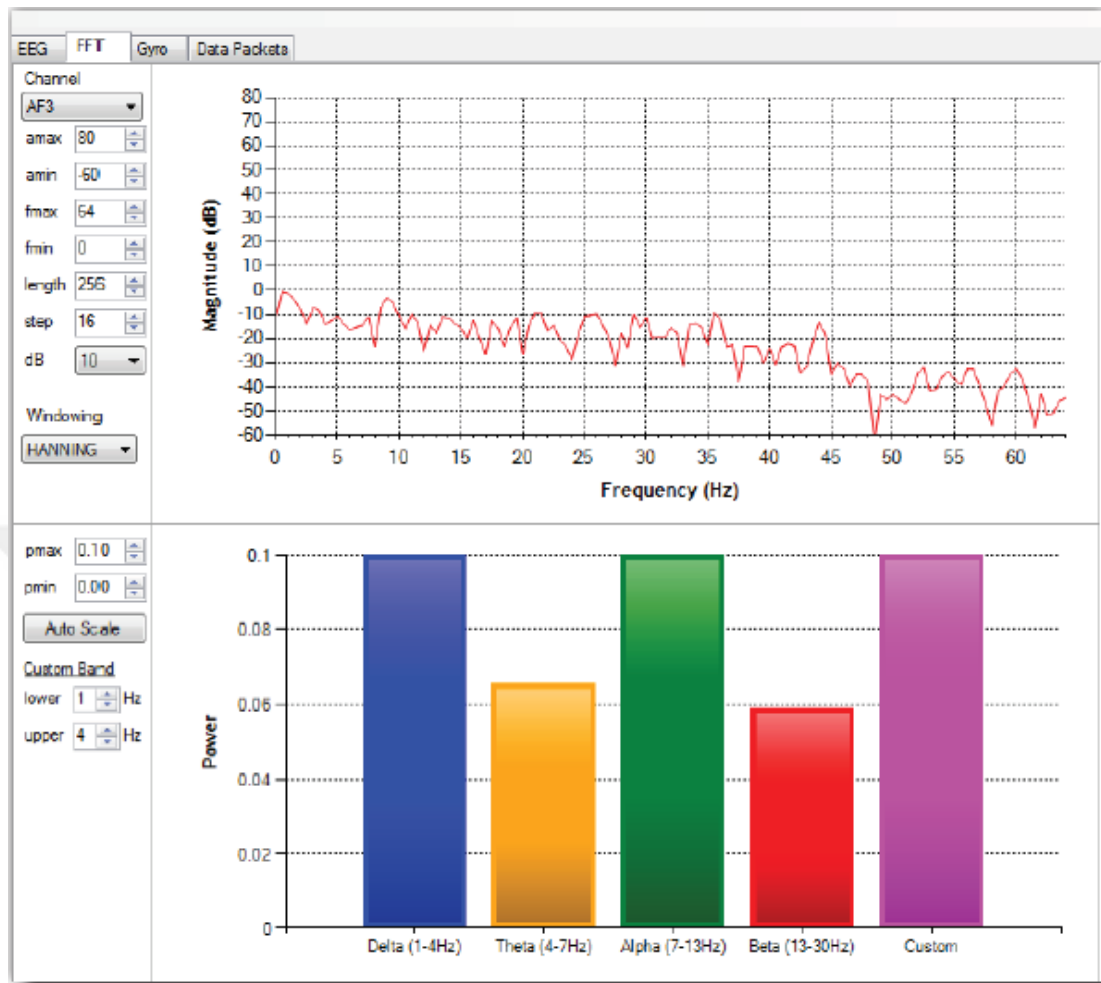


Figure 6.4 Emotiv FFT suit

The Gyro Suite displays the rotational acceleration of the head in horizontal and vertical axes (Figure 6.5). The gyro data used for the head movement based applications.

The graph has two signal lines:

Gyro X: the upper signal shows signal moving in the horizontal axis

Gyro Y: the lower signal shows signal moving in the vertical axis

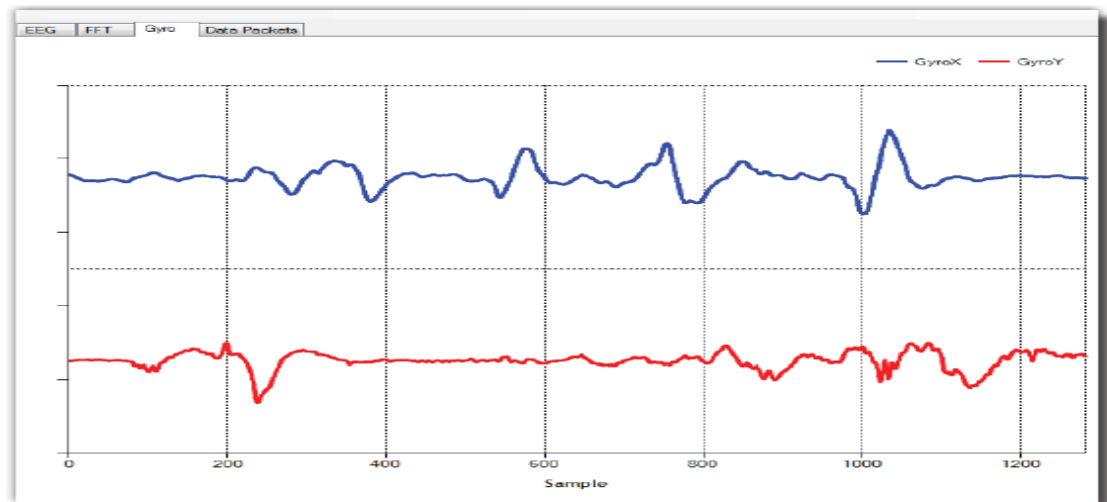


Figure 6.5 Emotiv gyro suit

The Data Packets Suite shows the data packet counter and the lost packet indicator (Figure 6.6). The wireless drop-outs can be clearly seen from this panel. The graphs display the clearly reading signals and the number of packet lost, respectively.

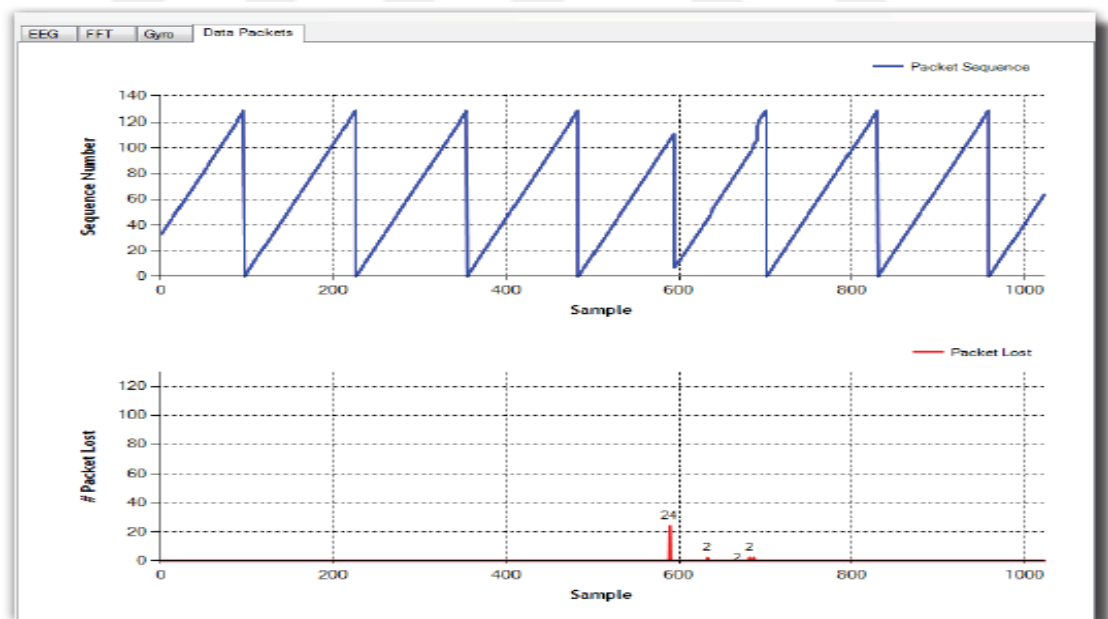


Figure 6.6 Emotiv data packet counter and packet loss display

Data File Format:

Data is saved by TestBench in a standard binary format, EDF, which is compatible with many EEG analysis programs such as EEGLab. Following the initial information line, each successive row in the data file corresponds to one data sample, or 1/128 second time slice of data.

Successive rows correspond to successive time slices, so for example one second of data is contained in 128 rows. Each column of the data file corresponds to an individual sensor location or other information tag.

Data tag descriptions:

COUNTER : The counter is used as a timebase, and runs from 0 to 128.

INTERPOLATED: It shows if a packet was dropped and it gives the interpolated value from surrounding values. When the interpolated value is equals to zero, this means the sample was good.

AF3..AF4 : EEG channels data.

RAW_CQ: This is a multiplexed conductivity measurement used to derive the contact quality indicator lights. It is possible to demultiplex this channel if more accurate conductivity measurements are required.

CQ_A F3..CQ_A F4: These numbers show the colour of the each channel's signal quality, where 0=BLACK, 1 =RED, 2=ORANGE, 3=YELLOW, 4=GREEN.

CQ_CMS, CQ_DRL: I gives the contact quality of the referance locations. The values 1 and 4 mean RED and GREEN respectively.

GYROX, GYROY: Horizontal and vertical difference readings since the previous sample.

MARKER: Timing markers manually or automatically entered in the file. If no marker was detected at the particular timing sample, a value of zero is added into the file, otherwise the number associated with the marker button, or the byte transmitted to the COM port, is entered in the MARKER column for that sample.

6.2 Sycamore BCI Software

In this thesis, the software Sycamore is developed for training, analyses and testing processes. The test screen is designed as below (Figure 6.7) :

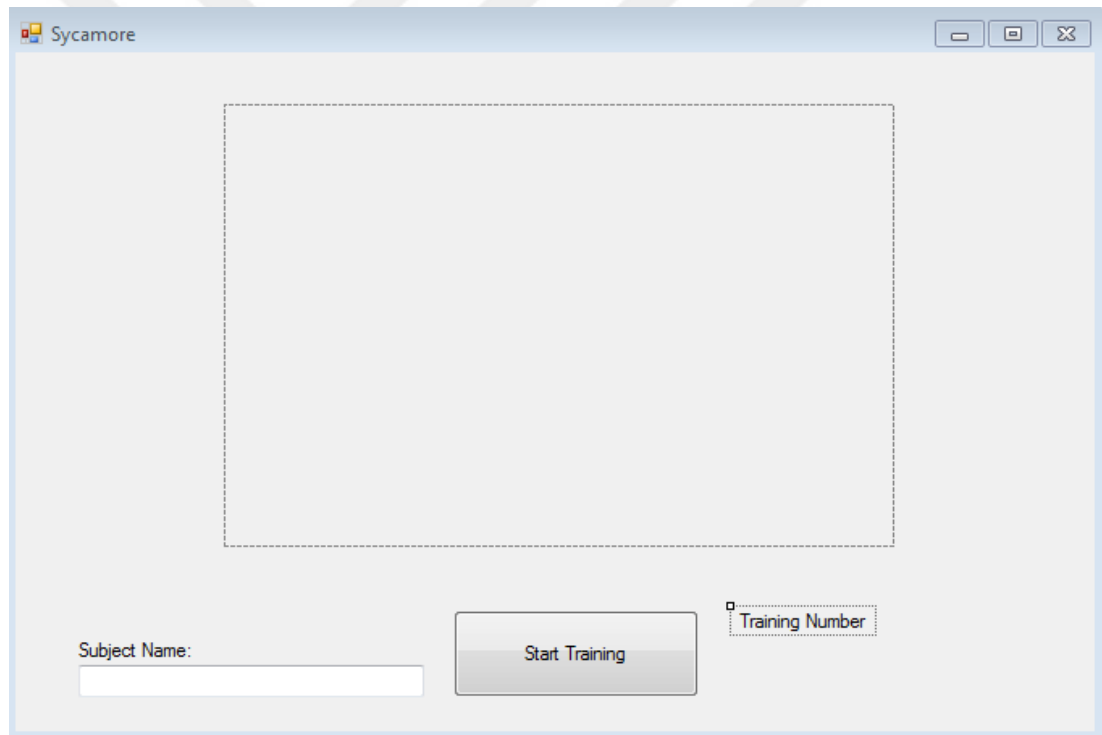


Figure 6.7 Sycamore training screen.

First, the user name of the participant has been written to “Subject Name” field and then push the “Start Training” button. The “Training Number” field shows the training number. In this study, each image is displayed for 1 sec and the black screen is displayed for 2 sec among the trainings because of the resting brain.

In the noiseless room, participants are seated in the chair and the training process is explained to them. The training process starts with the plus image, means “training will start and be ready” (Figure 6.8).

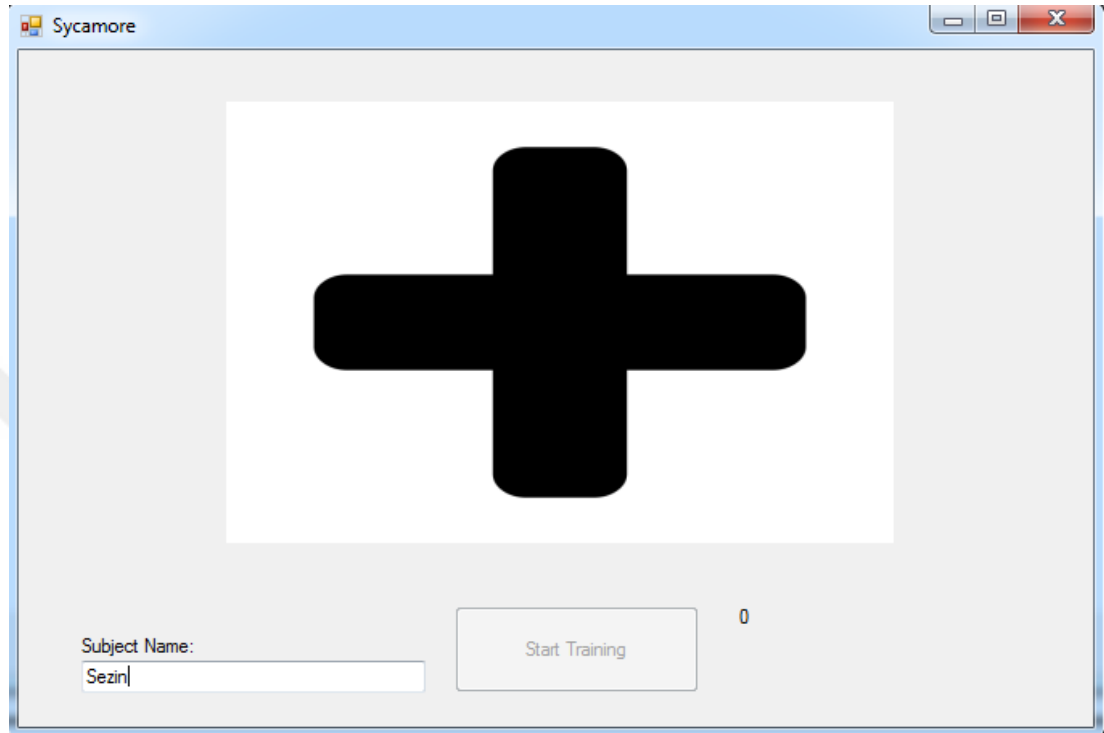


Figure 6.8 Sycamore starting image of training screen.

After the starting image “Plus”, training screen shows the mental task images with a random order (Figure 6.9-6.13). The participants are thinking the cognitive tasks left, right, up, down and no movement, while they are watching the corresponding images.

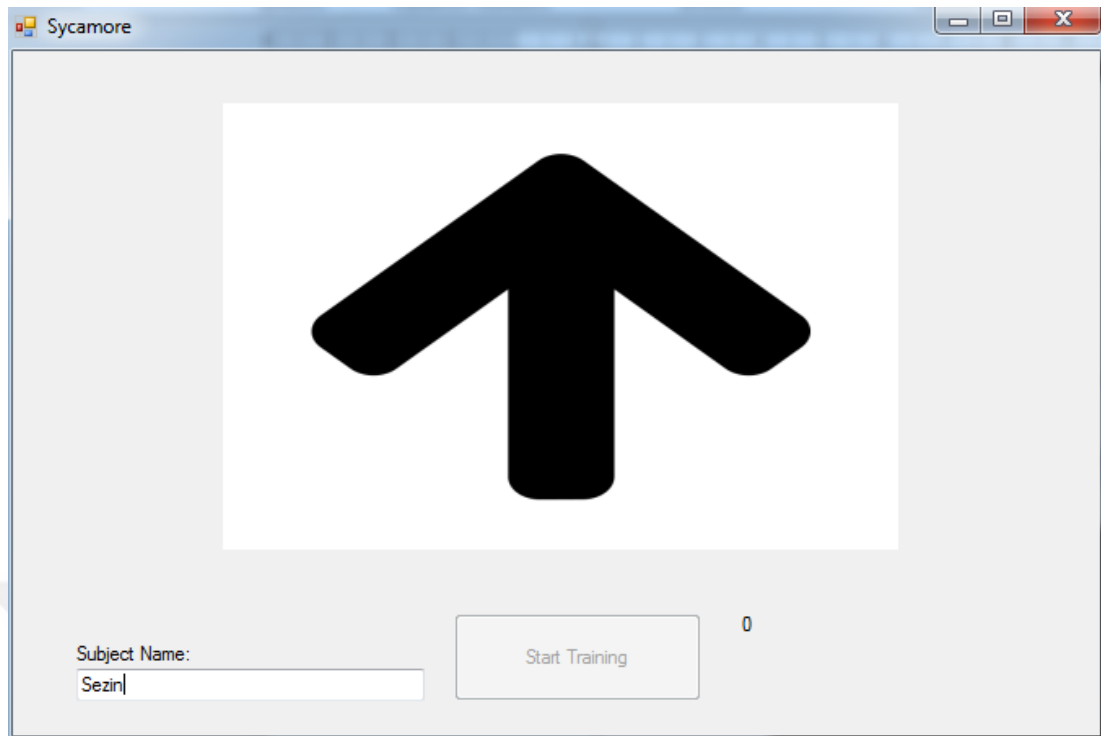


Figure 6.9 Sycamore up image of training screen.

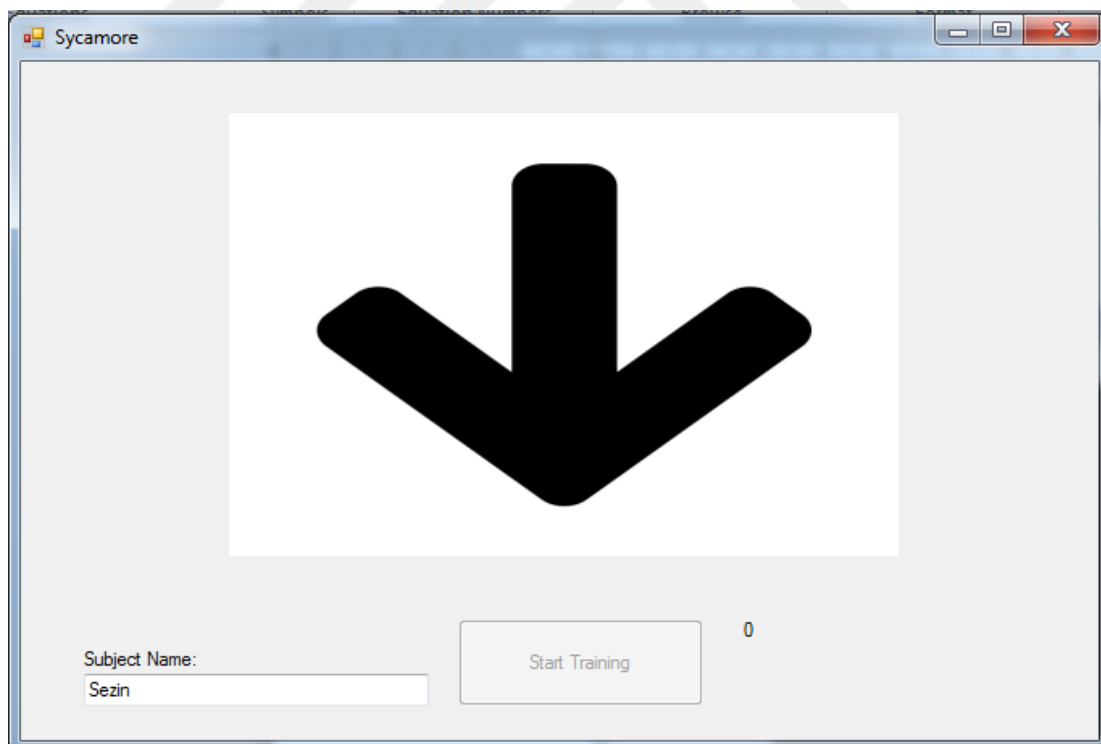


Figure 6.10 Sycamore down image of training screen.

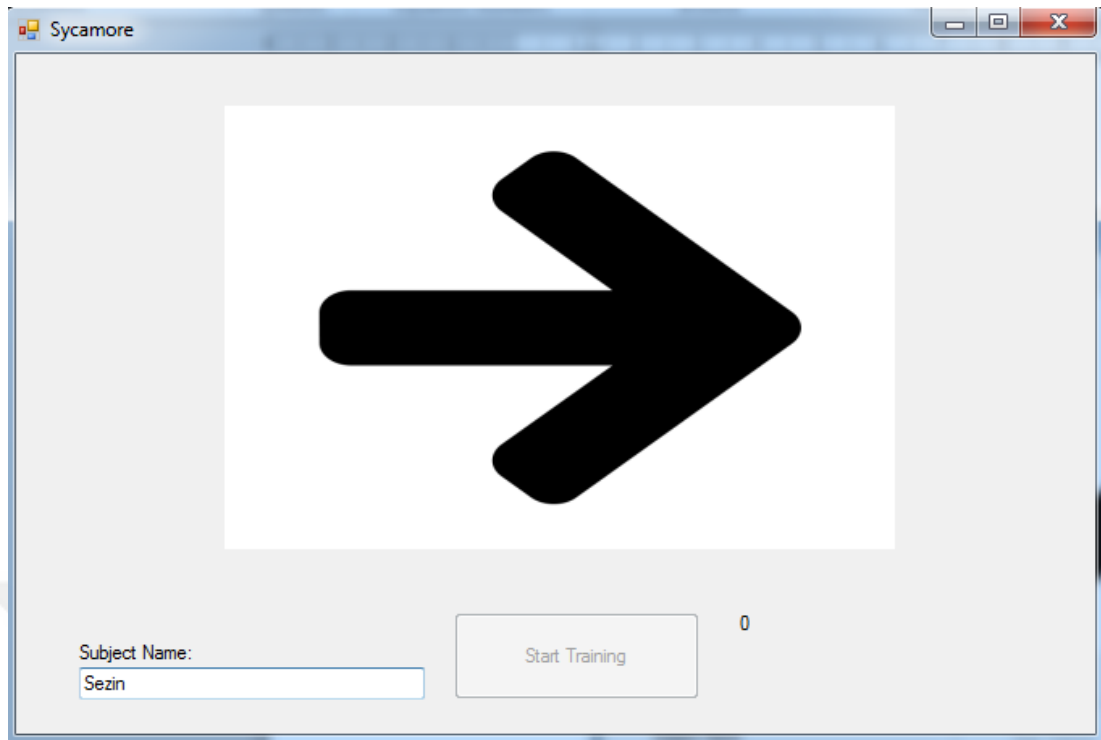


Figure 6.11 Sycamore right image of training screen.

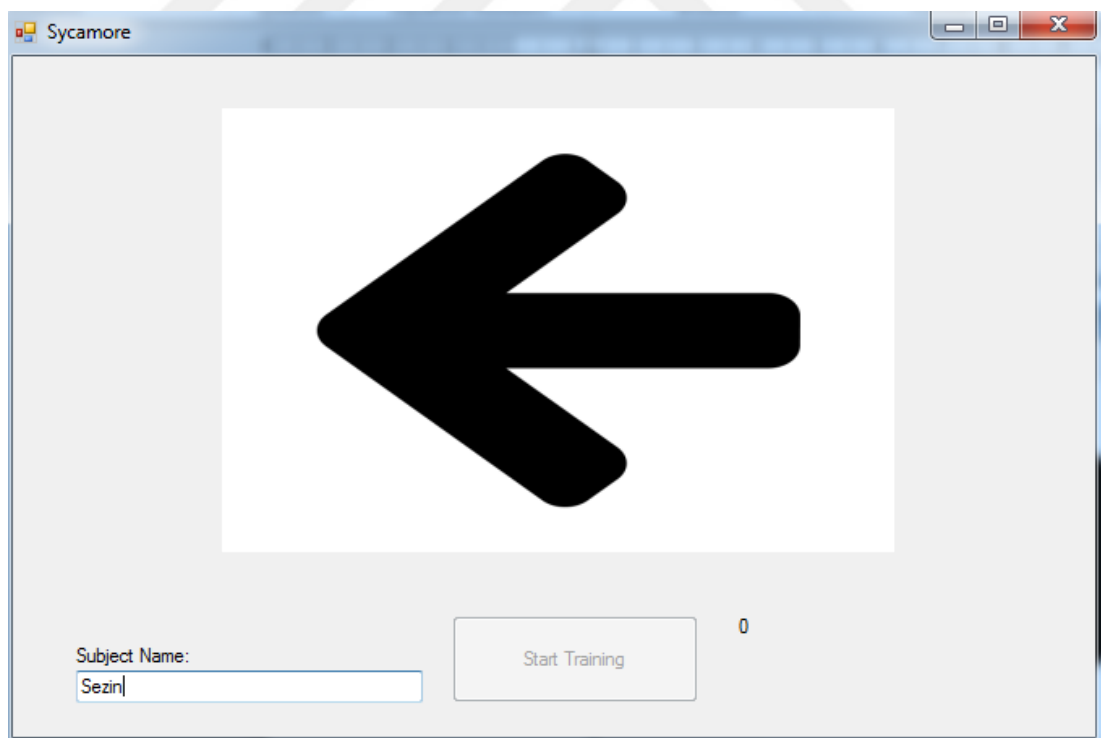


Figure 6.12 Sycamore left image of training screen.

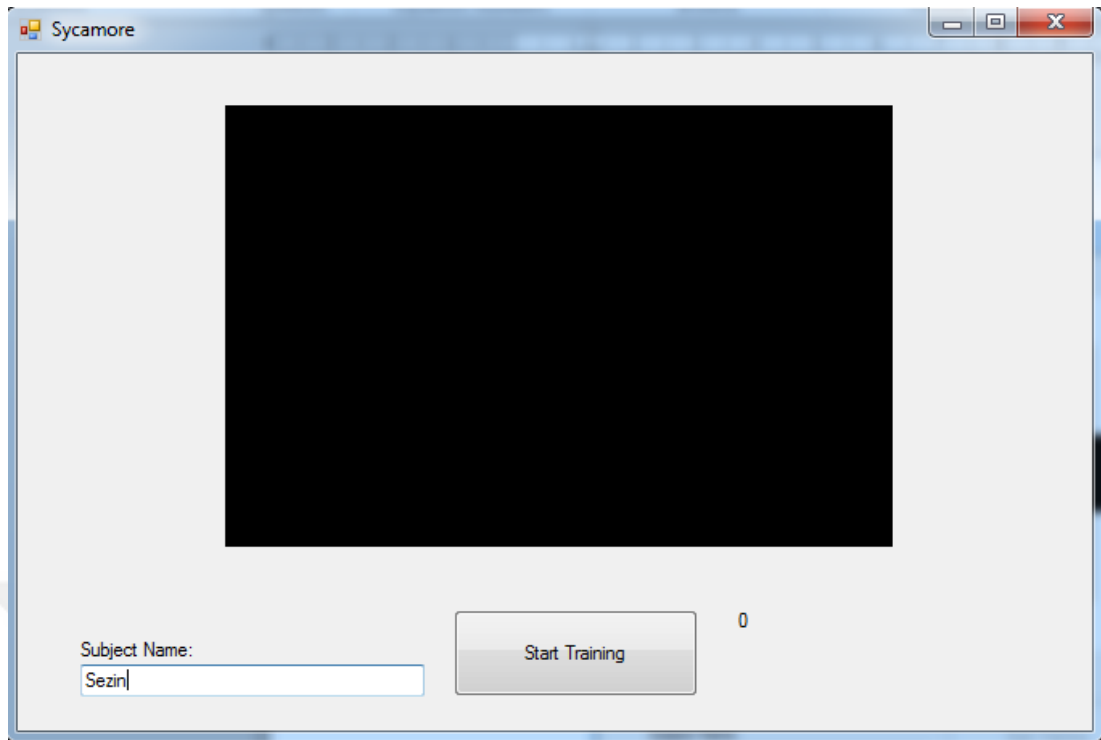


Figure 6.13 Sycamore no movement image of training screen.

The statistical similarity of the training data is measured by the following screen. The Z_m values are calculated for cognitive tasks.

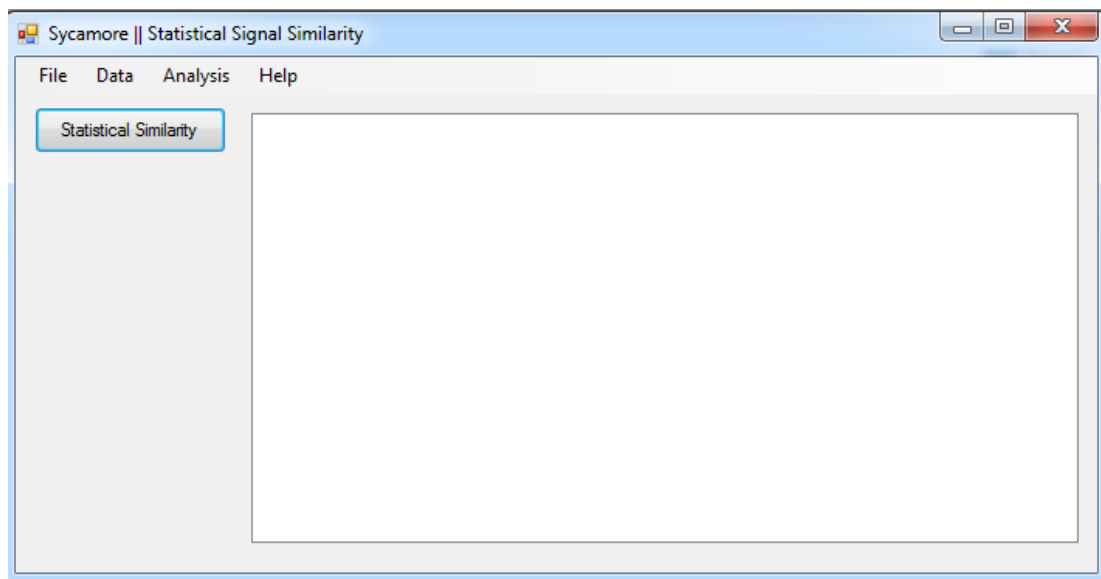


Figure 6.14 Sycamore statistical similarity calculation screen.

The multifractal detrended fluctuation analysis is calculated with the below window (Figure 6.15). The initial parameters scale, q order and signal are inserted to the corresponding fields and then mfdfa algorithm can be run.

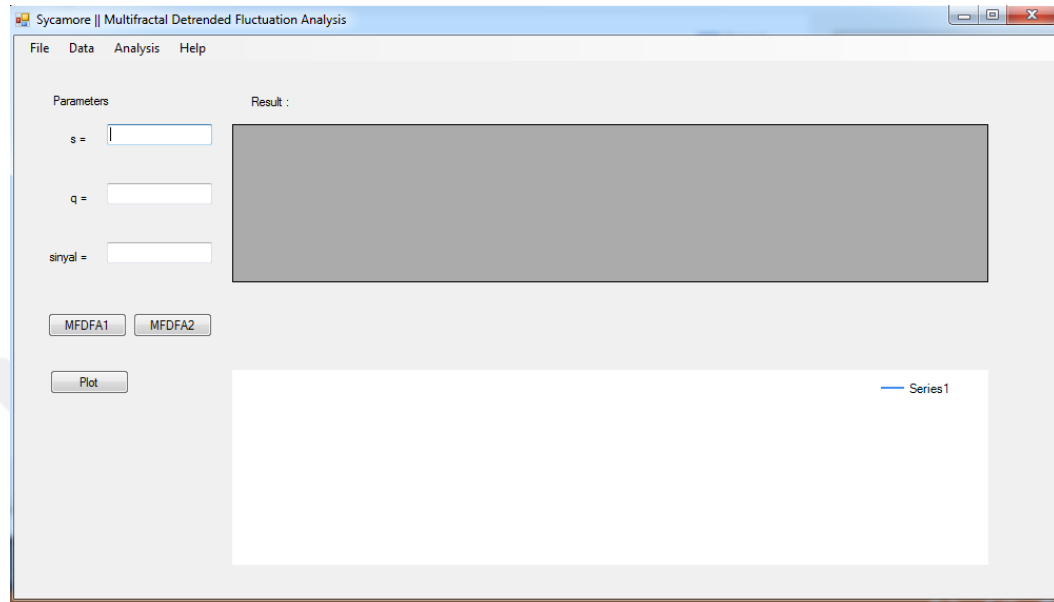


Figure 6.15 Sycamore MFDFA calculation screen.

In the online test screen, participants wear the Emotiv Epoc neuroheadset and captured signals are classified with the K-nearest neighbor and CxK-nearest neighbor algorithm according to extracted features (Figure 6.16). In the left side of the screen, electrode locations are displayed, and the feature extraction and classification method options are listed.

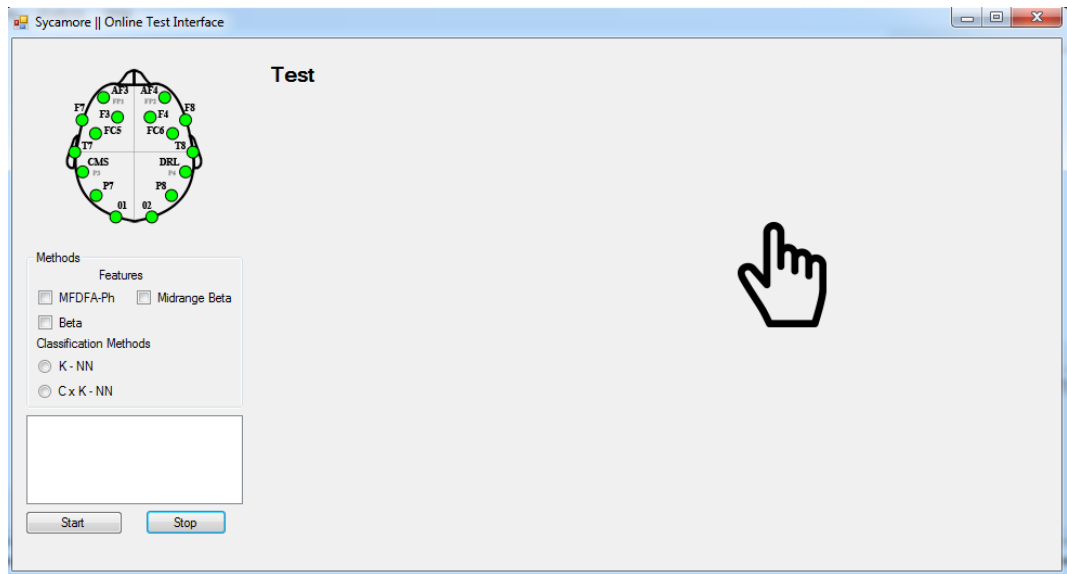


Figure 6.16 Sycamore BCI online test screen.

CHAPTER SEVEN

FEATURE EXTRACTION METHODS

The feature extraction of the specific features is the most important phase in BCI because of the complexity of the EEG signals. Different mental tasks have different characteristics. The feature vector consists of this specific information about the different mental tasks.

7.1 Multifractal Detrended Fluctuation analysis

In recent years the detrended fluctuation analysis (DFA) method (Kantelhardt et al., 2002) has become a widely-used technique for the determination of (mono-) fractal scaling properties and the detection of long-range correlations in noisy, nonstationary time series (Taqqu et al., 1995; Kantelhardt et al., 2001). It has successfully been applied to diverse fields such as DNA sequences (Buldyrev et al., 1998), heart rate dynamics (Ashkenazy et al., 2001), neuron spiking (Bahar et al., 2001), human gait (Hausdorff et al., 1997), long-time weather records (Talkner & Weber, 2000), economics time series (Mantegna & Stanley, 2000). One reason to employ the DFA method is to avoid spurious detection of correlations that are artifacts of non-stationarities in the time series.

Different mental tasks have different characteristics. The feature vector consists of this specific information about the different mental tasks.

Kantelhardt's MFDFA mathematical notation is used for the analysis. The steps required to calculate the MFDFA estimates are summarized below (Kantelhardt et al., 2002):

Input: Let, x_k is a time series of length N of compact support that $x_k = 0$ for an insignificant amount of values.

Step 1: First, compute the sequence of summary displacements

$$P(i) = \sum_{k=1}^i [x_k - \bar{x}], \quad i = 1, \dots, N. \quad (7.1)$$

Step 2: Then, partition $P(i)$ in a number of non-overlapping segments denoted by $N_l = N/l$, of equal length l . The same process is repeated from end to start to the series to consider the small parts that can remain at the end of the series. Thus we obtain total $2N_l$ segments.

Step 3: In this step, detrend the profile $P(i)$, $i=1, \dots, N$, for each segment of length l , by applying least square fit on each segment and calculating their respective variance, which is given as

$$F^2(l, v) = \frac{1}{l} \sum_{i=1}^l \{P[(v-1)l + i] - y_v(i)\}^2 \quad (7.2)$$

where v is a segment such that $v=1, \dots, N_l$, and

$$F^2(l, v) = \frac{1}{l} \sum_{i=1}^l \{P[N - (v - N_l)l + i] - y_v(i)\}^2 \quad (7.3)$$

for $v = N_l + 1, \dots, 2N_l$, where $y_v(i)$ is the fitting polynomial in the segment v .

Step 4: Then, calculate the q th order fluctuation function by averaging over all segments, as follows,

$$F_q(l) = \left\{ \frac{1}{2N_l} \sum_{v=1}^{2N_l} [F^2(l, v)]^{q/2} \right\}^{1/q} \quad (7.4)$$

where q can take value different from zero. To determine the dependency of generalized q dependent fluctuations on time scale l , repeat steps 2 to 4.

Step 5: Lastly, determine the scaling behavior of the fluctuating functions by analyzing the log-log plots of $F_q(l)$ versus l for each value of q .

$$F_q(l) \sim l^{h(q)} \quad (7.5)$$

where, $h(q)$ is the q -dependent generalized Hurst exponent (Kantelhardt et al., 2002). It is to be noted that for long-range power-law corrected series x_i , $F_q(l)$ increases as power-law for large values of l .

For each order of q , the scaling behavior of the fluctuation functions can be determined by the logarithmic chart of $F_q(l)$ versus l . The slope of $\log F_q(l)$ and $\log l$ is the generalized Hurst exponent $h(q)$.

The Hurst exponent H , varies between 0 and 1 (Feder & Fractals, 1988). The Hurst exponents can be interpreted as the correlation analysis of the time series.

The scaling exponent H ;

- $H = 0.5$ means that the time series are uncorrelated,
- $0.5 < H < 1$ implies long-term persistence,
- $0 < H < 0.5$ implies short-term persistence (Movahed et al., 2003).

7.2 Brain Bandpowers Extraction

The EEG data is collected in time-domain space. Because of the EEG signal complexity, signals seems like noise and irrelevant, but it is possible to obtain information from the data in frequency-domain. In the signal analysis working with the frequency-domain is more useful rather than the time domain.

The time-domain data show a signal changes over time, whereas a frequency-domain data shows how much of the signal lies within each frequency band over a range of frequencies. The signal can be converted between the time-domain and frequency-domain with a mathematical transformation methods, such as Fourier

transform. The Fourier transform converts the time function into a sum of sine waves of different frequencies.

The spectrum of the frequencies is the frequency domain representation of the signal. In the Fourier transform, data separated to window length intervals. The fast Fourier transform is faster if the signal window length is the power of two. Therefore, window lengths should be the power of two.

The algorithm 1 gives the frequency components of the offline signal. Emotiv EPOC amplifier collect data with 256Hz, and ocular, muscle and motion artefacts are not treated.

Algorithm 1 Steps:

Step1 : Remove any residual common mode signals with median subtraction.

Step2 : Limit slew rate to remove occasional noise spikes.

Step3 : Apply IIR High-pass filter.

Step4 : Select epoch length for FFT (256 = 2 seconds in this example).

Step5 : Grab next epoch .

(step forward 0.25 seconds in this example, using trailing 2 second sample)

Step6 : Apply Hanning window filter .

(removes wrap-around step artefact from FFT)

Step7 : Run the FFT.

Step8 : Calculate bin power for each frequency step.

(square of magnitude of the complex FFT output value)

Step9 : Add up the power in each frequency range.

7.2.1 Fast Fourier Transform

The fast Fourier transform (FFT) measure the discrete Fourier transform (DFT) of the complex valued series (Duhamel & Vetterli, 1990). It has been transformed the time domain data to the frequency domain data (Figure 7.1).

The discrete Fourier transform can be applied to the complex series but in large series the computation takes very long time. The fast Fourier transform method is faster than the DFT. So, the fast fourier algorithm is generalt used method (Brigham, 1988).

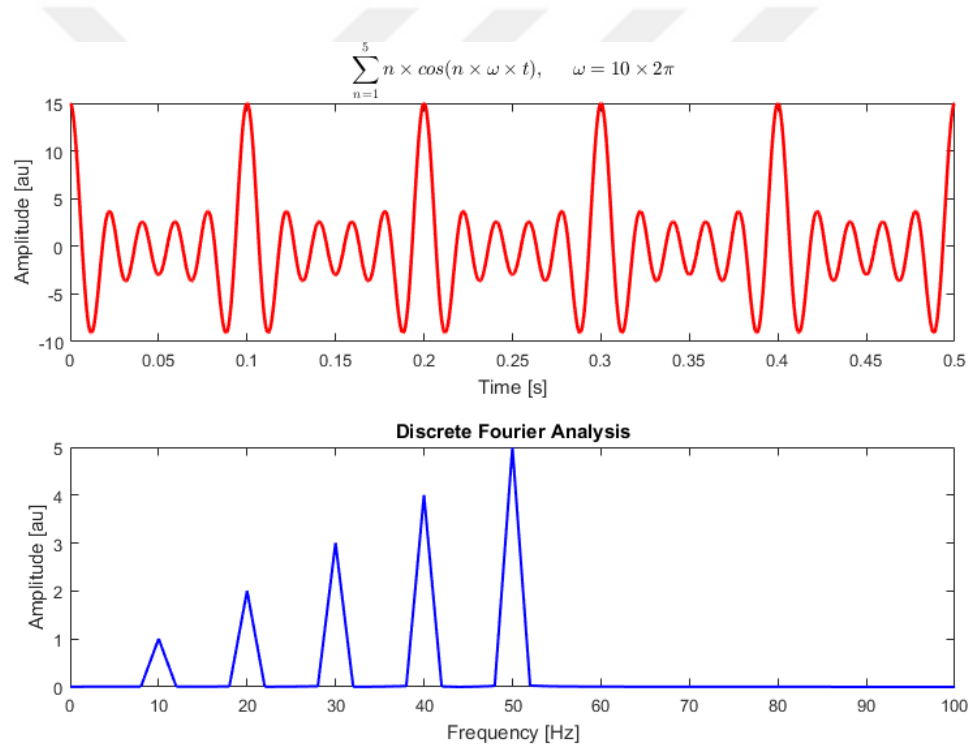


Figure 7.1 A discrete Fourier analysis of a sum of cosine waves at 10, 20, 30, 40, and 50 Hz.

The fast fourier transform is firstly mentioned in unpublished work of the Gauss (Bergland, 1969; Strang 1993). Then, Cooley & Tukey (1965) have developed the much faster algorithm as fast fourier transform.

There are many transformation algorithms but the fast Fourier transform is the more efficient than the other methods. The fast Hartley transform is as fast as fast

fourier transform (Bracewell, 1999). Also, Winograd transform algorithm improves the speed of discrete Fourier transform (Press et al., 1992; pp. 412-413, Arndt).

Fast fourier Transform function explained as follows:

Let $f(t)$ be the continuous signal. Let N samples are denoted: $f[0], f[1], f[2], \dots, f[k], \dots, f[N-1]$.

The Fourier transform of the signal $f(t)$;

$$F(j\omega) = \int_{-\infty}^{\infty} f(t)e^{-j\omega t} dt \quad (7.6)$$

7.2.2 Hanning Window

The Hanning function is typically used as a window function in digital signal processing to select a subset of a series of samples in order to perform a Fourier transform or other calculations (Rangayyan, 2002).

$$\omega(n) = \frac{1}{2} \left[1 - \cos \left(\frac{2\pi n}{N-1} \right) \right] \quad (7.7)$$

The Hanning window is generally satisfactory in 95% of cases. It has good frequency resolution and reduced spectral leakage (Anurag & Anand, 2016). When the nature of the signal is unknown but a smoothing window is wanted to apply, the Hanning window can be used.

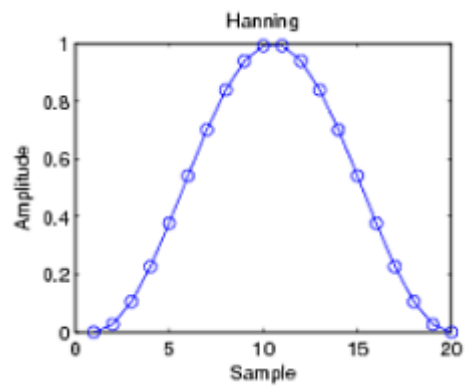


Figure 7.2 Hanning window.

CHAPTER EIGHT

CLASSIFICATION AND VALIDATION METHODS

In this chapter, the methods used in this study are detail explained. The statistical signal similarity method is used for the validation of the dataset. The K-Nearest Neighbor Algorithm and CxK – Nearest Algorithm are used as classification method.

8.1 Statistical Signal Similarity

Measure of similarity has been used for the comparison of one signal or image with another. Many basic processing operations, such as matched filtering, cross correlation, and beam formation, may be interpreted as being based on measures of similarity. These related operations typically form the foundation of the detection, classification, localization, association and registration algorithms employed in semiautonomous sensor systems (Kennedy, 2007).

A hypothesis test is performed with the null hypothesis being that there is no signal present and that the waveforms entering the beam former contain only zero-mean Gaussian-distributed noise.

The test statistic for all possible lag combinations corresponding to all physically measurable angles is computed. The most likely direction of the source is set equal to the angular coordinate for which the null hypothesis is least likely, i.e. the test statistic is maximized.

The delay-and-sum beam-former is applied as

$$y(n) = \sum_{m=0}^{M-1} x_m(n), \quad (8.1)$$

where $x_m(n)$ is the n th sample output from the m^{th} delay channel and $y(n)$ is the beam-formed output. The noise statistics of every sample from all sensors are

assumed to be identical, so the n^{th} sample in each delay channel is assumed to be an independent observation of the random variable X_n .

Analyzing the digitized waveforms (in x) over a window of length N , gives a total of N different random variables, with M observations of each variable. Under the null hypothesis the variables have a Gaussian (Normal) distribution,

$$X_n \sim N(\mu_n, \sigma_n^2). \quad (8.2)$$

At a given n , using the data from all M channels, the Maximum Likelihood Estimates (MLEs) $\hat{\mu}_n$ and $\hat{\sigma}_n^2$ of the (true) mean and variance μ_n and σ_n^2 , are computed using,

$$\hat{\mu}_n = \frac{y(n)}{M} \quad (8.3)$$

and

$$\hat{\sigma}_n^2 = \frac{1}{M} \left\{ \sum_{m=0}^{M-1} x_m(n)^2 - \frac{y(n)^2}{M} \right\}. \quad (8.4)$$

Under the null hypothesis the following relationships hold:

$$\text{If } Z_a = M \frac{(\hat{\mu}_n - \mu_n)^2}{\sigma_n^2} \text{ then } Z_a \sim \chi^2(1); \quad (8.5)$$

$$\text{If } Z_b = M \frac{\hat{\sigma}_n^2}{\sigma_n^2} \text{ then } Z_b \sim \chi^2(M-1). \quad (8.6)$$

Under the null hypothesis it is also assumed that the noise statistics of the sensor outputs are zero mean and time invariant so the parameters of each distribution are the same:

$$\mu_1 = \mu_2 = \dots = \mu_N = \mu = 0 \quad (8.7)$$

and

$$\sigma_1 = \sigma_2 = \dots = \sigma_N = \sigma^2. \quad (8.8)$$

Using the reproductive property of χ^2 variables, the following aggregate test statistics can be formed and analyzed:

$$\text{If } Z_c = \frac{M}{\sigma^2} \sum_{n=0}^{N-1} \hat{\mu}_n^2 \text{ then } Z_c \sim \chi^2(N); \quad (8.9)$$

$$\text{If } Z_d = \frac{M}{\sigma^2} \sum_{n=0}^{N-1} \hat{\sigma}_n^2 \text{ then } Z_d \sim \chi^2(N(M-1)). \quad (8.10)$$

So far it has been assumed that the true variance (2σ) of the (white) noise is known. This is an inconvenient and unnecessary assumption. It can be eliminated by dividing (8.9) by (8.10); furthermore, if the numerator and the denominator are scaled by the inverse of their respective degrees of freedom, i.e.

$$Z_M = \frac{Z_c / N}{Z_d / (N(M-1))}, \quad (8.11)$$

Then a variable distributed according to Snedecor's F distribution results; that is, after substituting (8.9) and (8.10) into, (8.11):

$$Z_M = (M-1) \frac{\sum_{n=0}^{N-1} \hat{\mu}_n^2}{\sum_{n=0}^{N-1} \hat{\sigma}_n^2}, \quad (8.12)$$

with

$$Z_M \sim F(N, N(M-1)). \quad (8.13)$$

Substituting the expressions for $\hat{\mu}_n$ and $\hat{\sigma}_n^2$, given in (8.13) and (8.14) respectively, into (8.12) yields,

$$Z_M = (M-1) \frac{\frac{1}{M} \sum_{n=0}^{N-1} y(n)^2}{\sum_{m=0}^{M-1} \sum_{n=0}^{N-1} x_m(n)^2 - \frac{1}{M} \sum_{n=0}^{N-1} y(n)^2}. \quad (8.14)$$

The Z_M test statistic is the ratio of two sum-of-squares quantities (8.12). If the square of the estimated mean (numerator) is regarded as the (delay-and-sum) signal power, and the variance (denominator) the noise power, then it may be convenient to convert Z_M into a Signal-to-Noise Ratio (SNR) in dB. Images may then be formed using many closely-spaced beams, and presented to an operator for visual inspection.

The hypothesis test is performed with the null hypothesis as below.

H_0 : *There is no signal present.*

The statistical similarity algorithm steps are in Algorithm 2:

Input: x is the input signal, $x = 1, \dots, N$.

Step 1: Calculate the differences of the signals as following equation.

$$x = (x_{t_i+1} - x_{t_i}) \quad (8.15)$$

Step 2: Calculate de similarity measurement value with the equation (8.14).

The Z_M test statistic is F distributed under the null hypothesis. The F distribution value is determined based on the degrees of freedom. The degrees of freedom parameters depend on the data window length (N) and the signal count which is the number of the inserted signal. The determined F value is used as threshold. If the calculated Z_M value bigger than the threshold, the null hypothesis is rejected and the signals are assumed to be present.

8.2 K-Nearest Neighbor Algorithm

The k-nearest neighbor (Hart et al., 2001) algorithm is a supervised classification method. Classes are determined before classification and characterized by sets of elements. The number of elements can be different among classes. This algorithm has been used to associate the sample to the class containing more neighbors.

It has been successfully used in many applications, such as pattern recognition (Mahmoud & Al-Khatib, 2011) and machine learning task (Malek et al., 2012). The classification method involves a two-step process:

1. Constructing a classification model from data,
2. Applying the model to test examples

The k-nearest neighbors of a given example z refer to the k points that are closest to z . The data point is classified based on the class labels of its neighbors. In the case where the neighbors have more than one label, the data point is assigned to the majority class of its nearest neighbors.

The choosing of the right value of key is important. If key is too small, than the nearest-neighbor classifier may be susceptible to over feeting because of noise in the training data. On the other hand, if k is too large, the nearest-neighbor classifier may miss classify the test instance because its list of nearest neighbors may include data points that are located far away from its neighborhood.

The nearest-neighbor classification method is given in algorithm 3. The algorithm computes the distance between each test example and all the training examples to determine its nearest-neighbor list. Such computation can be costly if the number of training examples is large. The aim of this method is to find the nearest neighbors of a test example (Figure 8.1).

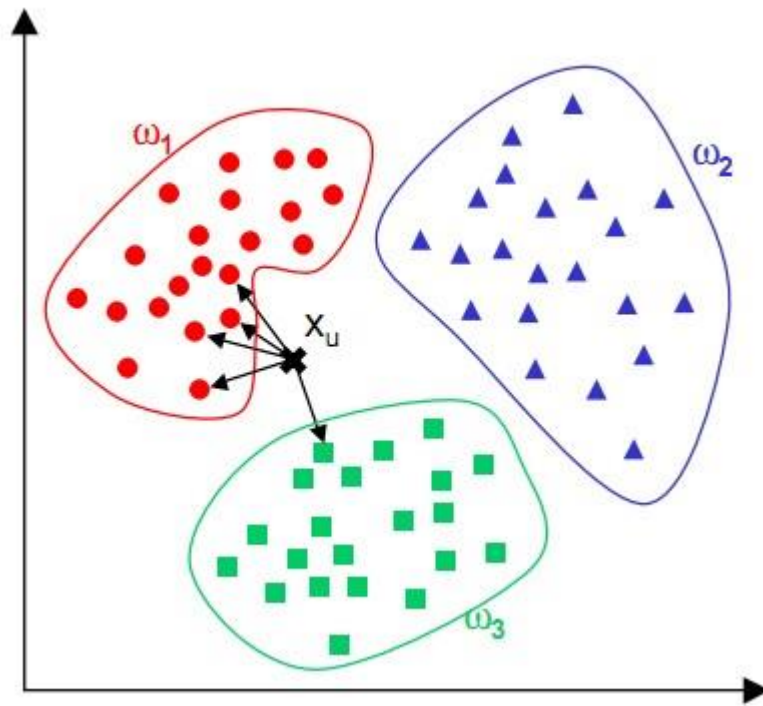


Figure 8.1 K-nearest neighbor

Algorithm 3 Steps:

Step 1: Let k be the number of nearest neighbors and D be the set of training examples.

Step 2: For each test example $z = (x', y')$ do,

Step3: Compute $d = (x', x)$, the distance between z and ever example, $(x, y) \in D$.

Step 4: Select $D_z \subseteq D$, the set of k closest training examples to z .

Step 4: Classified the test examples based on the majority class of its nearest neighbors.

$$y' = \arg \max_v \sum_{(x_i, y_i) \in D_z} I(v = y_i) \quad (8.16)$$

End for.

8.3 C × K-Nearest Neighbor Algorithm

In the artificial intelligence and other fields, the fundamental problem is recognition of patterns. Nearest neighbor (NN) algorithms are simple but effective methods for performing general and non-parametric classification (Cover & Hart, 1967). The empirical evaluation to data in various fields shows that NN is robust and has asymptotic error rate that is at most twice the Bayes error rate (Cover & Hart, 1967).

The problem is that predicting the class label of an unknown sample according to given known class labels which can be separated into C classes (Gao & Wang, 2007).

CxK- nearest neighbor algorithm is described as follows:

Algorithm 4:

Inputs: Unclassified data of training X , the set of labeled test samples $X = \{x_1, x_2, \dots, x_n\}$, the priori known classes $j = 1, 2, \dots, C$, the number of elements of each class C_j as n_j .

Output: Classified data of training X .

Step 1: Set K neighbors, $1 \leq K \leq n$.

Step 2: Calculate the distance between x and x_i^c according to the K number for each class C_j .

$$d(x, x_i^c) = \|x - x_i^c\| \quad (8.17)$$

Where $\|\cdot\|$ is the Euclidean norm.

Step 3: For each class C_j ,

If $i \leq K$ then assign x_i^c to the set of K-nearest neighbors in C_j .

Else

Delete the farthest sample the set of K-nearest neighbors and assign x_i^c to the set of K-nearest neighbors in C_j .

Step 4: Calculate the average distance d_j of x from K-nearest neighbors of class C_j .

Step 5: Mark the class with minimum distance $d_r = \min_j d_j$ and classify x in class r of the last minimum found.

8.4 k-fold Cross Validation Method

The Cross-Validation is a statistical method and used for the model evaluation. The basic form of the cross-validation is k-fold cross-validation. Also, the k-fold cross-validation is used for the performance estimation of the classifier. In k-fold cross-validation method, the data is partitioned to the k segments or folds. The one of these folds is used to train a model and the remaining folds are used as learning. Afterwards, in each iteration different fold of the dataset is held out for validations while the others $k-1$ folds are used for learning. The cross-validation process is then repeated k times, with each of the k subsamples used only once as the validation data.

The average of the results measured from the k steps is calculated to produce a one estimation. The each observation is used for both training and validation, and each observation only used for validation. This is the benefit of the k- fold cross-validation method.

In the literature, 10-fold cross-validation is commonly used (Zhang et al., 2015). The 10-fold cross-validation is the standard way of measuring the error rate of

a learning scheme on a particular dataset; for reliable results, 10 times 10-fold cross-validation (Figure 8.2).

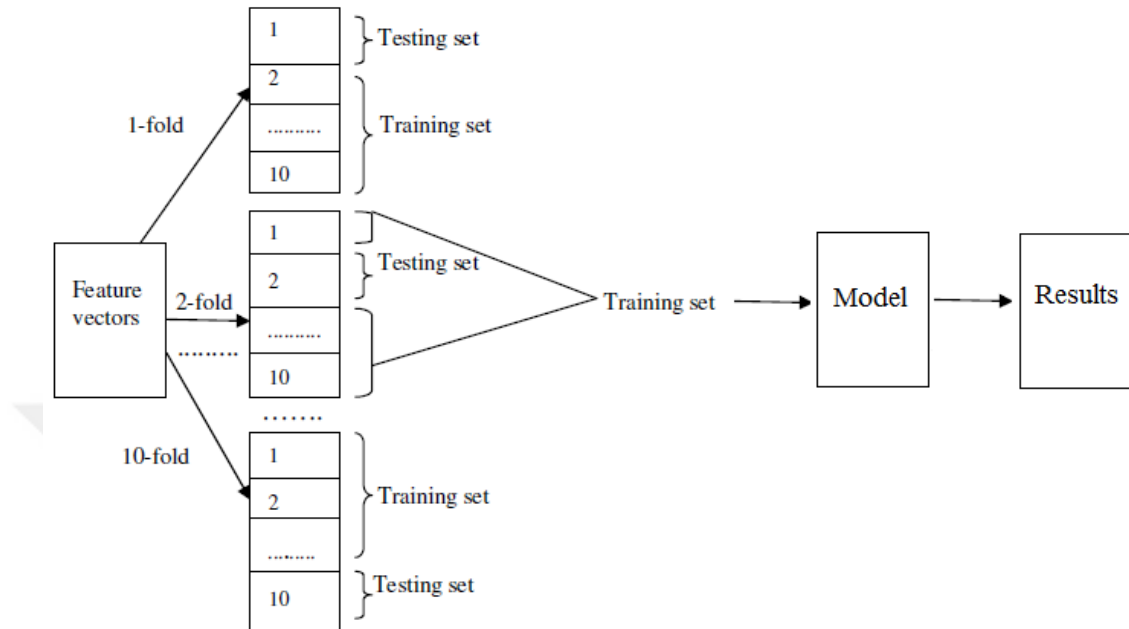


Figure 8.2 10-fold cross validation.

The two aim of the cross-validation is as follows:

- 1) The measuring performance estimation of the validation model.
- 2) The comparison of the performance between two or more different algorithms and determination of the best algorithm.

The above two goals are highly related, since the second goal is automatically achieved if one knows the accurate estimates of performance.

CHAPTER NINE

EXPERIMENTAL RESULTS

In this section, the data validation is made before the experiments. For this purpose, the statistical signal similarity is measured both within tasks and within sections. After the data validation process, the extracted features are classified by the soft computing methods.

9.1 Data Validation

The statistical similarity measure as Z_m statistics has been used for the each session and session means. Each session consists of 24 trainings and in each training the cognitive task images are shown for 1 sec. The statistical similarity between each mental task is measured for sessions. Also, the similarity within the sessions means for the same tasks has been measured. We expect that all tasks in each session is different from each other and the same tasks are similar for all sessions. The aim of this process, providing the consistency of the subject's data.

As it is seen from the measurement of the statistical similarity between mental tasks for all three sessions, Z_m statistics values of mental tasks are above or below from the threshold value which is F distribution value. But there is no channel which is all similarity values below the threshold (Table 9.1-9.3). Therefore, all channels are used for the further works.

Table 9.1 The statistical similarity between mental tasks for session 1.

Session 1 Comparison of Mental Tasks	AF3	F7	F3	FC5	T7	P7	O1	O2	P8	T8	FC6	F4	F8	AF4
Down-Blank	0.77	1.07	0.69	0.97	0.88	1.03	0.73	0.89	1.09	0.71	0.60	0.90	0.57	0.57
Left-Blank	0.94	1.29	0.92	1.56	1.06	0.73	1.00	0.81	0.63	0.81	0.96	0.86	0.80	0.90
Left-Down	0.98	0.75	1.12	0.81	1.07	0.82	1.39	1.53	1.13	1.39	1.41	1.13	1.16	1.16
Left-Right	1.51	1.21	1.40	2.09	0.80	1.03	1.02	0.93	0.97	0.94	1.05	1.08	1.35	1.35
Right-Blank	2.31	1.09	1.48	1.30	0.85	0.89	1.18	1.25	1.16	0.93	0.86	1.16	1.17	1.17
Right-Down	0.74	0.79	0.90	0.70	0.87	1.21	1.43	0.84	1.14	1.01	1.01	1.30	1.02	1.02
Up-Blank	0.97	0.94	0.94	1.10	1.01	1.30	0.73	0.77	1.11	1.07	1.69	1.16	1.16	1.16
Up-Down	1.02	1.47	0.86	1.90	1.67	1.39	0.89	1.35	1.55	1.08	1.42	1.05	1.25	1.25
Up-Left	0.99	1.02	0.97	0.96	0.99	1.00	1.18	1.52	0.92	0.74	0.90	1.05	0.80	0.80
Up-Right	0.88	0.94	1.16	0.74	0.92	1.27	1.24	1.03	1.03	1.33	0.98	0.99	1.27	1.27

Table 9.2 The statistical similarity between mental tasks for session 2.

Session 2 Comparison of Mental Tasks	AF3	F7	F3	FC5	T7	P7	O1	O2	P8	T8	FC6	F4	F8	AF4
Down-Blank	1.18	1.15	0.81	1.38	1.19	0.97	1.12	1.54	0.91	0.98	0.86	0.80	0.94	0.94
Left-Blank	1.40	1.16	0.97	0.90	0.53	1.02	1.52	0.89	0.95	1.02	0.94	0.98	1.16	1.46
Left-Down	0.98	0.75	1.12	0.81	1.07	0.82	1.39	1.53	1.13	1.39	1.41	1.13	1.16	1.16
Left-Right	1.51	1.21	1.40	2.09	0.80	1.03	1.02	0.93	0.97	0.94	1.05	1.08	1.35	1.35
Right-Blank	1.00	0.92	0.94	0.95	1.05	1.42	0.97	0.71	0.65	0.85	0.93	1.17	0.88	1.05
Right-Down	0.74	0.79	0.90	0.70	0.87	1.21	1.43	0.84	1.14	1.01	1.01	1.30	1.02	1.02
Up-Blank	1.05	1.00	1.41	1.18	1.10	1.12	1.07	0.88	0.72	0.85	1.08	1.44	1.03	1.05
Up-Down	1.02	1.47	0.86	1.90	1.67	1.39	0.89	1.35	1.55	1.08	1.42	1.05	1.25	1.25
Up-Left	0.96	1.13	1.03	1.00	1.10	0.85	1.33	0.99	1.27	1.29	1.00	1.51	1.47	1.47
Up-Right	0.79	0.85	1.15	0.90	1.12	1.41	1.52	0.97	0.97	1.19	1.07	0.83	0.78	0.78

Table 9.3 The statistical similarity between mental tasks for session 3.

Session 3 Comparison of Mental Tasks	AF3	F7	F3	FC5	T7	P7	O1	O2	P8	T8	FC6	F4	F8	AF4
Down-Blank	1.35	1.15	1.03	1.63	0.92	1.10	1.32	1.15	1.22	1.05	1.55	0.88	0.91	0.91
Left-Blank	1.84	1.08	1.19	1.31	0.70	0.86	0.75	0.91	0.77	0.91	0.87	1.08	1.60	1.60
Left-Down	0.79	0.81	0.90	0.81	0.91	1.00	1.67	1.07	1.26	1.27	0.66	0.79	1.04	1.04
Left-Right	1.22	1.19	1.24	1.67	1.40	1.17	1.56	0.81	1.23	1.34	1.07	0.95	1.01	1.01
Right-Blank	0.94	1.29	0.92	1.56	1.06	0.73	1.00	0.81	0.63	0.81	0.96	0.86	0.80	0.90
Right-Down	1.35	1.15	1.03	1.63	0.92	1.10	1.32	1.15	1.22	1.05	1.55	0.88	0.91	0.91
Up-Blank	1.00	0.92	0.94	0.95	1.05	1.42	0.97	0.71	0.65	0.85	0.93	1.17	0.88	1.05
Up-Down	0.97	0.94	0.94	1.10	1.01	1.30	0.73	0.77	1.11	1.07	1.69	1.16	1.16	1.16
Up-Left	0.77	1.07	0.69	0.97	0.88	1.03	0.73	0.89	1.09	0.71	0.60	0.90	0.57	0.57
Up-Right	1.03	0.86	0.74	0.84	0.80	1.02	0.71	0.81	0.98	0.72	0.94	1.08	1.07	1.07

According to the similarity results, each cognitive task is similar in all sessions (Table 9.4). Also, each cognitive task are different from each other in session avearege (Table 9.5). This shows that the handled signals are consistant for the following analysis.

Table 9.4 The statistical similarity of same mental tasks between sessions.

	AF3	F7	F3	FC5	T7	P7	O1	O2	P8	T8	FC6	F4	F8	AF4
Left	1.13	0.77	1.39	0.98	0.95	0.90	0.98	0.83	0.99	0.84	0.83	0.84	1.22	1.02
Right	0.96	1.28	1.19	1.07	0.73	0.91	0.96	0.94	0.66	0.95	0.88	1.24	1.10	0.49
Up	0.98	1.64	0.90	1.06	1.44	0.81	1.39	0.84	0.73	0.64	0.83	0.97	0.82	1.08
Down	0.98	0.96	0.98	1.31	0.95	1.05	0.66	1.21	1.47	0.96	1.07	0.76	1.41	0.85
Blank	0.97	1.05	0.85	0.95	1.09	0.81	0.80	1.41	0.89	1.17	0.99	0.95	0.93	0.83

Table 9.5 The statistical similarity of different mental tasks for session's average.

Sessions Average	AF3	F7	F3	FC5	T7	P7	O1	O2	P8	T8	FC6	F4	F8	AF4
Down-Blank	0.41	0.82	0.663	0.247	0.361	0.81	0.851	0.231	0.865	0.116	0.092	0.146	0.225	0.134
Left-Blank	0.9	0.11	6.288	0.081	0.3	0.867	0.753	0.207	0.296	0.249	0.025	0.846	0.057	0.625
Left-Down	0.16	1.5	0.839	0.16	0.9	0.892	0.282	0.733	0.164	0.571	0.516	0.002	0.259	0.198
Left-Right	0.28	0.012	0.19	0.173	0.4	0.094	0.47	0.165	0.306	0.031	0.707	0.518	0.984	0.353
Right-Blank	0.06	0.18	0.27	0.045	0.18	0.051	0.01	0.25	0.435	0.265	0.162	0.25	0.269	0.645
Right-Down	0.69	0.72	0.757	0.98	0.771	0.014	0.25	0.055	0.204	0.068	0.405	0.182	0.051	0.04
Up-Blank	0.002	1.22	0.16	1.317	0.158	0.56	1	0.001	0.007	0.195	32.87	0.0025	1.216	0.132
Up-Down	0.221	0.002	0.264	0.436	0.165	0.012	0.716	0.439	1.129	0.029	0.018	0.556	2.706	0.142
Up-Left	0.14	0.67	0.475	0.61	1.297	0.153	1.69	0.498	0.762	0.071	0.105	0.149	0.727	1.9
Up-Right	0.25	1.37	0.3	0.65	0.127	19.3	0.029	3.907	2.008	0.113	0.979	0.469	0.538	0.051

In this thesis dissertation, we work an online data. Before the online test the subject is taken to training phase. Training phase is consist of sessions and each session has 24 trainings. The subject has attended to three sessions in different days. Then the statistical similarity measure as Z_M statistics of sessions' mean signal has been used for the determining the better channel which has the distinctive features of mental tasks. We expect that all tasks in sessions' mean signal is different from each other.

The subject has trained with the visual stimuli. In Sycamore training screen, when plus image appeared the subject knowing that the training will start. When the arrows appear, the subject both follows the arrows and thinks the control right hand according to the arrow rotation. In the blank screen, the subject thinks nothing. There is the break for two second among trainings. In a section, trainings are repeated 24 times.

The plot of the all channels for the mental tasks is as follows (Figure 9.1).

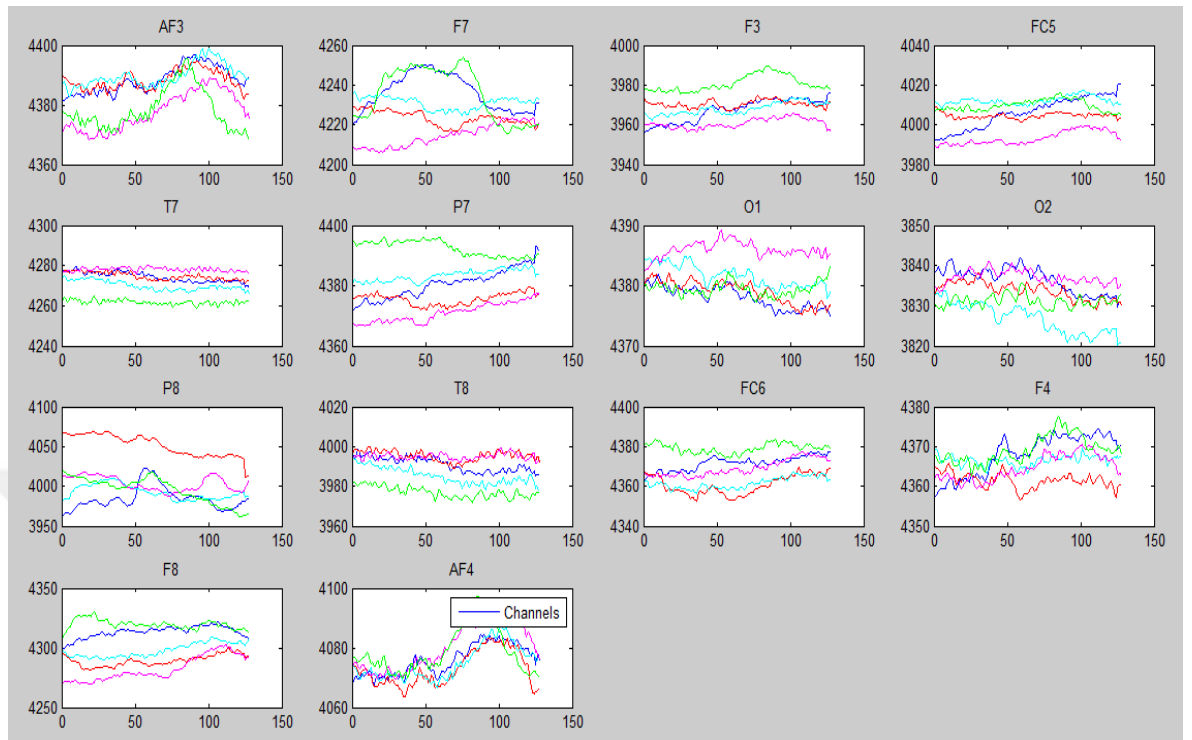


Figure 9.1 The signals of mental tasks for the electrode locations of Subject1.

The understanding of the difference of the mental tasks is very difficult from the above plot. Therefore, the features are classified by the soft computing algorithms.

The data validation is supplied by the measuring EEG band power frequency analysis. In the thinking and focusing situations, the power of the beta signals is higher than the other specific band powers (delta, theta, alpha, gamma). The alpha signals are active when the relaxing mode. Therefore, the data set is valuable when the power of the beta signals are higher than the alpha signals. It is show that the participant is focusing and thinking.

According to the beta and alpha signals power of the Subject 1 (Figure 9.2), the almost all power of the beta signals are higher than the power of the alpha signals. The difference of the power of beta and alpha signals are shows that the Subject 1 is thinking and concentrating in the training. The both maximum power of the signals have changed in a range 30-70 dB.

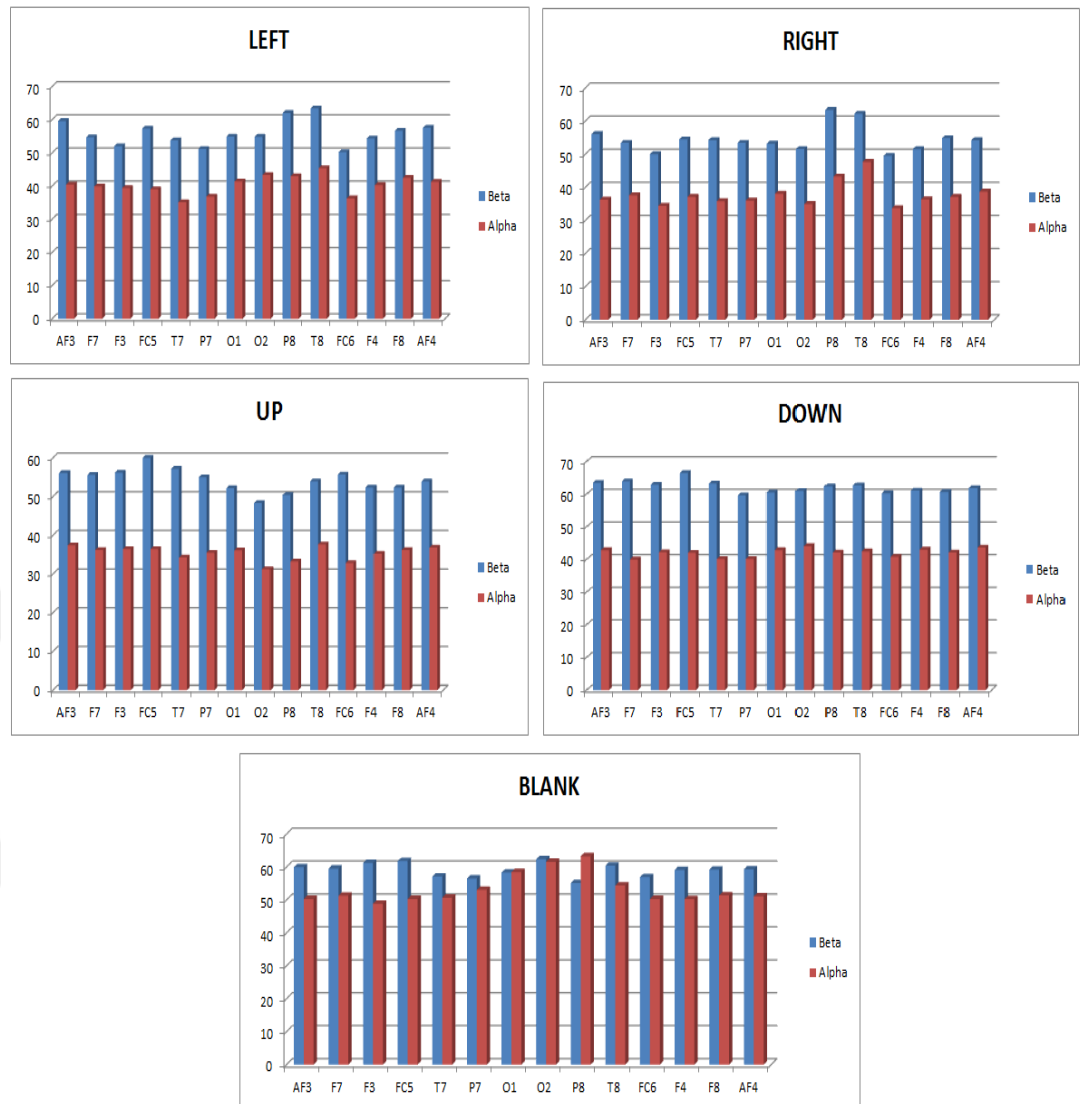


Figure 9.2 The power of the Beta and Alpha signals of Subject1.

In Figure 9.3 the beta and alpha signals power of the Subject 2, the almost all power of the beta signals are higher than the power of the alpha signals. There is a little difference between the power of beta and alpha signals. This is show that the Subject 2 is not full thinking and concentrating in the training. The both maximum power of the signals have changed in a range 30-60 dB.

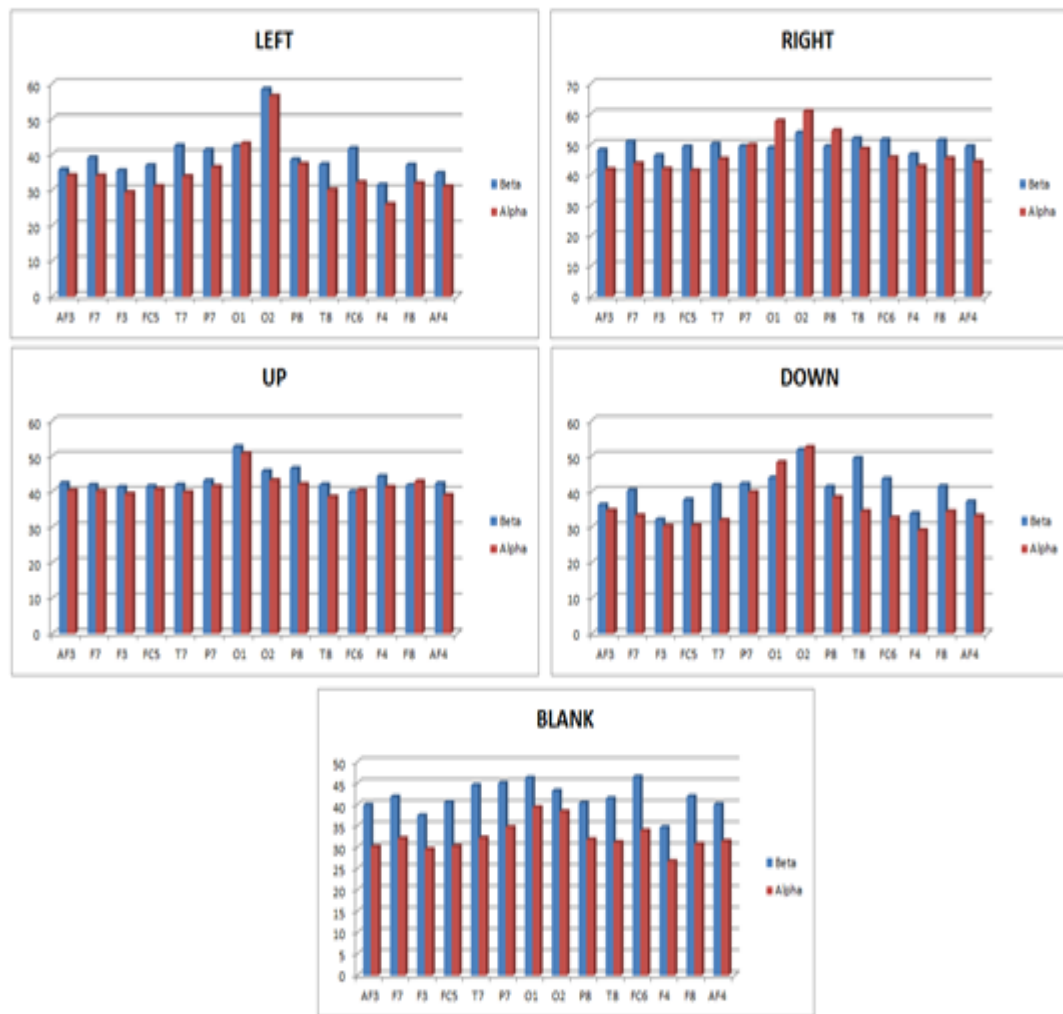


Figure 9.3 The power of the Beta and Alpha signals of Subject2.

In Figure 9.4, the beta and alpha signals power of the Subject 3, the almost all power of the beta signals are higher than the power of the alpha signals. The difference of the power of beta and alpha signals are shows that the Subject 3 is thinking and concentrating in the training. The both maximum power of the signals have changed in a range 30-70 dB.

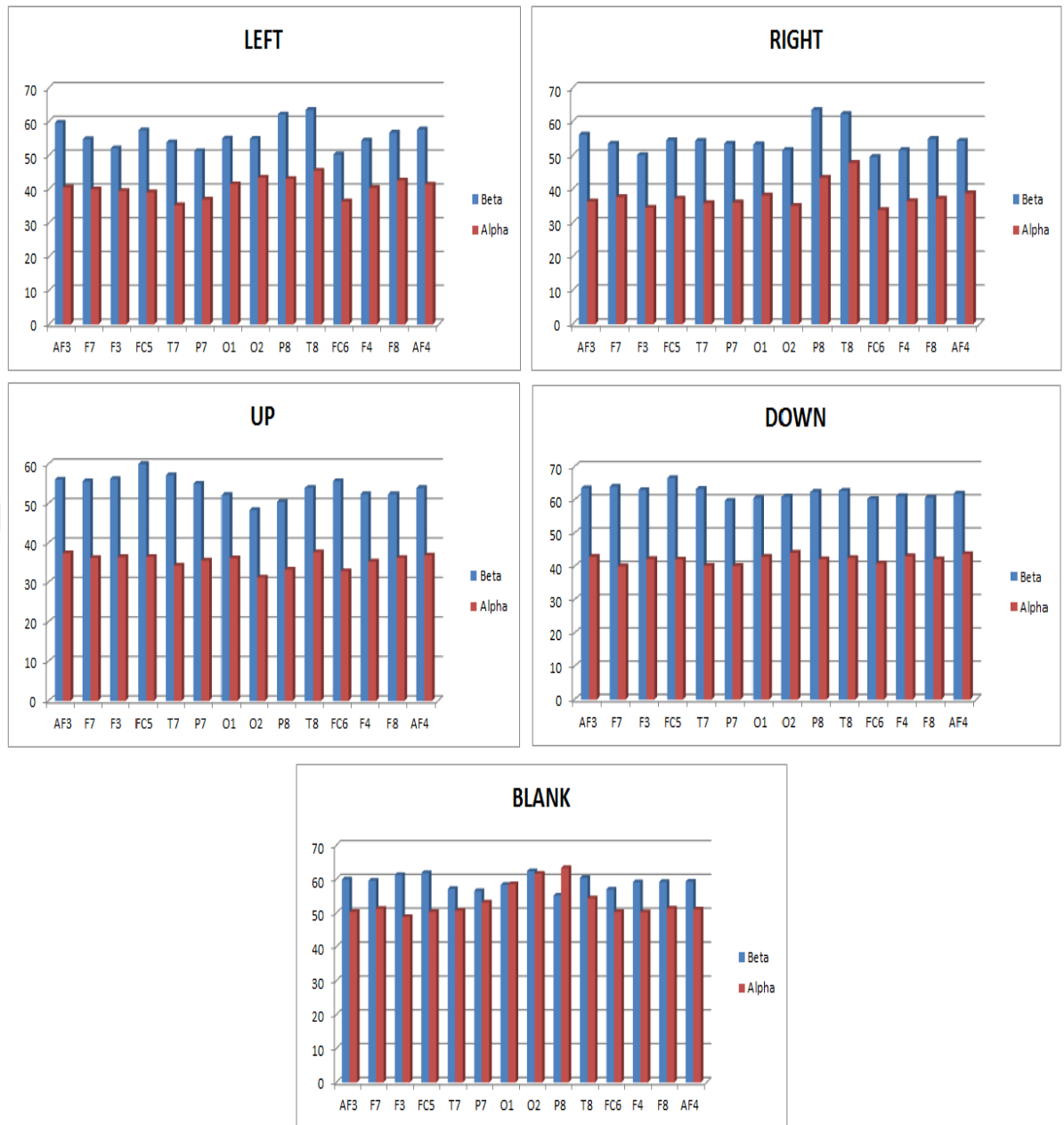


Figure 9.4 The power of the Beta and Alpha signals of Subject3.

In Figure 9.5 the beta and alpha signals power of the Subject 4, the almost all power of the beta signals are higher than the power of the alpha signals. There is a little difference between the power of beta and alpha signals. This is show that the Subject 4 is not full thinking and concentrating in the training. The both maximum power of the signals have changed in a range 20-50 dB. The range of the powers is lower than the other subjects.

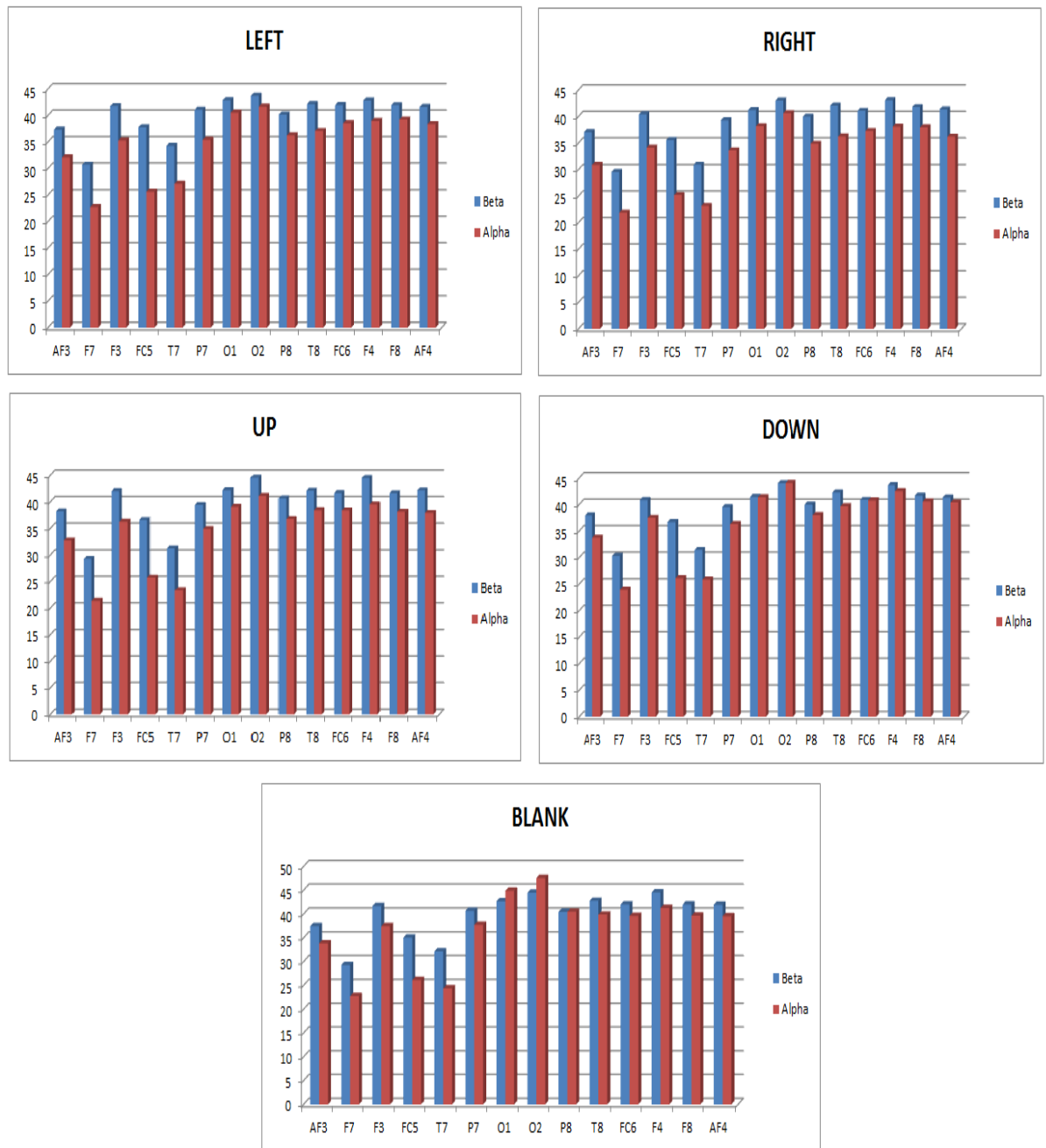


Figure 9.5 The power of the Beta and Alpha signals of Subject4.

In Figure 9.6, the beta and alpha signals power of the Subject 5, the almost all power of the beta signals are higher than the power of the alpha signals. There is a little difference between the power of beta and alpha signals. This is show that the Subject 4 is not full thinking and concentrating in the training. The both maximum power of the signals have changed in a range 30-60 dB.

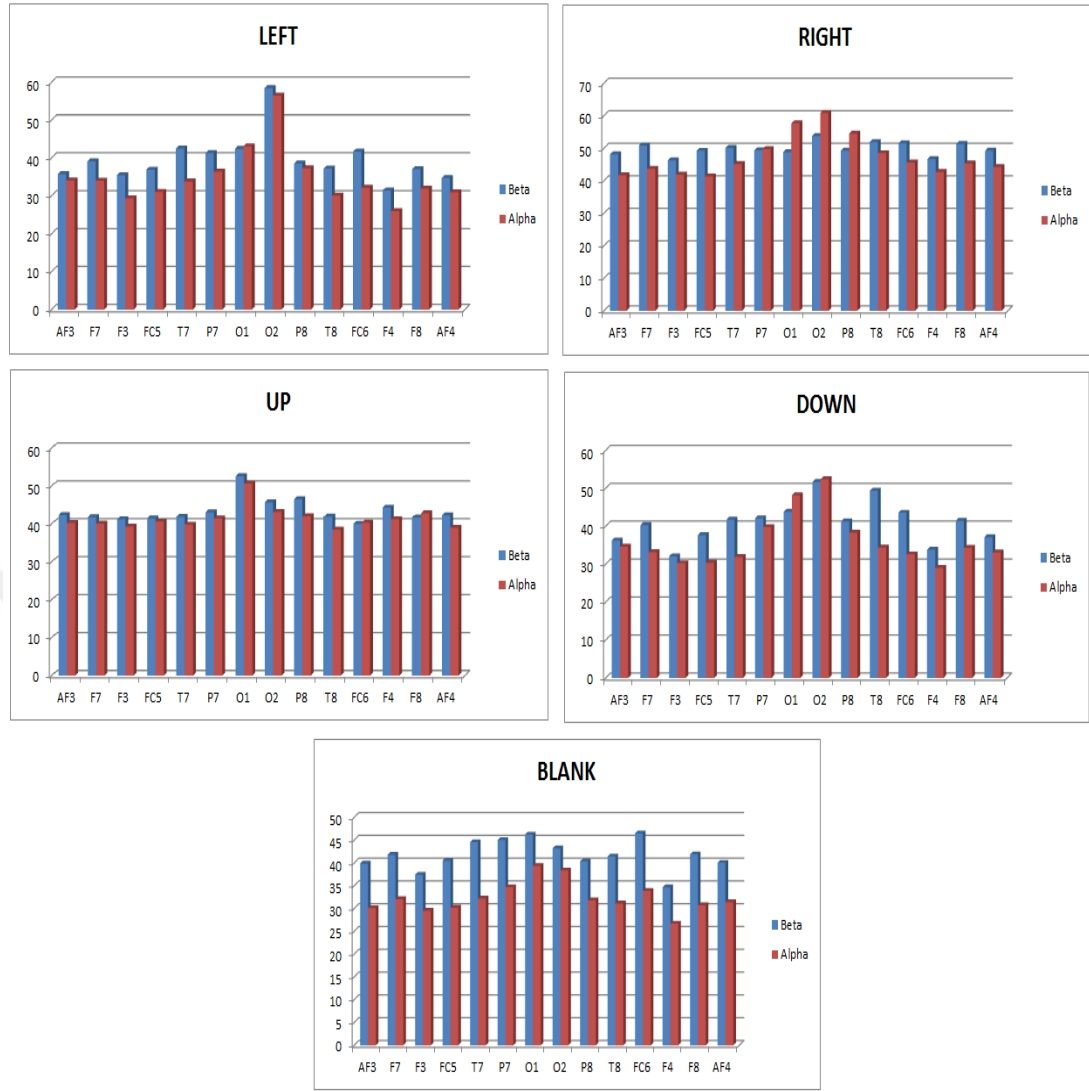


Figure 9.6 The power of the Beta and Alpha signals of Subject5.

9.2 Offline and Online Results

The electroencephalography (EEG) signals is non-linear, and non-stationary signals. Therefore, traditional methods of EEG analysis may overlook many properties of signals. Similarly, fractal analysis of EEG signals has shown scaling behaviors that may not be consistent with pure monofractal processes.

In this study, we have used MFDFA of 2^{nd} order fitting polynomial, varied q in the range -5 to 5 with 101 discrete intervals and scaling 128. The 2^{nd} order local

Hurst exponents (H_l), probability distribution of local Hurst exponents (P_h) and multifractal spectrum of local Hurst components (D_h) of the electrode locations are calculated. The probability distribution of Hurst exponents is used as feature vector. The Hurst exponent values of all mental tasks are in the interval of $0 < H < 0.5$. This indicates a long-range dependence.

The EEG data acquired from the Emotiv Epoc Neuro Headset for five subjects: 2 female and 3 male, age between 20 and 50, 2 left handed and 3 right handed, and all of them healthy people. Subjects have been seat on the chair with open eyes and they are relaxed. They both think of the movement of the right hand on left, right, up and down directions and also watch the images in the training screen. Each training data is collected for 24 times and the dimension of the each cognitive task is consists of 1 sec data for 14 channels, therefore 24x14x128 dimension data is captured.

In the preprocessing phase, the dataset is normalized by the min-max normalization method. The distribution of the Hurst exponent P_h , calculated by the MFDFA method, is handled from the normalized dataset. The P_h values are calculated separately for each cognitive task. Also, P_h values calculated for the raw dataset. The P_h values calculated from normalized dataset give better results; therefore normalized data is used for MFDFA calculations in further works.

The collected time-domain signal converted to the frequency-domain space with the fast Fourier transform method. Before the Fourier transform, the preprocessing methods are applied to the raw dataset. The Hanning window method, median filtering and high pass filtering methods are applied to the raw data respectively. Also, normalization preprocessing method is applied before the above preprocessing methods but the results has not found good. Therefore, normalization preprocessing phase is not used in the beta signal extraction process.

Midrange Beta and Beta signals are taken as features. The Midrange Beta signal is between 16 and 20 Hz. It is active in thinking and aware of the self and surrounding. The Beta signal is between 12 and 30 Hz.

The midrange beta and beta frequency bands, and P_h values are classified by the K-nearest neighbor and CxK-nearest neighbor algorithms. The offline classification results are handled for the 10-fold cross validation.

The P_h distribution of the Hurst exponent calculated by the MFDFA method, Midrange Beta and Beta signals are obtained and they are used as features. The classification of these features is made subject based and each cognitive task based. The 10% of the data set is randomly chosen as test set, and the rest of the data is chosen as train set in the 10-fold cross validation method.

The K-nearest classification results are shown in Table 9.6 for subject 1. According to the K-nearest neighbor classification results of the P_h values for each cognitive task, no movement, left and right cognitive tasks are the highest accuracy rates. The mean accuracy rate of P_h feature classification is 93%.

In the midrange beta classification results, left, up, and no movement cognitive tasks are the highest accuracy rates. The mean accuracy rate of midrange beta feature is equals to 85%.

Finally, in the beta feature classification results, no movement, up, right and down cognitive tasks have better accuracy rates. The mean accuracy rate of the beta feature is found as 92%.

From this table, we can say that the P_h values as a feature is very good rather than the midrange beta and beta features for subject 1.

Table 9.6 The accuracy rates of K – nearest neighbor algorithm for subject 1.

Subject 1	K – Nearest Neighbor Classification Method		
Task	Ph	Midrange Beta	Beta
Left	93%	89%	80%
Right	89%	82%	93%
Up	89%	87%	97%
Down	93%	83%	93%
No Movement	99%	85%	99%
Average	93%	85%	92%

Table 9.7 gives the K-nearest classification results of subject 2 for Ph, midrange beta and beta features. According to the K-nearest neighbor classification results of the P_h values for each cognitive task, no movement, left and down cognitive tasks are the highest accuracy rates. The mean accuracy rate of P_h feature classification is 89%.

In the midrange beta classification results, up, right and no movement cognitive tasks are the highest accuracy rates. The mean accuracy rate of midrange beta feature is equals to 84%.

Finally, in the beta feature classification results, no movement and left cognitive tasks have better accuracy rates. The mean accuracy rate of the beta feature is found as 84%. From this table, we can say that the P_h values as a feature is very good rather than the midrange beta and beta features for subject 2.

Table 9.7 The accuracy rates of K – nearest neighbor algorithm for subject 2.

Subject 2	K – Nearest Neighbor Classification		
Task	Ph	Midrange Beta	Beta
Left	91%	76%	84%
Right	86%	88%	83%
Up	83%	97%	82%
Down	89%	73%	83%
No Movement	97%	85%	86%
Average	89%	84%	84%

Table 9.8 gives the K-nearest classification results of subject 3 for Ph, midrange beta and beta features. According to the K-nearest neighbor classification results of

the P_h values for each cognitive task, almost the entire cognitive task has very good results. The mean accuracy rate of P_h feature classification is 95%.

In the midrange beta classification results, no movement, right and left cognitive tasks are the highest accuracy rates. The mean accuracy rate of midrange beta feature is equals to 80%.

Finally, in the beta feature classification results, no movement and right cognitive tasks have better accuracy rates. The mean accuracy rate of the beta feature is found as 82%. From this table, we can say that the P_h values as a feature is very good rather than the midrange beta and beta features for subject 3.

Table 9.8 The accuracy rates of K – nearest neighbor algorithm for subject 3.

Subject 3	K – Nearest Neighbor Classification		
Task	P_h	Midrange Beta	Beta
Left	93%	82%	78%
Right	91%	83%	83%
Up	95%	73%	81%
Down	95%	76%	80%
No Movement	100%	85%	86%
Average	95%	80%	82%

The K-nearest classification results are shown in Table 9.9 for subject 4. According to the K-nearest neighbor classification results of the P_h values for each cognitive task, all left signals are correctly classified, and also up, down and no movement signals are the high accuracy rates. The mean accuracy rate of P_h feature classification is 91%.

In the midrange beta classification results, up, left and down cognitive tasks are the highest accuracy rates. The mean accuracy rate of midrange beta feature is equals to 82%.

Finally, in the beta feature classification results, no movement, right and up cognitive tasks have better accuracy rates. The mean accuracy rate of the beta feature

is found as 84%. From this table, we can say that the P_h values as a feature is very good rather than the midrange beta and beta features for subject 4.

Table 9.9 The accuracy rates of K – nearest neighbor algorithm for subject 4.

Subject 4	K – Nearest Neighbor Classification		
Task	Ph	Midrange Beta	Beta
Left	100%	84%	80%
Right	82%	78%	87%
Up	93%	85%	84%
Down	91%	81%	82%
No Movement	91%	80%	88%
Average	91%	82%	84%

Table 9.10 gives the K-nearest classification results of subject 5 for P_h , midrange beta and beta features. According to the K-nearest neighbor classification results of the P_h values for each cognitive task, almost the entire cognitive task has very good results. The mean accuracy rate of P_h feature classification is 92%.

In the midrange beta classification results, up, left and down cognitive tasks are the highest accuracy rates. The mean accuracy rate of midrange beta feature is equals to 82%.

Finally, in the beta feature classification results, down, up and no movement cognitive tasks have better accuracy rates. The mean accuracy rate of the beta feature is found as 84%. From this table, we can say that the P_h values as a feature is very good rather than the midrange beta and beta features for subject 5.

Table 9.10 The accuracy rates of K – nearest neighbor algorithm for subject 5.

Subject 5	K – Nearest Neighbor Classification		
Task	Ph	Midrange Beta	Beta
Left	93%	84%	82%
Right	91%	78%	80%
Up	91%	85%	84%
Down	85%	81%	90%
No Movement	99%	80%	83%
Average	92%	82%	84%

Also, the new classification method CxK – nearest neighbor algorithm, proposed by the Ulutagay & Nasibov, 2016 is used for the classification of the P_h , midrange beta and beta features.

The CxK-nearest classification results are shown in Table 9.11 for subject 1. According to the CxK-nearest neighbor classification results of the P_h values for each cognitive task is very good. The entire cognitive task has over 90% accuracy rates. The mean accuracy rate of P_h feature classification is 95%.

In the midrange beta classification results, left, no movement and up cognitive tasks are the highest accuracy rates. The mean accuracy rate of midrange beta feature is equals to 86%.

Finally, in the beta feature classification results, all cognitive tasks have high accuracy rates. The mean accuracy rate of the beta feature is found as 94%. From this table, we can say that the P_h values as a feature has higher accuracy rates than the midrange beta and beta features for subject 1.

Table 9.11 The accuracy rates of CxK – nearest neighbor algorithm for subject 1.

Subject 1	C x K – Nearest Neighbor Classification		
Task	Ph	Midrange Beta	Beta
Left	95%	91%	88%
Right	93%	83%	95%
Up	93%	85%	97%
Down	94%	84%	94%
No Movement	99%	88%	95%
Average	95%	86%	94%

The CxK-nearest classification results are shown in Table 9.12 for subject 2. According to the CxK -nearest neighbor classification results of the P_h values for each cognitive task is very good. The almost entire cognitive task has over 90% accuracy rates. The mean accuracy rate of P_h feature classification is 91%.

In the midrange beta classification results, no movement, up and right cognitive tasks are the highest accuracy rates. The mean accuracy rate of midrange beta feature is equals to 90%.

Finally, in the beta feature classification results, all cognitive tasks have high accuracy rates. The mean accuracy rate of the beta feature is found as 89%. From this table, we can say that the P_h values as a feature has better accuracy rates than the midrange beta and beta features for subject 2.

Table 9.12 The accuracy rates of CxK – nearest neighbor algorithm for subject 2.

Subject 2	C x K – Nearest Neighbor Classification		
Task	Ph	Midrange Beta	Beta
Left	95%	82%	88%
Right	90%	93%	90%
Up	86%	95%	86%
Down	91%	84%	87%
No Movement	94%	95%	94%
Average	91%	90%	89%

The CxK-nearest classification results are shown in Table 9.13 for subject 3. According to the CxK-nearest neighbor classification results of the P_h values for each cognitive task is very good. The entire cognitive task has over 90% accuracy rates. The mean accuracy rate of P_h feature classification is 96%.

In the midrange beta classification results, no movement, left and right cognitive tasks are the highest accuracy rates. The mean accuracy rate of midrange beta feature is equals to 90%.

Finally, in the beta feature classification results, right, no movement and up cognitive tasks have higher accuracy rates. The mean accuracy rate of the beta feature is found as 84%. From this table, we can say that the P_h values as a feature is very good rather than the midrange beta and beta features for subject 3.

Table 9.13 The accuracy rates of CxK – nearest neighbor algorithm for subject 3.

Subject 3	C x K – Nearest Neighbor Classification		
Task	Ph	Midrange Beta	Beta
Left	95%	93%	83%
Right	93%	92%	88%
Up	97%	85%	84%
Down	98%	88%	81%
No Movement	99%	94%	85%
Average	96%	90%	84%

The CxK-nearest classification results are shown in Table 9.14 for subject 4. According to the CxK-nearest neighbor classification results of the P_h values for each cognitive task is very good. The almost entire cognitive task has over 90% accuracy rates. The mean accuracy rate of P_h feature classification is 94%.

In the midrange beta classification results, left, down and no movement cognitive tasks are the highest accuracy rates. The mean accuracy rate of midrange beta feature is equals to 89%.

Finally, in the beta feature classification results, no movement and right cognitive tasks have high accuracy rates. The mean accuracy rate of the beta feature is found as 89%. From this table, we can say that the P_h values as a feature is very good rather than the midrange beta and beta features for subject 4.

Table 9.14 The accuracy rates of CxK – nearest neighbor algorithm for subject 4.

Subject 4	C x K – Nearest Neighbor Classification		
Task	Ph	Midrange Beta	Beta
Left	98%	93%	87%
Right	88%	85%	92%
Up	95%	88%	88%
Down	93%	91%	86%
No Movement	94%	90%	93%
Average	94%	89%	89%

The CxK-nearest classification results are shown in Table 9.15 for subject 5. According to the CxK-nearest neighbor classification results of the P_h values for each

cognitive task is very good. The entire cognitive task has over 90% accuracy rates. The mean accuracy rate of P_h feature classification is 92%.

In the midrange beta classification results, no movement, up and left cognitive tasks are the highest accuracy rates. The mean accuracy rate of midrange beta feature is equals to 89%.

Finally, in the beta feature classification results, all cognitive tasks have high accuracy rates. The mean accuracy rate of the beta feature is found as 89%. From this table, we can say that the P_h values as a feature is very good rather than the midrange beta and beta features for subject 5.

Table 9.15 The accuracy rates of CxK – nearest neighbor algorithm for subject 5.

Subject 5	C x K – Nearest Neighbor Classification		
Task	Ph	Midrange Beta	Beta
Left	96%	90%	89%
Right	94%	88%	92%
Up	91%	91%	85%
Down	90%	87%	94%
No Movement	97%	92%	90%
Average	92%	89%	89%

The overall average classification accuracy for each cognitive task has been calculated for k-nearest neighbor and CxK-nearest neighbor algorithm (Table 9.16).

The comparison of the classification accuracies:

- The classification accuracies change between 94% and %96 for left EEG signals.
- The classification accuracies change between 88% and %92 for right EEG signals.
- The classification accuracies change between 90% and %92 for up EEG signals.
- The classification accuracies change between 90% and %93 for down EEG signals.
- The classification accuracies change between 97% and %97 for no movement EEG signals.

Table 9.16 The overall accuracy rates of CxK and K – nearest neighbor algorithm for all cognitive tasks.

	K-NN			CxK-NN		
	Ph	MidrangeBeta	Beta	Ph	MidrangeBeta	Beta
Left	94%	83%	81%	96%	90%	87%
Right	88%	82%	85%	92%	88%	91%
Up	90%	85%	85%	92%	89%	88%
Down	90%	79%	86%	93%	87%	88%
No Movement	97%	83%	88%	97%	92%	91%

The Table 9.17 shows that the K-nearest neighbor classification accuracy rates of all subjects. Subject 1 and Subject 3 have Silva Mind Control education. The Silva mind control method has been founded and developed in 1960 through parapsychologist Jose Silva to help his children do better in school and increase their chance of success in life. This method is dynamic meditation technique. It consists of mental training method. The Silva Method teaches people control their subconscious and negative programming.

Therefore subject 1 and subject 3 has better in cognitive tests. The P_h feature has higher accuracy rate (92%) than midrange beta (82%) and beta signal (85%) features for overall accuracy.

According to the overall average classification results of K-nearest neighbor algorithm:

- The classification accuracy rate is ranges between 89% and 95% for P_h .
- The classification accuracy rate is ranges between 80% and 85% for midrange beta.
- The classification accuracy rate is ranges between 82% and 92% for beta.

Table 9.17 The accuracy rates of K – nearest neighbor algorithm for all subjects.

K – Nearest Neighbor Algorithm			
	MF DFA - Ph	Midrange Beta	Beta
Subject 1	93%	85%	92%
Subject 2	89%	84%	84%
Subject 3	95%	80%	82%
Subject 4	91%	82%	84%
Subject 5	90%	82%	83%
Average	92%	82%	85%

In the CxK – nearest neighbor algorithm results for all subjects is displayed in Table 9.18. Subject 1 and subject 3 have higher accuracy results for P_h features again. According to the total classification accuracy results of subjects, P_h has higher accuracy rate (94%) than midrange beta (8%) and beta signal (89%) features.

According to the overall average classification results of CxK-nearest neighbor algorithm:

- The classification accuracy rate is ranges between 92% and 95% for P_h .
- The classification accuracy rate is ranges between 86% and 90% for midrange beta.
- The classification accuracy rate is ranges between 84% and 94% for beta.

Table 9.18 The accuracy rates of CxK – nearest neighbor algorithm for all subjects.

C x K – Nearest Neighbor Algorithm			
	MF DFA - Ph	Midrange Beta	Beta
Subject 1	95%	86%	94%
Subject 2	92%	90%	89%
Subject 3	96%	88%	84%
Subject 4	94%	89%	89%
Subject 5	92%	89%	89%
Average	94%	88%	89%

When the k-nearest neighbor algorithm and CxK-nearest neighbor algorithm results are compared:

- The k-nearest neighbor classification accuracy rate is 92% while CxK-nearest neighbor classification rate is 94% for P_h signals.
- The k-nearest neighbor classification accuracy rate is 82% while CxK-nearest neighbor classification rate is 88% for P_h signals.
- The k-nearest neighbor classification accuracy rate is 85% while CxK-nearest neighbor classification rate is 89% for P_h signals.

Because of the sensitivity to the dimensionality of the feature vector, K-nearest neighbor algorithm is not very common in BCI research (Borisoff et al., 2004). However, it has been efficient with low dimension feature vectors. Also, k-nearest neighbor algorithm has been used in a multiclass environment (Schlögl et al., 2005) and applied to cursor movements on a vertical axis, when classifying slow cortical potentials (Kayikcioglu & Aydemir, 2010).

The CxK-nearest neighbor algorithm has given better results in our offline analysis. This classification method is newly used method in EEG classification.

In the online analysis, subjects seat on the chair and relax before the online test. The test is beginning with the “Start” button and the online test is ended with the “Stop” button (Figure 6.16). The 1 sec data is captured in online analysis. The features are extracted from this 1sec with dimension 128 data and then classified by the C-KNN and K-NN algorithms. The session’s average data set ($128 \times 5 = 640$ for five class) taken in the training phase is used as test set and the online captured data is used as training set. The P_h values are used as feature in online analysis.

The classification accuracy is measured by true classification number of the training count. In the online analysis, the overall average classification results of K-nearest neighbor algorithm:

- The overall classification accuracy rate is 78% for left movement. The almost all subject has the same and good succes rate for the left command.

- The overall classification accuracy rate is 64% for right movement. The subject 1 and subject 5 have higher performance than the others. The overall accuracy rate of the right movement command has the lowest accuracy rate. The K-NN classifier is not good for right movement command as the remaining commands.
- The overall classification accuracy rate is 74% for up movement. The subject 3 and subject 4 have better accuracy performance.
- The overall classification accuracy rate is 74% for down movement.
- The overall classification accuracy rate is 78% for no movement movement.

The better accuracy rates have been found for the left and no movement commands (78%). Then down and up accuracy rates follow them (74%). The accuracy rate of the right command has the lowest classification accuracy (64%).

Table 9.19 The accuracy rates of the online analysis for K-NN classifier.

	K-NN				
	Left	Right	Up	Down	No Movemet
Subject 1	80%	70%	70%	80%	80%
Subject 2	80%	60%	70%	80%	80%
Subject 3	70%	60%	80%	80%	80%
Subject 4	80%	60%	80%	70%	70%
Subject 5	80%	70%	70%	60%	80%
Average	78%	64%	74%	74%	78%

The online classification results for CxK - nearest neighbor algorithm of all subjects is displayed in Table 9.20.

According to the overall avarege classification results of CxK-nearest neighbor algorithm:

- The overall classification accuracy rate is 84% for left movement.
- The overall classification accuracy rate is 70% for right movement.
- The overall classification accuracy rate is 74% for up movement.
- The overall classification accuracy rate is 78% for down movement.
- The overall classification accuracy rate is 86% for blank movement.

Table 9.20 The accuracy rates of the online analysis for CxK-NN classifier.

	CxK-NN				
	Left	Right	Up	Down	No Movement
Subject 1	80%	60%	70%	70%	90%
Subject 2	80%	70%	60%	70%	80%
Subject 3	80%	70%	80%	90%	90%
Subject 4	90%	70%	90%	80%	80%
Subject 5	90%	80%	70%	80%	90%
Average	84%	70%	74%	78%	86%

In the literature, there are many BCI applications. The results are compared with the other works. Bashar & Bhuiyan, (2016) is applied the k-nearest neighbor algorithm to the BCI competition II Graz motor imagery EEG data set. It has 140 trials each for left and right hand. In their work, the classes of the neighbors are weighted according to the similarity of each neighbor where the similarity index is the cosine value between two sample vectors of Euclidean distance. They have found the accuracy rates 86% and 96% for left and right cognitive task classification.

The many classifiers are used on the BCI competition Graz motor imagery data set. The classifiers are probabilistic neural network (PNN), support vector machine (SVM), generalized regression neural network (GRNN), adaptive neuro fuzzy inference system (ANFIS), discriminant analysis (DA), Naive Bayes (Sakthivel et al., 2014) and k-nearest neighbor algorithm. The below methods have been classified two cognitive tasks left and right (Table 9.21).

Table 9.21 The accuracy rates of the different classifiers in the literature.

Methods	Proposed by	Classifier	Classification Accuracy (%)
(MEMD + STFT)	Bashar and Bhuiyan, 2016	kNN	90.71
DWT and AR model	Xu et al., 2008	LDA	90
Multiple auto correlation	Wang et al., 2014	LVQ	90
		Neural network	90
Higher order features	Zhou et al., 2008	LDA	89.29
Morlet wavelet	Lemm et al., 2004	Bayes quadratic	89.29
Wavelet based features	Xu et al. , 2009	FSVM	87.86
		MLP	84.29
		BGN	83.57
Discriminative area selection	Hsu, 2015	FHNN	83.1
AAR	Tavakolian et al., 2007	Bayes quadratic	82.86
		LDA	65.6
		Gaussian classifiers	65.4
PSD	Solhjoo et al.,2004	Mahalanobis distance	63.1
KNN	Hari et al., 2016		75
SVM	Hari et al., 2016		72
NB	Hari et al., 2016		60
LDA	Hari et al., 2016		73
DT	Hari et al., 2016		75
Cross Correlation	Hari et al., 2016		74

Bhattacharyya et al. (2015) is proposed “Interval type-2 fuzzy logic based multiclass ANFIS algorithm for real-time EEG based movement control of a robot arm” study. In this paper, Bhattacharyya et al. (2015) have used the MFDFA method for feature extraction and then they classify the feature by the methods in Table 9.20.

They, classify 5 cognitive tasks: forward, backward, left, right and no movement. The classification accuracy rates are displayed in Table 9.22 for offline analysis. According to the results, the best classifier is OVO-IT2FLF-ANFIS with 90.93%.

In our proposed study, K-nearest neighbor algorithm classifies 5 cognitive tasks with 92% and CxK-nearest neighbor algorithm classifies the same tasks with 94% accuracy rate.

Table 9.22 The offline analysis accuracy rates of the different classifiers of the Bhattacharyya et al. (2015) method.

Classifier algorithm	Accuracy Rate
OVA-IT2FLF-ANFIS	88.91
OVO-IT2FLF-ANFIS	90.93
OVA-LDA	78.57
OVO-LDA	79.43
OVA-KNN	82.67
OVO-KNN	82.13
OVA-SVM	85.16
OVO-SVM	86.25
OVA-NB	85.75
OVO-NB	85.75

The online classification results of proposed method by Bhattacharyya et al. (2015) are shown in Table 9.23.

Table 9.23 The online analysis accuracy rates of the different classifiers of the Bhattacharyya et al. (2015) method.

Subject ID	OVA-IT2FLF-ANFIS (%)	OVO-IT2FLF-ANFIS (%)
1	75	80
2	60	80
3	50	60
4	60	65
5	60	70
6	65	65
7	70	75
8	70	70
9	60	65
10	70	65
11	70	75
Mean	64.5	70

CHAPTER TEN

CONCLUSION

In this thesis EEG signals are acquired and classified using k-nearest neighbor and CxK- nearest neighbor algorithms. The training, analysis and online test applications are developed with C# language. The developed program Sycamore BCI is consolidated with accepted programs, MATLAB and WEKA. The MATLAB program is used for extracting P_h values and brain wave signals, and preprocessing. The WEKA program is used for the K-NN classification. Also, these processes are developed in Sycamore BCI program.

The data set is captured with our program from the Emotiv Epoc Neuroheadset. Up, down, left, right and no movement features are extracted and they are used for classification. The classification performance is measured by the classification accuracy rate. The different BCI applications are developed for obtaining a higher performance. Any device can be controlled using EEG data with the successful classification application.

To compare the accuracy rates of the classifications, participants of different ages and gender are selected and the data set acquired from the different participants is classified. The performance of classification has varied due to the subjects. The effect of the user in BCI experience is discussed in detail.

The factor analysis is used to prevent the curse of dimensionality for each cognitive task. But the experimented factors are not same for left, right, up, down and no movement cognitive tasks. We need to use all the channels because intersection of the cognitive tasks factors corresponds to all the channels. The extracted features also decrease the dimension of the dataset.

The k-nearest neighbor algorithm is used for the classification of the EEG signals, but the CxK-nearest neighbor algorithm is not used before for the classification of the cognitive tasks. This method gives a more acceptable accuracy rate than the k-

nearest neighbor algorithm. In recent years, there is a serious competition between many methods which are developed for the BCI analysis. There is also a competition between the successful algorithms. We suppose a new method to the BCI literature. We successfully develop a software application which can perform data acquisition, online and offline analysis simultaneously.

The multi-class classification of cognitive EEG signal is done and the classification results are found acceptable. Also, the recently developed method, CxK nearest neighbor algorithm could be used for the multi-class classification of the cognitive EEG signal. The classification is done for the P_h , midrange beta and beta features. The P_h features with the CxK-NN algorithm classification gives much better results (94%) compared with the literature. Finally, The CxK-NN method improves the accuracy rate of motor imagery EEG signal classification.

It seems every improvement in BCI studies may rapidly present a better life quality for mankind.

REFERENCES

- Agarwal, R., Gotman, J., Flanagan, D. & Rosenblatt, B. (1998) Automatic EEG analysis using long-term monitoring in the ICU. *Electroencephalography and Clinical Neurophysiology*, 107(1), pp. 44-58.
- Altenmuller, E.O., & Gerloff, C. (1999). *Psychophysiology and the EEG*. In: Niedermeyer E, Lopes da Silva FH, editors. *Electroencephalography: basic principles, clinical applications and related fields* (4th Ed.). Baltimore, MD: Williams and Wilkins, 637–655.
- Anderson, C.W., Stolz, E.A., & Shamsunder, S. (1998). Multivariate autoregressive models for classification of spontaneous electroencephalographic signals during mental tasks. *IEEE Trans Biomed Engineering*, 45, 277–286.
- Anurag, S., & Anand, K.S. (2016). Window function analysis in OFDM system for PAPR reduction. *International Journal of Innovative Research in Computer and Communication Engineering* 4(6).
- Arndt, J. (2017). FFT code and related Stuff. Retrieved May 01, 2017 from <http://www.jjj.de/fxt/>.
- Ashkenazy, Y., Ivanov, P. Ch., Havlin, S., Peng, C.K., Goldberger, A. L., & Stanley, H. E. (2001). Magnitude and sign correlations in heartbeat fluctuations. *Physical Review Letters*, 86, 1900-1903.
- Astefanoaei C, Pretegiani E, Optican LM, Creanga D, & Rufa A. (2013). Eye movement recording and nonlinear dynamics analysis – the case of saccades. *Romanian Journal of Biophysics*, 23, 81–92.

- Astefanoaei, C., Pretegiani, E., Optican, L.M., Creanga, D., & Rufa, A. (2013). Eye movement recording and nonlinear dynamics analysis – the case of saccades. *Romanian Journal of Biophysics*, 23, 81–92.
- Ausloos, M. (2012). Measuring complexity with multifractals in texts. Translation effects. *Chaos, Soliton & Fractals*, 11(45), 1349–57.
- Bahar, S., Kantelhardt, J.W., Neiman, A., Rego, H.H. A., Russell, D. F., Wilkens, L., et al. (2001). Long range temporal anti-correlations in paddlefish electroreceptors. *Europhysics Letter*, 56, 454-460.
- Bashar, S. K., & Bhuiyan, M. I. H. (2016). Classification of motor imagery movements using multivariate empirical mode decomposition and short time Fourier transform based hybrid method. *Engineering Science and Technology, an International Journal*, 3(19) , 1457–1464.
- Berger, H. (1929). Uber das Electrenkephalogramm des Menchen. *Arch Psychiatr Nervenkr*, 87, 527–570.
- Bergland, G. D. (1969). Guided tour of the fast Fourier transform. *IEEE Spectrum*, 6, 41-52.
- Bhattacharyya, S., Basu, D., Konara, A., & Tibarewala, D.N. (2015). Interval type-2 fuzzy logic based multiclass ANFIS algorithm for real-time EEG based movement control of a robot arm. *Robotics and Autonomous Systems*, 68, 104–115.
- Blankertz, B., Dornhege, G., Krauledat, M., Muller, K. & Curio, G. (2007). The non-invasive Berlin Brain-Computer interface: Fast acquisition of effective performance in untrained subjects. *Neuroimage*, 37, 539-550.

- Borisoff, J.F., Mason, S.G., Bashashati, A., & Birch, G.E. (2004). Brain-computer interface design for asynchronous control applications: Improvements to the LF-ASD asynchronous brain switch. *IEEE Trans Biomed Engineering*, 51, 985–992.
- Bracewell, R. (1999). *The Fourier transform and its applications*. (3rd Ed.) New York: McGraw-Hill.
- Brigham, E.O. (1988). *The fast Fourier transform and applications*. Englewood Cliffs, NJ: Prentice Hall.
- Bronzino, J. D. (1995). *Principles of Electroencephalography*. In: J.D. Bronzino Ed. The Biomedical Engineering Handbook, Florida: CRC Press, 201-212.
- Buldyrev, S. V., Dokholyan, N.V., Goldberger, A.L., Havlin, S., Peng, C.K., Stanley, H.E. et al. (1998). Analysis of DNA sequences using methods of statistical physics. *Physica A*, 249, 430-438.
- Carlson, N. R. (2002). *Foundations of physiological psychology*. (5th Ed.) Boston, Mass. London : Allyn and Bacon.
- Cooley, J. W. & Tukey, O. W. (1965). An Algorithm for the machine calculation of complex fourier series. *Mathematics of Computation*, 19, 297-301.
- Cooper, R., Osselton, J.W., & Shaw, J.C. (1980). *EEG technology* (3rd Ed.). London, UK: Butterworths.
- Cover, T.M., & Hart, P.E. (1967). Nearest neighbor pattern classification, *IEEE Transactions on Information Theory*, 13, 21–27.
- Cox, J.R., Nolle, F.M., & Arthur, R.M. (1972). Digital analysis of the electroencephalogram, the blood pressure wave, and the electrocardiogram. *Proceedings of the IEEE*, 60(10):1137-1164.

- Duhamel, P. & Vetterli, M. (1990). Fast Fourier transforms: A tutorial review. *Signal Processing*, 19, 259-299.
- Dutta, S., Ghosh, D., Shukla, S., & Dey, S. (2014). Multifractal parameters as an indication of different physiological and pathological states of the human brain. *Physica A*, 396, 155–63.
- Farwell, L.A., & Donchin, E. (1998). Talking off the top of your head: toward a mental prosthesis utilizing event-related brain potentials. *Electroencephalography and Clinical Neurophysiology*, 70(6), 510-23.
- Feder, J. (1988). *Fractals*. New York, USA: Plenum Press.
- Frahm, J., Bruhn, H., Merboldt, K.D., & Hänicke, W. (1992). Dynamic MR imaging of human brain oxygenation during rest and photic stimulation. *Journal of Magnetic Resonance Imaging*, 2, 501-5.
- Graimann, B., Allison, B., Mandel, C., Luth, T., Valbuena, D. & Graser, A. (2009). Non-invasive brain-computer interfaces for semi-autonomous assistive devices. *Robust Intelligent Systems*, Chapter 6, 113-138.
- Grave de Peralta Menendez R., Gonzalez Andino S., Lantz G., Michel CM, & Landis T. (2001) Noninvasive localization of electromagnetic epileptic activity. I. Method descriptions and simulations. *Brain Topography*, 14(2), 131-7.
- Gray, P. (2002). *Psychology* (4th Ed.). New York: Worth Publishers. ISBN 0-7167-5162-3.
- Hari Krishnaa, D., Pashaa, I.A., & Satya Savithrib, T. (2016). Classification of EEG motor imagery multi class signals based on cross correlation. *Procedia Computer Science*, 85, 490 – 495.

- Hart, P.E., Stock, D.G., & Duda, R.O. (2001). *Pattern classification* (2nd Ed.). Wiley, Hoboken, NJ, USA.
- Hausdorff, J.M., Mitchell, S.L., Firtion, R., Peng, C.K., Cudkowicz, M.E., Wei, J.Y., et al. (1997). Altered fractal dynamics of gait: reduced stride-interval correlations with aging and Huntington's disease. *Journal of Applied Physiology*, 82(1), 262-9.
- Hsu, W.Y. (2015). Brain–computer interface: the next frontier of telemedicine in human–computer interaction. *Telematics and Informatics*, 32(1), 180–192.
- Hurst, H.E. (1951). Long-term storage capacity of reservoirs, *Transactions of the American Society of Civil Engineers*, 116, 770-808.
- Ihlen, E.A., & Vereijken, B. (2010). Interaction-dominant dynamics in human cognition: Beyond $1/f(\alpha)$ fluctuation. *Journal of Experimental Psychology: General*, 139(3):436-63.
- Kantelhardt, J.W., Zschiegner, S.A., Koscielny-Bunde, E., Havlin, S., Bunde, A., & Stanley, H.E. (2002). Multifractal detrended fluctuation analysis of nonstationary time series. *Physica A*, 316, 87–114.
- Kantelhardt, J.W., Koscielny-Bunde, E., Rego, H.H.A., Havlin, S., & Bunde, A. (2001). Detecting long-range correlations with detrended fluctuation analysis. *Physica A: Statistical Mechanics and its Applications*, 295(3), 441-454.
- Kantelhardt, J.W. (2009). *Fractal and multifractal time series*. In: Meyers RA, editor. *Encyclopedia of Complexity and Systems Science* ed.: Springer. 3754–3779.

- Kayikcioglu, T., & Aydemir, O. (2010). A polynomial fitting and k-NN based approach for improving classification of motor imagery BCI data. *Pattern Recognition Letters*, 31, 1207–1215.
- Keirn, Z.A., & Aunon, J.I. (1990). A new mode of communication between man and his surroundings. *IEEE Transactions on Biomedical Engineering*, 37, 1209–1214.
- Kelty-Stephen, D.G., & Nixon, J. (2013). Notes on a journey from symbols to multifractals. *Ecological Psychology*, 25, 1–62.
- Kennedy, H.L. (2007). A new statistical measure of signal similarity. *Information, Decision and Control*, DOI: 10.1109/IDC.2007.374535.
- Kooi KA, Tucker RP, & Marshall RE. (1978). *Fundamentals of Electroencephalography* (2nd Ed.). Harper & Row, Hagerstown, MD.
- Kumar, S., Gu, L., Ghosh, N., & Mohanty, S.K. (2013). Multifractal detrended fluctuation analysis of optogenetic modulation of neural activity. *Proceeding SPIE 8586 Optogenetics: Optical Methods for Cellular Control*, 858608.
- Lang, W., Cheyne, D., Hollinger, P., Gerschlager, W., & Lindinger, G. (1996). Electric and magnetic fields of the brain accompanying internal simulation of movement. *Cognitive Brain Research*, 3, 125–129.
- Lemm, S., Schäfer, C., & Curio, G. (2004). Bci competition 2003-data set iii: probabilistic modeling of sensorimotor μ rhythms for classification of imaginary hand movements. *IEEE Transactions on Biomedical Engineering*, 51(6), 1077–1080.
- Lotte, F., Congedo, M., Lécuyer, A., & Lamarche, F. (2007). A review of classification algorithms for EEG-based brain–computer interfaces. *Journal of Neural Engineering*, 4.

- Mahmoud, S.A. & Al-Khatib, W.G. (2011). Recognition of Arabic (Indian) bank check digits using log-gabor filters. *Applied Intelligence*, 3(35), 445–456.
- Malek, H., Ebadzadeh, M.M., & Rahmati, M. (2012). Three new fuzzy neural networks learning algorithms based on clustering, training error and genetic algorithm. *Applied Intelligence*, 3(37), 280–289.
- Mantegna, R.N., & Stanley, H.E. (2000). *An introduction to econophysics*. Cambridge: Cambridge University Press.
- McFarland, D.J., Miner, L.A., Vaughan, T.M., & Wolpaw, J.R. (2000). Mu and beta rhythm topographies during motor imagery and actual movement. *Brain Topography*, 3, 177–186.
- McFarland, D.J., Neat, G.W., Read, R.F., & Wolpaw, J.R. (1993). An EEG-based method for graded cursor control. *Psychobiology*, 21, 77-81.
- Movahed, M.S., Jafari, G., Ghasemi, F., Rahvar, S., & Tabar, M.R.R. (2006). Multifractal detrended fluctuation analysis of sunspot time series. *Journal of Statistical Mechanics: Theory and Experiment*, doi:10.1088/1742-5468/2006/02/P02003.
- Nussbaumer, H.J. (1982). *Fast Fourier transform and convolution algorithms* (2nd Ed.). New York: Springer-Verlag.
- Ogawa, S., Lee, T.M., Kay, A.R., & Tank, D.W. (1990). Brain magnetic resonance imaging with contrast dependent on blood oxygenation. *Proceedings of the National Academy of Sciences, U S A*. 87(24), 9868–9872.
- Papoulis, A. (1962). *The Fourier integral and its applications*. New York: McGraw-Hill.

- Pfurtscheller, G., & Neuper, C. (1997). Motor imagery activates primary sensorimotor area in man. *Neuroscience Letter*, 239, 65–68.
- Pfurtscheller, G., & Lopes da Silva, F.H. (1999). Event-related EEG/MEG synchronization and desynchronization: basic principles. *Clinical Neurophysiology*, 110(11), 1842–1857.
- Pfurtscheller, G., Muller-Putz, G.R., Schlögl, A., Graimann, B., Leeb, R., Brunner, C., et al. (2006). 15 years of BCI research at Graz University of technology: current projects. *IEEE Transactions on Neural Systems and Rehabilitation Engineering: A publication of the IEEE Engineering in Medicine and Biology Society*, 14, 205-210.
- Press, W. H., Flannery, B.P., Teukolsky, S.A., & Vetterling, W. T. (1992). *Fast Fourier transform. Ch. 12 in Numerical Recipes in FORTRAN: The Art of Scientific Computing*. (2nd Ed.) Cambridge, England: Cambridge University Press, 490-529.
- Purves, D., Augustine, G.J., Fitzpatrick, D., Katz, L.C. Lamantia, A.S. & McNamara, J.O. (2004). *Neuroscience. Sinauer associates*. (3rd Ed.). Sunderland, Massachusetts, USA: Inc. Publishers.
- Qing-Bin, G., & Zheng-Zhi, W. (2007). Center-based nearest neighbor classifier. *Pattern Recognition*, 40, 346 – 349.
- Ramirez, R.W. (1985). *The FFT: Fundamentals and concepts*. Englewood Cliffs, NJ: Prentice-Hall.
- Rangayyan, R.M. (2002). *Biomedical signal analysis: A case-study approach*. John Wiley & Sons, Inc., ISBN 0-471-2081 1-6.

- Sakthivel, N., Nair, B.B., Elangovan, M., Sugumaran, V., & Saravanmurugan, S. (2014). Comparison of dimensionality reduction techniques for the fault diagnosis of mono block centrifugal pump using vibration signals. *Engineering Science and Technology an International Journal*, 17(1), 30–38.
- Schacter, D. L., Gilbert, D. L. & Wegner, D. M. (2009). *Psychology*. (2nd Ed.). New York: Worth Publishers.
- Schlögl, A., Lee, F., Bischof, H., & Pfurtscheller, G. (2005). Characterization of four-class motor imagery EEG data for the BCI-competition 2005. *Journal of Neural Engineering*, 2, L14. 229.
- Schmeisser, E.T., McDonough, J.M., Bond, M., Hislop, P.D., & Epstein, A.D. (2001). Fractal analysis of eye movements during reading. *Optometry and Vision Science*, 78(11), 805-14.
- Seber, G.A.F., (2004). *Multivariate Observations*. Wiley, ISBN: 978-0-471-69121-1.
- Sellers, E.W., & Donchin, E. (2006). A P300-based brain-computer interface: Initial tests by ALS patients. *Clinical Neurophysiology: Official Journal of the International Federation of Clinical Neurophysiology*, 117, 538-548.
- Shelhamer, M.J. (2005). Sequences of predictive saccades are correlated over a span of approximately 2 s and produce a fractal time series. *Journal of Neurophysiology*, 93(4), 2002-11.
- Solhjoo, S., & Moradi, M. (2004). Mental task recognition: a comparison between some of classification methods. *BIOSIGNAL 2004 International EURASIP Conference*, 24–26.
- Stan, C., Cristescu, M.T., Luiza, B.I., & Cristescu, C.P.J. (2013). Investigation on series of length of coding and non-coding DNA sequences of bacteria using

- multifractal detrended cross-correlation analysis. *Journal of Theoretical Biology*, 321 (21), 54-62.
- Strang, G. (1993). Wavelet transforms versus Fourier transforms. *Bulletin of the American Mathematical Society*, 28, 288-305.
- Suckling, J., Wink, A.M., Bernard, F.A., Barnes, A., & Bullmore, E.J. (2008). Endogenous multifractal brain dynamics are modulated by age, cholinergic blockade and cognitive performance. *Journal of Neuroscience Methods*, 174(2), 292-300.
- Talkner, P. & Weber, R.O. (2000). Power spectrum and detrended fluctuation analysis: application to daily temperatures . *Physical Review E*, 62, 150.
- Taqqu, M., Teverovsky, V., & Willinger, W. (1995). Estimators for long-range dependence: an empirical study. *Fractals*, 3(4):785–798.
- Ulutağay, G. & Nasibov, E. (2016) C × K-Nearest Neighbor Classification with Ordered Weighted Averaging Distance. *Novel Applications of Intelligent Systems*, 586, 105-122, doi: 10.1007/978-3-319-14194-7_6.
- Teplan, M., (2002). Fundamentals of EEG measurement. *Measurement science review*, 2(2), 1-11.
- Van Loan, C. (1992). *Computational Frameworks for the Fast Fourier Transform*. Philadelphia, PA: SIAM.
- Velliste, M., Perel, S., Spalding, M.C., Whitford, A.S., & Schwartz, A.B. (2008). Cortical control of a prosthetic arm for self-feeding. *Nature*, 453, 1098-1101.
- Walker, J. S. (1996). *Fast Fourier transform*. (2nd Ed.) Boca Raton, FL: CRC Press.

- Wang, J., Ning, X., & Chen, Y. (2003). Multifractal analysis of electronic cardiogram taken from healthy and unhealthy adult subjects. *Physica A*, 323, 368–561.
- Wang, X., Wang, A., Zheng, S., Lin, Y., & Yu, M. (2014). A multiple autocorrelation analysis method for motor imagery EEG feature extraction. *The 26th Chinese Control and Decision Conference (2014 CCDC), IEEE*, 3000–3004.
- Wolpaw, J.R., & McFarland, D.J. (1994). Multichannel EEG-based brain-computer communication. *Electroencephalography and Clinical Neurophysiology*, 90, 444–449.
- Xu, B., & Song, A. (2008). Pattern recognition of motor imagery EEG using wavelet transform. *Journal of Biomedical Science and Engineering*, 1(01), 64.
- Xu, Q., Zhou, H., Wang, Y., & Huang, J. (2009). Fuzzy support vector machine for classification of EEG signals using wavelet-based features. *Medical Engineering & Physics*, 31(7), 858–865.
- Zhang, H., Yang, S., Guo, L., Zhao, Y., Shao, F., & Chen, F. (2015). Comparisons of isomiR patterns and classification performance using the rank-based MANOVA and 10-fold cross-validation. *Gene*, 569, 21–26.
- Zheng, Y., Gao, J., Sanchez, J.C., Principe, J.C., & Okun, M.S. (2005). Multiplicative multifractal modeling of human neuronal activity. *Physics Letters A*, 344, 253–64.
- Zhou, S.M., Gan, J.Q., & Sepulveda, F. (2008). Classifying mental tasks based on features of higher-order statistics from EEG signals in brain–computer interface. *Information Sciences*, 178(6), 1629–1640.